

STATE OF CALIFORNIA DEPARTMENT OF TRANSPORTATION
TECHNICAL REPORT DOCUMENTATION PAGE
 TR0003 (REV. 10/98)

1. REPORT NUMBER CA10-1043	2. GOVERNMENT ASSOCIATION NUMBER	3. RECIPIENT'S CATALOG NUMBER	
4. TITLE AND SUBTITLE Microsimulation Modeling of High Occupancy Toll (HOT) Concept in HOV Lanes		5. REPORT DATE October 2009	
		6. PERFORMING ORGANIZATION CODE	
7. AUTHOR(S) Will Recker, Lianyu Chu, Shin-Ting (Cindy) Jeng		8. PERFORMING ORGANIZATION REPORT NO.	
9. PERFORMING ORGANIZATION NAME AND ADDRESS Institute of Transportation Studies University of California, Irvine Irvine, CA 92697-3600		10. WORK UNIT NUMBER 193	
		11. CONTRACT OR GRANT NUMBER 65A0235	
12. SPONSORING AGENCY AND ADDRESS California Department of Transportation Division of Research and Innovation, MS-83 1227 O Street Sacramento CA 95814		13. TYPE OF REPORT AND PERIOD COVERED Final Report	
		14. SPONSORING AGENCY CODE	
15. SUPPLEMENTAL NOTES None			
16. ABSTRACT This project developed a new HOV driver behavioral model that incorporates an access preference/choice model for examining travel time savings and a traffic model for calculating the acceptable gap to get in/out of buffer-separated HOV lane facilities. The model is incorporated into the Paramics simulator as a plug-in developed through API (Application Programming Interface) programming. In order to extend its capability for calibration and implementation, several user-specified parameters were incorporated during the model development process, including ingress and egress points selection control, and provision traffic information updates. The parameters of the model were tested and evaluated using both a sample, idealized, segment of freeway as well as a simulation network of the SR-57 freeway in Orange County, California. Sensitivity analyses were performed to evaluate the reasonableness of the model; the freeway network was further investigated for model validation purposes. The results demonstrate the reasonableness of the proposed model under various traffic conditions. The proposed model also was demonstrated to better capture the weaving maneuvers observed on the SR-57 freeway.			
17. KEY WORDS HOV lanes, Buffer-separated facility, Behavioral lane access model		18. DISTRIBUTION STATEMENT No restrictions. This document is available to the public through the National Technical Information Service, Springfield, VA 22161	
19. SECURITY CLASSIFICATION (of this report) None		20. NUMBER OF PAGES 101	21. PRICE

DISCLAIMER STATEMENT

This document is disseminated in the interest of information exchange. The contents of this report reflect the views of the authors who are responsible for the facts and accuracy of the data presented herein. The contents do not necessarily reflect the official views or policies of the State of California or the Federal Highway Administration. This publication does not constitute a standard, specification or regulation. This report does not constitute an endorsement by the Department of any product described herein.

For individuals with sensory disabilities, this document is available in Braille, large print, audiocassette, or compact disk. To obtain a copy of this document in one of these alternate formats, please contact: the Division of Research and Innovation, MS-83, California Department of Transportation, P.O. Box 942873, Sacramento, CA 94273-0001.

FINAL REPORT

Caltrans RTA 65A0235

**Microsimulation Modeling of High Occupancy
Toll (HOT) Concept in HOV Lanes**

October, 2009

FINAL REPORT

Caltrans RTA 65A0235

Microsimulation Modeling of High Occupancy Toll (HOT) Concept in HOV Lanes

Prepared by:

Will Recker, Shin-Ting (Cindy) Jeng

Institute of Transportation Studies
University of California, Irvine
Irvine, CA 92697

Lianyu Chu
California Center for Innovative Transportation
University of California, Berkeley
Berkeley, CA 94720

October, 2009

Table of Contents

1. Introduction.....	5
2. Literature Review of HOV Lane Choice Modeling	7
2.1 HOV Lane Choice Model	7
2.2 HOV Modeling in Microsimulation Models.....	7
3. HOV Driver Behavior Model Development	8
3.1 Determining Preferred HOV Ingress/Egress Points	8
3.2 Acting on Preferences	15
3.3 Lane-changing Behavior	15
3.4 Extracting Results to the Viewpoint of the HOV-lane Bound Vehicle	16
3.5 Probability that Preferred Entry Point <i>i/e i</i> can be Accessed	18
4. Paramics Buffer-separated HOV Access API Development.....	24
4.1 Paramics Buffer-separated HOV Access API Schematic	24
4.2 Sample Network.....	25
4.3 Implementation of Ingress Preference Model and Traffic Model	26
5. Model Sensitivity Analysis and Validation	33
5.1 Calibration Parameters and Control Parameters	33
5.2 Sensitivity Analysis of the Sample Network	34
5.3 Sensitivity Analysis using the SR-57 Network.....	54
5.4 Model Validation and Discussion.....	60
6. Conclusions.....	66
References.....	67
Appendix A: Plugin Input Specifications and Plugin Pseudo Code.....	69
Appendix B: Derivation of Preference to Enter HOV Lane at Ingress/Egress (<i>i/e i</i>)	73
Appendix C: Derivation of Preference to Exit HOV Lane at Ingress/Egress (<i>i/e j</i>)	80
Appendix D: Derivation of Lane-changing Behavior	87

List of Tables

Table 5-1 OD table for Case 1 and Case 2.....	35
Table 5-2 OD table for Case 3 and Case 4.....	35

List of Figures

Figure 3-1. Determining preferred HOV Ingress/Egress Points.....	8
Figure 3-2. Preference to enter the HOV lane at Ingress/Egress (i/e) i	9
Figure 3-3. Preference for exiting HOV lane at Ingress/Egress (i/e) j	12
Figure 3-4. Acceptable Gap at time $t = t_0$	16
Figure 3-5. Acceptable Gap at time $t = t_0 + t^*$	17
Figure 3-6. Acceptable Gap at time $t = t_0 + t_g$	17
Figure 3-7. State of traffic system relative to preferred Ingress/Egress point i/e i	19
Figure 3-8. Four-lane freeway example of Acceptable Gap conditions relative to successfully accessing preferred Ingress/Egress point i/e i	20
Figure 3-9. Four-lane freeway example of Acceptable Gap conditions relative to unsuccessfully accessing preferred Ingress/Egress point i/e i	21
Figure 3-10. Plot of d_{gk} for the set of “reasonable” parameter values: $a = 1.5$	23
Figure 3-11. Plot of d_{gk} for the set of “reasonable” parameter values: $a = 3.0$	23
Figure 4-1. Paramics buffer-separated HOV access API Schematic.....	25
Figure 4-2. Paramics network skeleton.....	26
Figure 4-3. Weave distance at buffer-separated HOV facilities (Caltrans, 2003).....	26
Figure 5-1. Summary of Case 1 results: Ramp to Ramp	36
Figure 5-2. Case 1 results variation with parameter a	37
Figure 5-2. Case 1 results variation with parameter a (cont.)	38
Figure 5-2. Case 1 results variation with parameter a (cont.)	39
Figure 5-3. The differences of travel time at each section.....	40
Figure 5-3. The differences of travel time at each section (cont.).....	41
Figure 5-3. The differences of travel time at each section (cont.).....	42
Figure 5-4. Comparison of non-congestion and congestion scenarios	43
Figure 5-5. Summary of Case 2 results: Mainline to Ramp	44
Figure 5-6. Case 2 results variation with parameter a	45
Figure 5-6. Case 2 results variation with parameter a (cont.)	46
Figure 5-6. Case 2 results variation with parameter a (cont.)	47
Figure 5-7. Summary of Case 3 results: Ramp to Mainline	48

Figure 5-8. Case 3 results variation with parameter a	49
Figure 5-8. Case 3 results variation with parameter a (cont.)	50
Figure 5-9. Summary of Case 4 results: Mainline to Mainline.....	51
Figure 5-10. Case 4 results variation with parameter a	52
Figure 5-10. Case 4 results variation with parameter a (cont.)	53
Figure 5-11. Freeway Network for Sensitivity Analysis: SR-57 Network.....	54
Figure 5-12. SR-57 Network sensitivity analysis results for different values of α	56
Figure 5-12. SR-57 Network sensitivity analysis results for different values of α (cont.)	57
Figure 5-13. SR-57 Network sensitivity analysis results for different values of a	58
Figure 5-13. SR-57 Network sensitivity analysis results for different values of a (cont.).....	59
Figure 5-14. Model validation: Usage of ingress point 1 vs 5-min flow	60
Figure 5-15. Model Validation: Travel time savings at ingress point 1	61
Figure 5-16. Model Validation: Speed at ingress point 1	61
Figure 5-17. Model Validation under free flow conditions: Usage of ingress point 1	62
Figure 5-18. Model Validation under free flow conditions: Travel Time Savings	62
Figure 5-19. Model Validation under free flow conditions: Speed	63
Figure 5-20. Ingress/egress point usages with dynamic feedback control.....	63
Figure 5-21. Travel time saving comparison	64
Figure 5-22. Speed-Density comparison at ingress point 1	65
Figure 5-23. Speed-Density comparison at ingress point 2	66

1. Introduction

High-Occupancy Vehicle (HOV) lanes, commonly known as carpool lanes, have been accepted as a cost-effective and environmental-friendly alternative in many metropolitan areas. Provision of HOV lanes is a demand management strategy intended to encourage travelers to switch their modes of travel to transit, vanpools, or carpools. A secondary benefit commonly anticipated is the reduction of the demand on the mixed-flow lanes, resulting in reduction in traffic congestion and improved air quality. The Federal Highway Administration (FHWA) encourages the installation of HOV lanes as an important part of an area-wide approach to help metropolitan areas address the needs that they have identified for mobility, safety, productivity, environment, and quality of life. In recent times, HOV lane construction has become a major freeway improvement strategy.

Currently, HOV lanes exist in more than 23 metropolitan areas—predominantly in the congested corridors of the regions. In California, the types of HOV facilities can be classified as being either (a) continuous-access HOV lanes (e.g., HOV lanes in the Bay area) or (b) limited-access buffer-separated with ingress/egress points (e.g. HOV lanes in Southern California). Both types of HOV facilities can operate either as part-time or as full-time.

Despite wide adoption of HOV facilities, there still remain questions on the effectiveness of current HOV systems (Hill, 2000; Wellander and Leotta, 2000). One criticism is that HOV lanes are under-utilized—a situation that is thought by at least some critics to apply to many HOV lanes across the nation. Another criticism is that HOV lanes get congested and thus are not sufficiently attractive alternatives during peak periods to justify their negative aspects (Varaiya, 2007). Federal Highway Administration (FHWA)'s Safe, Accountable, Flexible, Efficient Transportation Equity Act: A Legacy for Users (SAFETEB-LU) provides HOV lane operation guidelines, that recommends that HOV lanes be operated at a speed greater than 45 mph for 90% of the peak period. It is noted that HOV lanes in some regions, such as southern California, are currently operated at a critical condition since they have congestion during peak periods, but are under-utilized during off peaks.

To improve the effectiveness of HOV lane operation, two strategies have been adopted recently. One strategy is to allow hybrid vehicles to use HOV lanes in order to utilize the remaining, unused, capacity of HOV lanes. This policy has been deployed in a few states and some others are considering it. Based on experiences drawn from Virginia and California, such a policy may cause HOV lanes to become congested. Under circumstances in which HOV lanes are currently close to capacity or already congested such a policy is judged as not appropriate (Brownstone et al., 2007). Another strategy is conversion of HOV lanes to High Occupancy Toll (HOT) lanes, which combines HOV and pricing strategies by allowing solo drivers to gain access to HOV lanes by paying a toll. So far, seven states, including California, Colorado, Florida, Minnesota, Texas, Utah, and Washington, have implemented HOT lanes either on some of their existing under-utilized HOV lanes or by adding a parallel lane dedicated to HOT. Many states are currently planning or in the process of converting HOV to HOT lanes (Ungemah, 2006). Varaiya (2007) analyzed loop detector data along California HOV lanes using the Performance

Measurement System (PeMS), and suggested that an effective HOV lane operation is to convert 2-lane HOV facilities to HOV/HOT operation.

In reality, any particular HOV lane operation strategy may not be an appropriate option for every situation. That is, the benefits and impacts may vary by location and situation. It is thus very important to find ways to evaluate alternative strategies during the decision making process, and prior to any implementation. Traditionally, transportation planning models have been employed to evaluate alternative solution strategies to addressing a transportation problem. However, this “macroscopic” analysis method typically is based on BPR (Bureau of Public Roads) functions, which yield a monotonically increasing travel time and do not capture the dynamics in traffic and driver behavior. Obviously, the method is not appropriate for HOV lane analysis since HOV is not only a demand management policy that motivates solo drivers to switch to carpools but also is an advanced traffic management strategy that encourages HOV-eligible drivers to select either HOV lanes or mixed-flow lanes based on traffic conditions. An alternative approach is microscopic traffic simulation. Microscopic traffic simulation emulates traffic systems at a level that includes detailed specification of roads, individual drivers, and vehicles. It has become an increasingly popular and effective tool for analyzing a wide variety of dynamic problems not amendable to study by other means. It is well suited for the HOV lane analysis (Breiland et al., 2006). However, its use in the evaluation of HOV/HOT strategies is explicitly tied to its ability to model HOV behavior, both in terms of demand as well as traffic considerations.

The principal question addressed here is whether or not current micro-simulation models have adequate capability to model HOV facility and HOV driver behavior, particularly with respect to buffer-separated facilities. In addressing this question, our understanding of driver behavior as it relates to HOV lane selection can be described as follows:

- HOV drivers select HOV lane or mixed-flow lanes based on their distance to the exiting off-ramp, their familiarity of the traveled freeway, their driving aggressiveness, their historically experienced or currently perceived or predicted traffic condition along the HOV lane and mixed-flow lanes.
- HOV lanes are utilized more when mixed-flow lanes get congested.
- HOV lanes may still be used even when the mixed-flow lanes are free-flow due to factors not related to travel time savings, such as feeling more relaxed or comfortable in using HOV lanes.
- Under buffer-separated HOV lane operation, HOV-eligible drivers may not be able to enter the HOV lane at the first available ingress point because traffic conditions may not allow them to change all lanes successfully.
- Under buffer-separated HOV lane operation, HOV drivers may not exit HOV lanes at the last possible egress point because: (a) they may not know whether or not there is still an egress point before the existing off-ramp; (b) they may feel that the current traffic conditions along mixed-flow lanes is too congested to allow them to change lanes successfully if they take the last egress point before the exiting off-ramp.

The review of the literature on modeling HOV behavior in the next section shows that, although the leading micro-simulation models (Paramics, TransModeler, and Vissim) purport to be able to model HOV lanes and HOV drivers, their modeling capabilities are nonetheless limited. This

project aims to develop a HOV driver behavior model that is able to better mimic the real-world HOV drivers' behavior. The model is incorporated into the Paramics simulator as a plugin developed through API (Application Programming Interface) programming. The parameters of the model are further tested and evaluated using the simulation network, the SR-57 freeway in Orange County, California.

2. Literature Review of HOV Lane Choice Modeling

2.1 HOV Lane Choice Model

Travel time savings and requirements for changing lanes are generally considered as the primary variables in modeling HOV lane choice. Several early studies (Kostyniuk, 1982; Teal, 1987, Giuliano et al., 1990) found that longer commutes were more likely to choose carpooling, in order to gain more benefit from travel time saving.

To best describe the lane choice behavior for HOV drivers, a number of researchers have adopted discrete choice models. Small (1977) first introduced a multinomial logit model of lane choice to estimate HOV lane shares from the demand side. Chu (1993) included a nested logit model which further addressed both mode and departure time choice. McDonald and Noland (2001) also applied a nested logit model extended from Chu's study but with a three-level nested logit model instead of two-level to accommodate the time of day choice. Dahlgren (2002) applied a binary logit model to estimate HOV lane usage based on the time differential between the HOV and non-HOV lanes.

In order to reflect the lane choice effects due to travel time changes over time, Mahmassani, et al. (2000 and 2001) suggested a dynamic network simulation-assignment approach with different generalized cost (including travel time and travel cost) for High-Occupancy Toll (HOT) lanes. Furthermore, a review by Choudhury (2005) concluded that the limitation of the exclusive lane choice model (i.e. HOV/HOT lane choice model) primary developed for planning purpose are: 1) "aggregate demand models based on empirical values obtained from previous research," and 2) "do not involve any rigorous estimation of the model parameters." However, Choudhury (2005) also pointed out that the microsimulation models can be effective tool to: 1) "model the dynamic variation in traffic conditions," and 2) "perform detailed analyses of traffic situations involving exclusive lanes."

2.2 HOV Modeling in Microsimulation Models

To a varying degree, all the top three micro-simulation models, Paramics, TransModeler, and Vissim are able to model HOV lanes and HOV drivers' behaviors. Although Paramics and Vissim are more widely used, they are both relatively weak with respect to modeling HOV driver behavior. As a relatively newly developed micro-simulator, TransModeler provides more HOV modeling features and also is closest to the driver behavior described in the first section. However, all of them assume that there must be a travel time advantage on HOV lanes in order for HOV-eligible drivers to use them. There is no HOV driver behavior associated with the use of HOV lanes for reasons other than travel time savings.

Since Paramics has powerful API functionalities, our HOV driver behavior model is implemented in Paramics as a plugin for purposes of testing the basic formulation. For simplicity, the model is developed and tested for buffer-separated HOV lanes.

Currently, Paramics handles the ingress/egress decisions for eligible HOV users of buffer-separated carpool lanes as a route choice problem. Because HOV vehicles are constrained to follow these prescribed routes—the current implementation forces vehicles into the first ingress point possible—simulated vehicles can be observed to block mainline mixed-flow lanes in order to make these maneuvers. This can lead to unrealistic congestion, particularly under peak conditions where the HOV lanes are most heavily utilized.

Therefore, we propose a probabilistic HOV driver behavioral model based on discrete choice modeling derived from random utility principles, which includes a preferred access choice model for examining travel time savings and a traffic model for calculating the acceptable gap to get in/out the HOV lane. Its theoretical capability is extended to real-world application via providing additional “implementation” parameters, such as ingress and egress points selection control, and traffic information update frequency. The model details are discussed in Section 3 and Section 4, while initial “reasonableness” tests are provided in Section 5.

3. HOV Driver Behavior Model Development

3.1 Determining Preferred HOV Ingress/Egress Points

Consider the trip of an HOV-eligible vehicle from an entry ramp O to an exit ramp D. Let the n HOV lane ingress/egress points (i/e) between O and D be labeled consecutively from 1, 2, \dots , n , with corresponding sections of the freeway between i/e i and i/e $(i-1)$ labeled as section I as shown in Figure 3-1; here, and in subsequent figures, ingress/egress points are displayed as gaps (i.e., spaces) in the solid line separating the HOV lane from the mainline lines, which are displayed as dashed lines.

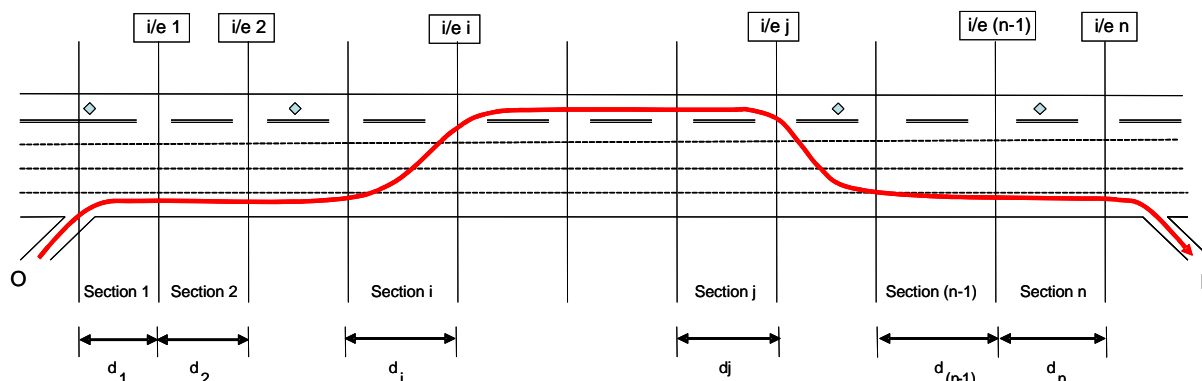


Figure 3-1. Determining preferred HOV Ingress/Egress Points

For the trip from O to D, let U_q^F denote the utility derived from travel on the mainline freeway section q . Similarly, let U_q^{HOV} denote the utility derived from travel on HOV section q . (Note: Presumably, in the case of an HOV lane the utility would be reflected only in the travel time savings, while in the case of an HOT lane the utility would be reflected by the difference in the value of time associated with the travel time savings and the toll.) For simplicity, we assume that the decision associated with HOV use can be segmented into two distinct decisions based on perceived real-time information regarding traffic conditions:

1. the decision/preference regarding where to try to enter the HOV lane; i.e., choice to enter the HOV lane at ingress/egress (i/e) i , and
2. the decision/preference regarding where to try to exit the HOV lane in order to exit the ramp at D; i.e., choice to exit the HOV lane at ingress/egress (i/e) j .

Note: The decision of whether or not to continue on the HOV lane at any particular time and/or the decision to reenter the HOV lane after exiting it but before reaching exit ramp D can be treated in the same manner by simply substituting the vehicle's current position on the freeway (lane and postmile) in the place of O.

3.1.1 Preference to enter HOV lane at ingress/egress (i/e) i

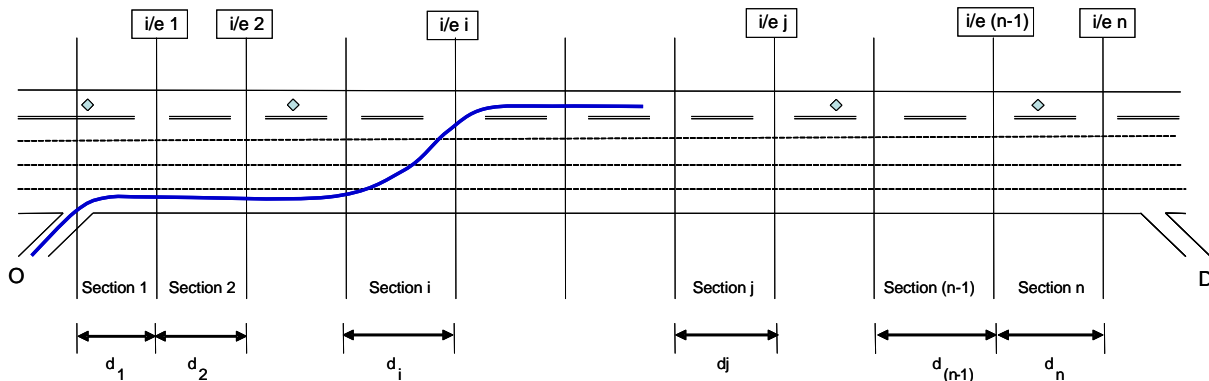


Figure 3-2. Preference to enter the HOV lane at Ingress/Egress (i/e) i

Consider a driver's choice (or preference) to enter the HOV facility at entry point (i/e) i , conditioned on the decision to exit the facility at exit point (i/e) j . Consistent with standard random utility assumptions, let the utility of this choice be denoted by:

$$U_i^e = \sum_{q=1}^i U_q^F + \sum_{l=i+1}^j U_l^{HOV} ; i < j \leq n \tag{1}$$

where U_i^e denotes the travel time utility of entering the HOV lane at i/e point i (under the presumption of exiting at i/e point j). (Note: the decision to enter the HOV lane at $j = n$ is *de facto* the decision not to enter the HOV lane at all; i.e., to use only the mainline freeway between

O and D.) Assume $U_i^e = V_i^e + \xi_i^e$, where V_i^e denotes the utility (actually a disutility) associated with the expected travel time (or, generalized cost in the case of HOT lanes) using entry point i and ξ_i^e denotes the random delay associated with unknown traffic effects. Assume ξ_i^e are multivariate normal distributed, i.e.,

$$\mathbf{U}^e = \text{MVN}(\mathbf{V}^e, \mathbf{\Sigma}^e) \quad (2)$$

where $\mathbf{\Sigma}^e$ is the covariance matrix.

Assume that the covariance between any two alternatives is only in the links they share in common; i.e.,

$$\text{Cov}(U_i^e, U_k^e) = \text{Var}(\xi_1^F + \xi_2^F + \dots + \xi_i^F + \xi_{k+1}^{HOV} + \xi_{k+2}^{HOV} + \dots + \xi_j^{HOV}) = \sigma_{F_i H_k}^2 ; i, k = 1, \dots, j \quad (3)$$

Assume, for simplicity, that the mainline freeway variances are independent of the HOV lane variances, i.e.,

$$\begin{aligned} \sigma_{F_i H_k}^2 &= \text{Cov}(U_i^e, U_k^e) = \text{Var}(\xi_1^F + \xi_2^F + \dots + \xi_i^F) + \text{Var}(\xi_{k+1}^{HOV} + \xi_{k+2}^{HOV} + \dots + \xi_j^{HOV}) \\ &= \sigma_{F_i}^2 + \sigma_{H_k}^2 \end{aligned} \quad (4)$$

Let P_i^e denote the probability that HOV lane entry i will be preferred for the trip from O to D. Then

$$P_i^e = \Pr[U_i^e \geq U_k^e ; \forall k \in \mathbf{R}] \quad (5)$$

where

$$\mathbf{R} = \{1, 2, 3, \dots, i, \dots, j\} \quad (6)$$

Define

$$\begin{aligned} \mathbf{R}' &= \{\forall k < i ; k \in \mathbf{R}\} \\ \mathbf{R}'' &= \{\forall k > i ; k \in \mathbf{R}\} \end{aligned} \quad (7)$$

Then,

$$P_i^e = \Pr[U_i^e \geq U_k^e ; \forall k \in \mathbf{R}'] \cdot \Pr[U_i^e \geq U_k^e ; \forall k \in \mathbf{R}''] \quad (8)$$

But, assuming completely myopic driver behavior: i.e., that the driver will enter the HOV lane at the first opportunity for which the decision to enter is better than the decision to enter the next available i/e point:

$$\Pr[U_i^e \geq U_k^e ; \forall k \in \mathbf{R}'] = \Pr[\Delta U_{i,i-1}^e \geq 0 \mid \Delta U_{i-1,i-2}^e \geq 0] \cdot \Pr[\Delta U_{i-1,i-2}^e \geq 0 \mid \Delta U_{i-2,i-3}^e \geq 0] \cdot \dots \quad (9)$$

$$\cdot \Pr[\Delta U_{3,2}^e \geq 0 \mid \Delta U_{2,1}^e \geq 0] \cdot \Pr[\Delta U_{2,1}^e \geq 0]$$

Or, since the $\Delta U_{k,k-1}^e$ are independent:

$$\Pr[U_i^e \geq U_k^e ; \forall k \in \mathbf{R}'] = \prod_{k=1}^{i-1} \Pr[\Delta U_{k+1,k}^e \geq 0] \quad (10)$$

Then,

$$P_i^e = \prod_{k=1}^{i-1} \Pr[\Delta U_{k+1,k}^e \geq 0] \cdot \Pr[U_i^e \geq U_k^e ; \forall k \in \mathbf{R}''] \quad (11)$$

Once again invoking the assumption of myopic behavior,

$$\Pr[U_i^e \geq U_k^e ; \forall k \in \mathbf{R}''] = \Pr[U_i^e \geq U_{i+1}^e] = 1 - \Pr[\Delta U_{i+1,i}^e \geq 0] \quad (12)$$

Then,

$$P_i^e = \left(1 - \Pr[\Delta U_{i+1,i}^e \geq 0]\right) \cdot \prod_{k=1}^{i-1} \Pr[\Delta U_{k+1,k}^e \geq 0] \quad (13)$$

But,

$$\Delta U_{k+1,k}^e \text{ is } N[(V_{k+1}^e - V_k^e), \hat{\sigma}_k^2]; \quad k = 1, \dots, j-1 \quad (14)$$

So,

$$\Pr[\Delta U_{k+1,k}^e \geq 0] = \Phi\left[\frac{(V_{k+1}^e - V_k^e)}{\hat{\sigma}_k}\right] \quad (15)$$

where $\Phi[\cdot]$ is the cumulative normal distribution function. Then

$$P_i^e = \left(1 - \Phi\left[\frac{(V_{i+1}^e - V_i^e)}{\hat{\sigma}_i}\right]\right) \cdot \prod_{k=1}^{i-1} \Phi\left[\frac{(V_{k+1}^e - V_k^e)}{\hat{\sigma}_k}\right] \quad (16)$$

The complete mathematical derivation is shown in Appendix B. Assuming that the V_k^e are a function only of travel time (or, of the value of time + toll), then estimation of P_i^e involves only

estimating the $\hat{\sigma}_k^2$ which, theoretically are simply the variances in travel time as computed, for example, from historical loop data for each section. As an alternative, field trajectory data together with travel time data drawn from loop detector data could be used in maximum likelihood estimation. As mentioned earlier, the same procedure can be used in “real time” as a reassessment process based on traffic dynamics simply by resetting the counter to the next ingress point available at the current time—computation time permitting, reassessment could be performed at each simulation step. Implementation in Paramics could be accomplished by a random draw from the computed probabilities P_i^e .

3.1.2 Preference to Exit HOV Lane at Ingress/Egress (i/e) j

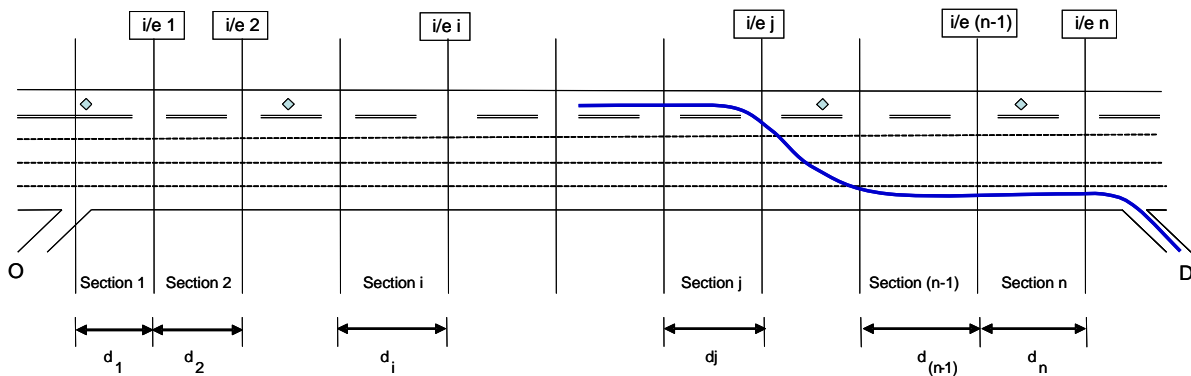


Figure 3-3. Preference for exiting HOV lane at Ingress/Egress (i/e) j

Consider next a driver’s choice (or preference) to exit the HOV facility at exit point (i/e) j, conditioned on the decision to enter the facility at entry point (i/e) i. Consistent with standard random utility assumptions, let the utility of this choice be denoted by:

$$U_j^x = \sum_{q=j+1}^n U_q^F + \sum_{l=i+1}^j U_l^{HOV} ; i < j \leq n; j = i+1, \dots, n \quad (17)$$

where U_j^x denotes the travel time utility of exiting the HOV lane at i/e point j (under the presumption of entering at i/e point i).

Assume $U_j^x = V_j^x + \xi_j^x$, where V_j^x denotes the disutility associated with the expected travel time using exit point j and ξ_j^x denotes the random delay associated with unknown traffic effects.

Assume ξ_j^x are multivariate normal distributed, i.e.,

$$U^x = MVN(V^x, \Sigma^x) \quad (18)$$

where Σ^x is the covariance matrix.

Assume that the covariance between any two alternatives is only in the links they share in common; i.e.,

$$\text{Cov}(U_k^x, U_j^x) = \text{Var}(\xi_{j+1}^F + \xi_{j+2}^F + \dots + \xi_n^F + \xi_{i+1}^{HOV} + \xi_{i+2}^{HOV} + \dots + \xi_k^{HOV}) = \sigma_{F_j H_k}^2 \quad (19)$$

Assume, for simplicity, that the mainline freeway variances are independent of the HOV lane variances, i.e.,

$$\begin{aligned} \sigma_{H_k F_j}^2 &= \text{Cov}(U_k^x, U_j^x) = \text{Var}(\xi_{i+1}^{HOV} + \xi_{i+2}^{HOV} + \dots + \xi_k^{HOV}) + \text{Var}(\xi_{j+1}^F + \xi_{j+2}^F + \dots + \xi_n^F); k = i+1, \dots, j; k \leq j \\ &= \sigma_{H_k}^2 + \sigma_{F_j}^2 \end{aligned} \quad (20)$$

Let P_{i+k}^x denote the probability that HOV lane exit $i+k$ will be preferred for the trip from O to D. Then

$$P_{i+k}^x = \Pr[U_{i+k}^x \geq U_{i+l}^x; \forall l \in \mathbf{R}] \quad (21)$$

where

$$\mathbf{R} = \{i+1, i+2, i+3, \dots, i+k, \dots, n\} \quad (22)$$

Define

$$\begin{aligned} \mathbf{R}' &= \{\forall l < i+k; l \in \mathbf{R}\} \\ \mathbf{R}'' &= \{\forall l > i+k; l \in \mathbf{R}\} \end{aligned} \quad (23)$$

Then,

$$P_{i+k}^x = \Pr[U_{i+k}^x \geq U_l^x; \forall l \in \mathbf{R}'] \cdot \Pr[U_{i+k}^x \geq U_l^x; \forall l \in \mathbf{R}''] \quad (24)$$

But, assuming completely myopic driver behavior: i.e., that the driver will exit the HOV lane at the first opportunity for which the decision to exit is better than the decision to exit the next available i/e point:

$$\begin{aligned} \Pr[U_{i+k}^x \geq U_l^x; \forall l \in \mathbf{R}'] &= \Pr[\Delta U_{i+k, i+k-1}^x \geq 0 \mid \Delta U_{i+k-1, i+k-2}^x \geq 0] \cdot \Pr[\Delta U_{i+k-1, i+k-2}^x \geq 0 \mid \Delta U_{i+k-2, i+k-3}^x \geq 0] \cdot \dots \\ &\quad \cdot \Pr[\Delta U_{i+3, i+2}^x \geq 0 \mid \Delta U_{i+2, i+1}^x \geq 0] \cdot \Pr[\Delta U_{i+2, i+1}^x \geq 0] \end{aligned} \quad (25)$$

Or, since the $\Delta U_{l, l-1}^x$ are independent:

$$\Pr[U_{i+k}^x \geq U_l^x; \forall l \in \mathbf{R}'] = \prod_{l=1}^{k-1} \Pr[\Delta U_{i+l+1, i+l}^x \geq 0] \quad (26)$$

Then

$$P_{i+k}^x = \prod_{l=1}^{k-1} \Pr[\Delta U_{i+l+1,i+l}^x \geq 0] \cdot \Pr[U_{i+k}^x \geq U_l^x ; \forall l \in \mathbf{R}^n] \quad (27)$$

Once again invoking the assumption of myopic behavior,

$$\Pr[U_{i+k}^x \geq U_l^x ; \forall l \in \mathbf{R}^n] = \Pr[U_{i+k}^x \geq U_{i+k+1}^x] = 1 - \Pr[\Delta U_{i+k+1}^x \geq 0] \quad (28)$$

Then,

$$P_{i+k}^x = \left(1 - \Pr[\Delta U_{i+k+1,i+k}^x \geq 0]\right) \cdot \prod_{l=1}^{k-1} \Pr[\Delta U_{i+l+1,i+l}^x \geq 0] \quad (29)$$

But,

$$\Delta U_{i+k+1,i+k}^x \text{ is } N\left[(V_{i+k+1}^x - V_{i+k}^x), \tilde{\sigma}_{i+k}^2\right]; k = 1, \dots, n-1 \quad (30)$$

So,

$$\Pr[\Delta U_{i+k+1,i+k}^x \geq 0] = \Phi\left[\frac{(V_{i+k+1}^x - V_{i+k}^x)}{\tilde{\sigma}_{i+k}}\right] \quad (31)$$

where $\Phi[\cdot]$ is the cumulative normal distribution function. Then

$$P_{i+k}^x = \left(1 - \Phi\left[\frac{(V_{i+k+1}^x - V_{i+k}^x)}{\tilde{\sigma}_{i+k}}\right]\right) \cdot \prod_{l=1}^{k-1} \Phi\left[\frac{(V_{i+l+1}^x - V_{i+l}^x)}{\tilde{\sigma}_{i+l}}\right] \quad (32)$$

The complete mathematical derivation is shown in Appendix C. As in the ingress case, assuming that the V_{i+k}^x are a function only of travel time (or, of the value of time + toll), then estimation of P_{i+k}^x involves only estimating the $\tilde{\sigma}_{i+k}^2$ which, theoretically are simply the variances in travel time as computed, for example, from historical loop data for each section. As an alternative, field trajectory data together with travel time data drawn from loop detector data could be used in maximum likelihood estimation. As in the ingress case, the same procedure can be used in “real time” as a reassessment process based on traffic dynamics simply by resetting the k counter to the next egress point available at the current time—computation time permitting, reassessment could be performed at each simulation step. Implementation in Paramics could be accomplished by a random draw from the computed probabilities P_{i+k}^x .

3.2 Acting on Preferences

P_i^e and P_{i+k}^x specify only the preferences of a particular HOV-eligible driver for a set of ingress/egress points for the trip from O to D. In order to act on these preferences, there must be sufficient opportunity to make the necessary traffic maneuvers (i.e., lane changes) to actually select any particular preferred ingress/egress point. Let \widehat{P}_i^e denote the probability of actually selecting HOV entry point i/e i . Then \widehat{P}_i^e is equal to the probability that HOV entry point i/e i is preferred (P_i^e) times the probability that there is sufficient opportunity to negotiate across lanes of traffic to make that choice, given that it is the preferred entry point. Assuming independence of these two events:

$$\widehat{P}_i^e = P_i^e \cdot P_i^w(\bar{d}_i, n_l, \nu | \text{entry point } i \text{ is preferred}) \quad (33)$$

where $P_i^w(\bar{d}_i, n_l, \nu | \text{entry point } i \text{ is preferred})$ is the probability that the preferred HOV entry point i/e i can be reached in time to enter, given the current distance \bar{d}_i between the HOV-eligible vehicle and HOV entry point i/e i , the number of lanes n_l that need to be traversed, and the intensity of traffic ν on the mainline freeway.

Using similar arguments, we define \widehat{P}_{i+k}^x as the probability of actually selecting HOV exit point i/e $i+k$, and specify it as

$$\widehat{P}_{i+k}^x = P_{i+k}^x \cdot P_{i+k}^w(\bar{\bar{d}}_{i+k}, n_l, \nu | \text{exit point } i \text{ is preferred}) \quad (34)$$

where $\bar{\bar{d}}_{i+k}$ is the distance from HOV exit point i/e $i+k$ to the exit ramp D, and n_l, ν are as previously defined.

3.3 Lane-changing Behavior

Probabilities \widehat{P}_i^e and \widehat{P}_{i+k}^x are inherently tied to presumed lane-changing behavior. In what follows, we first consider the nature of gaps in a traffic stream of a single lane as viewed from a fixed observer. We then extract findings to the case in which the viewpoint is that of the HOV-lane bound vehicle.

Consider a population of drivers, each of whom has a gap acceptance function, $\alpha(G)$, which defines the probability that the driver can/will switch lanes when faced with a gap G in the traffic in the adjacent lane. For simplicity, suppose further that

$$\alpha(G) = H(G - T) \quad (35)$$

where $H(\cdot)$ is the Heaviside function and T is a random variable with probability density $\mu(T)$.

Then the population gap acceptance function is

$$\alpha_p(G) = \int_0^\infty H(G-t) \cdot \mu(t) dt = \int_0^G \mu(t) dt \tag{36}$$

The complete mathematical derivation and implementation of the lane changing model are whond ? in Appendix D.

3.4 Extracting Results to the Viewpoint of the HOV-lane Bound Vehicle

Consider the situation at some time t_0 ; assume steady state conditions exist in which the average speeds in each lane of traffic are relatively constant. Denote the speed of traffic in the current lane of the HOV-bound vehicle by v_0 and the speed of traffic in the lane adjacent to the HOV-bound vehicle by v_w , as shown below:

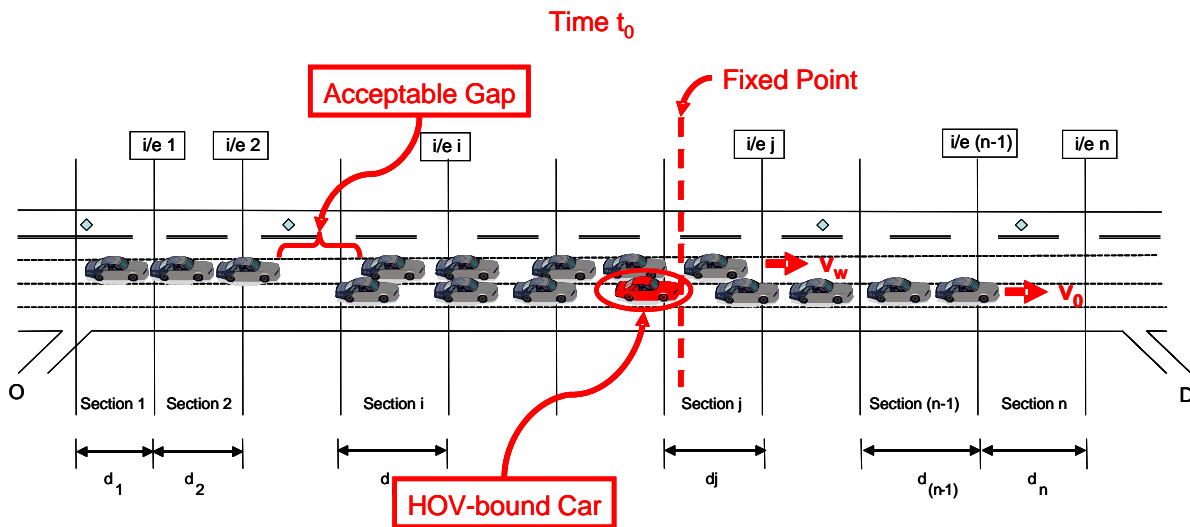


Figure 3-4. Acceptable Gap at time $t = t_0$

Consider next the situation at time $t_0 + t^*$, where t^* is drawn from the distribution

$$\Omega(t) = e^{-t/\nu} \delta(t) + e^{-T/\nu} \sum_{n=1}^\infty \frac{(-1)^n}{(n-1)! \nu^n} \left\{ e^{-nT/\nu} (1-nT)^{(n-1)} H(1-nT) - e^{-(n-1)T/\nu} [t-(n-1)T]^{(n-1)} H[t-(n-1)T] \right\} \tag{37}$$

Note that t^* represents the (random) time lapse from t_0 until an acceptable lane-changing gap in the traffic in the neighboring lane passes the fixed point, as shown in the figure below:

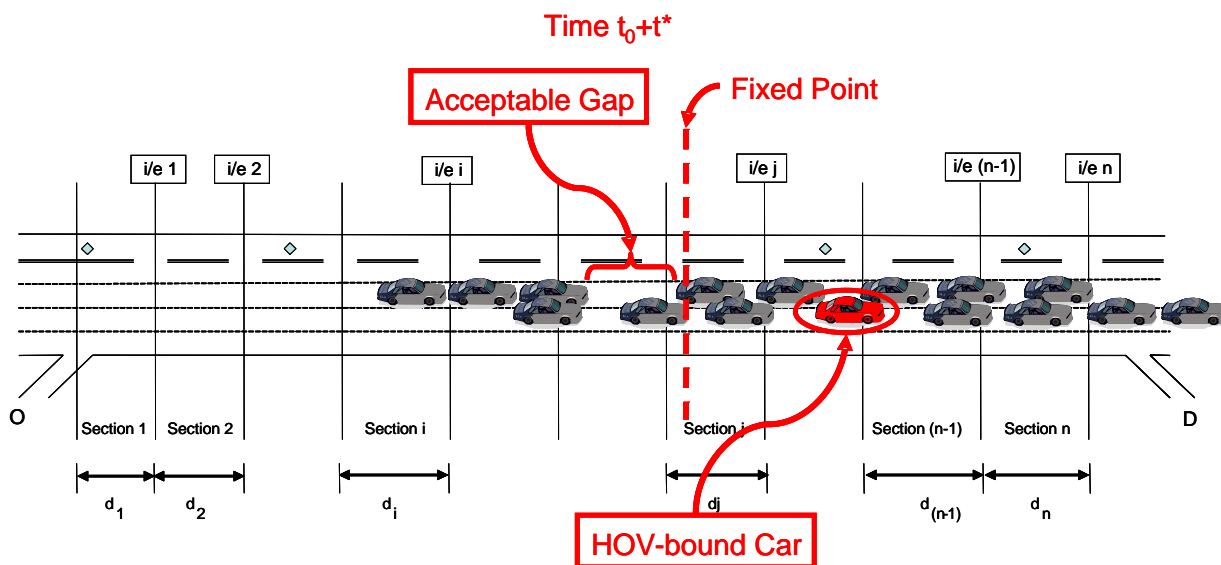


Figure 3-5. Acceptable Gap at time $t = t_0 + t^*$

For the case in which v_w , the speed of traffic in the lane adjacent to the HOV-bound vehicle is greater than v_0 , the speed of traffic in the current lane of the HOV-bound vehicle, the “acceptable gap” will catch up to the HOV-bound vehicle at time $t_0 + t_g$, as shown below:

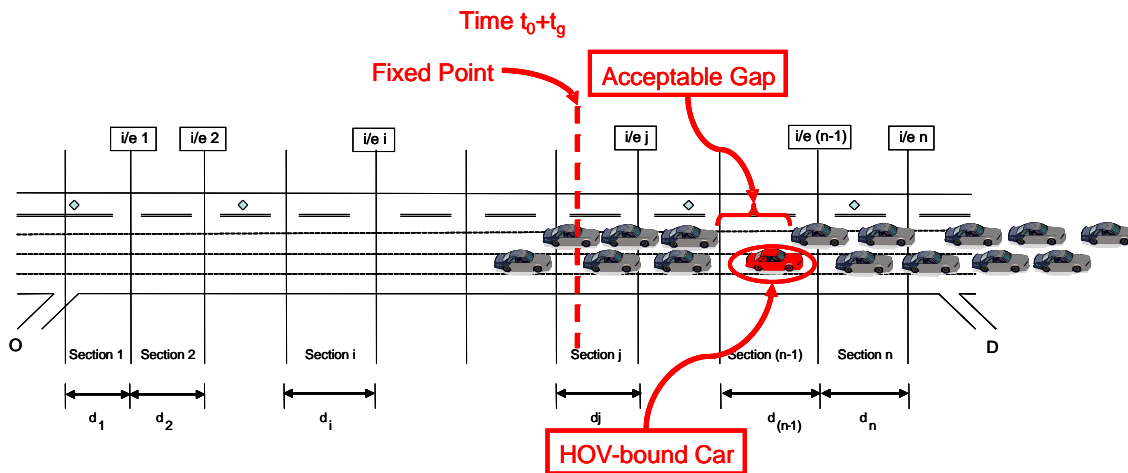


Figure 3-6. Acceptable Gap at time $t = t_0 + t_g$

where

$$t_g = \frac{v_w t^*}{(v_w - v_0)} \tag{38}$$

Then, the distance traveled by the HOV-bound vehicle at time $t_0 + t_g$, as measured from the fixed point is simply

$$d_g = \frac{v_w t^*}{(v_w - v_o)} \cdot v_o \quad (39)$$

Similarly, assuming spatial symmetry for the gap arrival pattern, in the case in which v_w , the speed of traffic in the lane adjacent to the HOV-bound vehicle is less than v_o , the speed of traffic in the current lane of the HOV-bound vehicle, the HOV-bound vehicle will catch up to the “acceptable gap” at time $t_0 + t_g$, where

$$t_g = \frac{v_o t^*}{(v_o - v_w)} \quad (40)$$

and the distance traveled by the HOV-bound vehicle at time $t_0 + t_g$, as measured from the fixed point is simply

$$d_g = \frac{v_o t^*}{(v_o - v_w)} \cdot v_o \quad (41)$$

In general, then, (39) and (41) imply

$$d_g = \frac{v_w t^*}{|v_w - v_o|} \cdot v_o \quad (42)$$

3.5 Probability that Preferred Entry Point i/e i can be Accessed

Recall:

$$\hat{P}_i^e = P_i^e \cdot P_i^w(\bar{d}_i, n_i, \nu | \text{entry point } i \text{ is preferred})$$

where $\hat{P}_i^e = P_i^e \cdot P_i^w(\bar{d}_i, n_i, \nu | \text{entry point } i \text{ is preferred})$ is the probability that HOV entry point i/e i can be reached in time to enter, given: it is preferred, the current distance \bar{d}_i between the HOV-eligible vehicle and HOV entry point i/e i , the number of lanes n_i that need to be traversed, and the intensity of traffic ν on the mainline freeway.

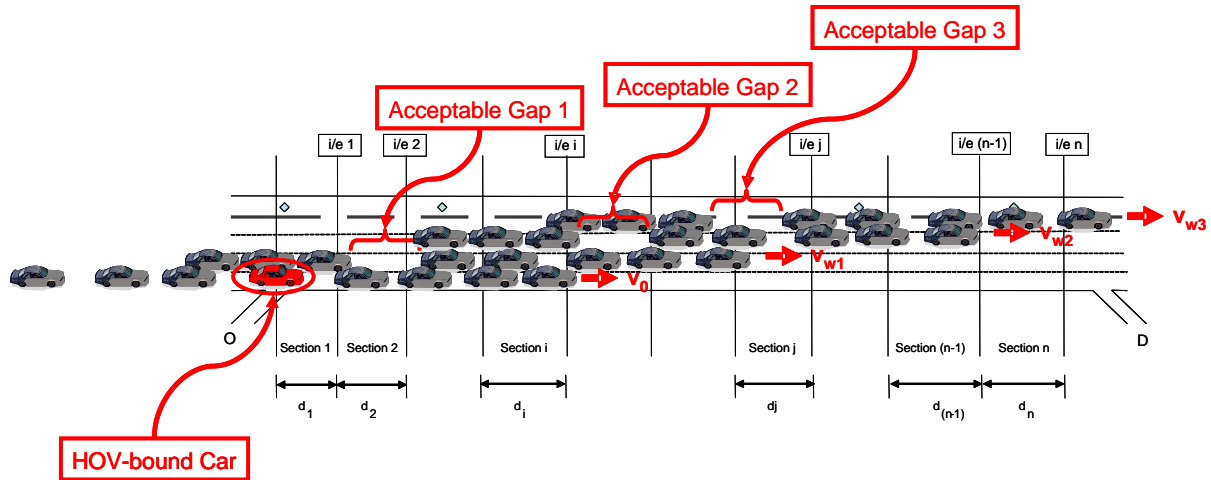


Figure 3-7. State of traffic system relative to preferred Ingress/Egress point $i/e\ i$

Consider a freeway with n_l lanes. Then,

$$P_i^w(\bar{d}_i, n_l, v) = \Pr(d_{g1} + d_{g2} + \dots + d_{g(n_l-1)} \leq \bar{d}_i) \quad (43)$$

where the d_{gk} are obvious generalizations of the d_g defined above. That is,

$$d_{gk} = \frac{v_k t_k^*}{|v_k - v_{k-1}|} \cdot v_k ; k = 1, 2, \dots, n_l - 1 \quad (44)$$

where

d_{gk} = the distance traveled from the point upon entering lane $k-1$ before an acceptable gap appears in lane k to move into lane k (one lane closer to the HOV lane).

v_k = the average speed of traffic in lane k ; i.e., v_{wk}

v_{k-1} = the average speed of traffic in lane $k-1$; i.e., the speed of traffic in the lane from which the HOV-bound vehicle is switching.

t_k^* = an estimate of the (random) time lapse from the time that the HOV-bound vehicle first enters lane $k-1$ (i.e., equivalent to t_0 in the above expressions) until an acceptable lane-changing gap in the traffic in the neighboring lane k passes the fixed point at which the HOV-bound vehicle entered lane $k-1$.

Then,

$$\begin{aligned}
 P_i^w(\bar{d}_i, n_i, v) &= \Pr(d_{g1} + d_{g2} + \dots + d_{g(n_i-1)} \leq \bar{d}_i) = \Pr\left(\sum_{k=1}^{n_i-1} d_{gk} \leq \bar{d}_i\right) \\
 &= \Pr\left(\sum_{k=1}^{n_i-1} \frac{v_k t_k^*}{|v_k - v_{k-1}|} \cdot v_k \leq \bar{d}_i\right)
 \end{aligned}
 \tag{45}$$

The comparison of

$$\sum_{k=1}^{n_i-1} \frac{v_k t_k^*}{|v_k - v_{k-1}|} \cdot v_k \leq \bar{d}_i$$

for a four-lane freeway (plus an HOV lane) with \bar{d}_i measured from the HOV-eligible vehicle's entry point at time t_0 is shown in the figure below:

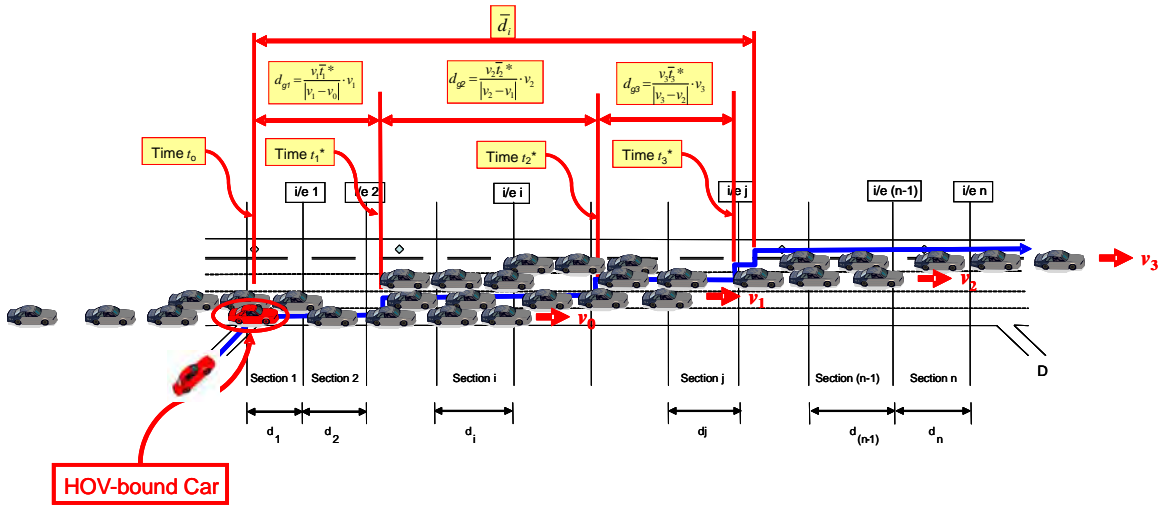


Figure 3-8. Four-lane freeway example of Acceptable Gap conditions relative to successfully accessing preferred Ingress/Egress point $i/e i$

Finding an exact expression for $\Pr(d_{g1} + d_{g2} + \dots + d_{g(n-1)} \leq \bar{d}_i)$ is probably not possible, but we can offer a rough approximation in the form of

$$\Pr(d_{g1} + d_{g2} + \dots + d_{g(n-1)} \leq \bar{d}_i) \rightarrow H\left[\bar{d}_i - (d_{g1} + d_{g2} + \dots + d_{g(n-1)})\right]
 \tag{46}$$

where $H(\cdot)$ is the Heaviside function. For example, application of Eq.(96) to the situation depicted in the figure above would lead to

$$\Pr(d_{g1} + d_{g2} + d_{g3} \leq \bar{d}_i) \rightarrow H\left[\bar{d}_i - (d_{g1} + d_{g2} + d_{g3})\right] = H[> 0] = 1
 \tag{47}$$

Whereas, for the situation shown in the figure below:

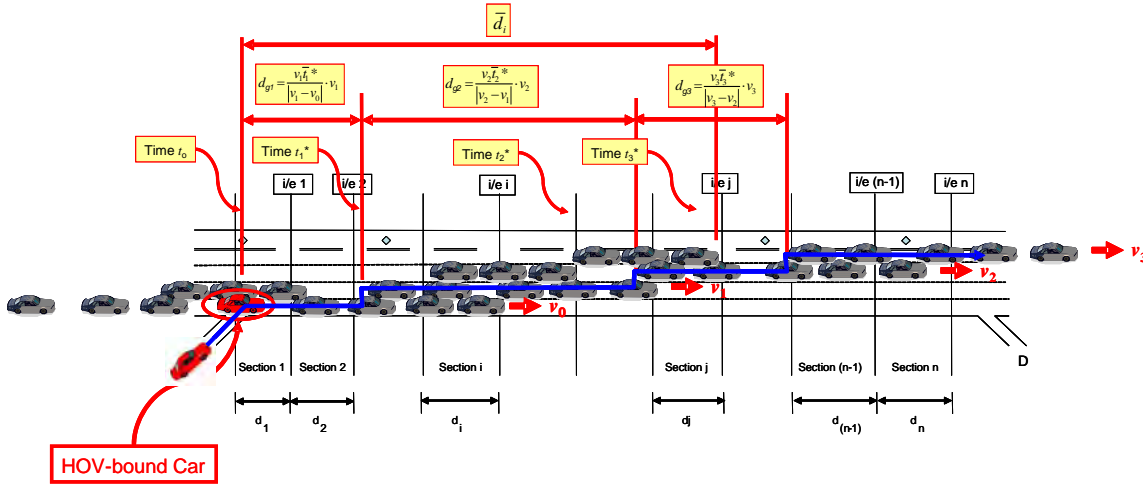


Figure 3-9. Four-lane freeway example of Acceptable Gap conditions relative to unsuccessfully accessing preferred Ingress/Egress point $i/e i$

$$\Pr(d_{g1} + d_{g2} + d_{g3} \leq \bar{d}_i) \rightarrow H[\bar{d}_i - (d_{g1} + d_{g2} + d_{g3})] = H[<0] = 0 \quad (48)$$

In this, there are at least two plausible ways to estimate the quantity $(d_{g1} + d_{g2} + \dots + d_{g(n-1)})$:

1. through a random draw of the appropriate density function $\Omega(t)$ for each lane, resulting in values for the various t_k^* for the k lanes needed to cross, from which the d_{gk} can be computed.
2. by replacing each t_k^* with its expected value \bar{t}_k as computed from the expression derived above; i.e., $\bar{t} = \nu \left[\exp\left(\frac{T}{\nu}\right) - 1 - \frac{T}{\nu} \right]$. Then calculating d_{gk} as

$$\begin{aligned} d_{gk} &= \frac{\nu_k \bar{t}_k^*}{|\nu_k - \nu_{k-1}|} \cdot \nu_k ; k = 1, 2, \dots, n_l - 1 \\ &= \frac{\nu_k \nu_k \left[\exp\left(\frac{T}{\nu_k}\right) - 1 - \frac{T}{\nu_k} \right]}{|\nu_k - \nu_{k-1}|} \cdot \nu_k ; k = 1, 2, \dots, n_l - 1 \end{aligned} \quad (49)$$

where

T = Acceptable gap (sec)

ν_k = traffic intensity, i.e., λ_k^{-1} (sec/veh), in lane k

3.5.1 Estimating Acceptable Gap, T

We assume that a lane-changing vehicle requires a spatial gap, T_S , in the adjacent lane of traffic that is at least equal to a car length, L_{car} ; i.e.,

$$T_S = a \cdot L_{car} \quad ; a \geq 1$$

Let ρ_k (veh/ft) denote the local density of traffic in lane k that, on average, would permit a lane change from lane $(k-1)$. Then

$$T_S = \rho_k^{-1}$$

Then, from continuity, the corresponding flow rate that would support a lane-change maneuver at lane k speed of v_k is $\hat{\lambda}_k = \rho_k v_k$ (veh/sec). Or, equivalently, the headway between vehicles would have to be $T = \hat{\lambda}_k^{-1}$. Under these conditions, the local spacing between vehicles in lane k is simply ρ_k^{-1} . Or,

$$\rho_k^{-1} = \hat{\lambda}_k^{-1} v_k \Rightarrow \hat{\lambda}_k^{-1} = \rho_k^{-1} v_k^{-1}$$

Or, substituting $T_S = \rho_k^{-1}$ and $T = \hat{\lambda}_k^{-1}$,

$$T = T_S v_k = a L_{car} v_k^{-1}$$

Then,

$$\begin{aligned} d_{gk} &= \frac{v_k v_k \left[\exp\left(\frac{T}{v_k}\right) - 1 - \frac{T}{v_k} \right]}{|v_k - v_{k-1}|} \cdot v_k \\ &= \frac{v_k v_k \left[\exp\left(\frac{a L_{car}}{v_k v_k}\right) - 1 - \frac{a L_{car}}{v_k v_k} \right]}{|v_k - v_{k-1}|} \cdot v_k \quad ; k = 1, 2, \dots, n_l - 1 \quad ; a \geq 1 \end{aligned}$$

3.5.2 Additional Speed Adjustment Consideration

We assume that the vehicle in lane $(k-1)$ can decrease (but not increase) its speed by some fraction, $b \leq 1$, of its current speed in order to maximize $|v_k - v_{k-1}|$, i.e., in the above expression we replace $|v_k - v_{k-1}|$ with $\max(|v_k - v_{k-1}|, |v_k - b v_{k-1}|)$, resulting in

$$d_{gk} = \frac{v_k v_k \left[\exp\left(\frac{aL_{car}}{v_k v_k}\right) - 1 - \frac{aL_{car}}{v_k v_k} \right]}{\max(|v_k - v_{k-1}|, |v_k - bv_{k-1}|)} \cdot v_k ; k = 1, 2, \dots, n_l - 1 ; a \geq 1 ; b \leq 1 \quad (50)$$

Sample plots of d_{gk} for sets of “reasonable” parameter values are displayed below:

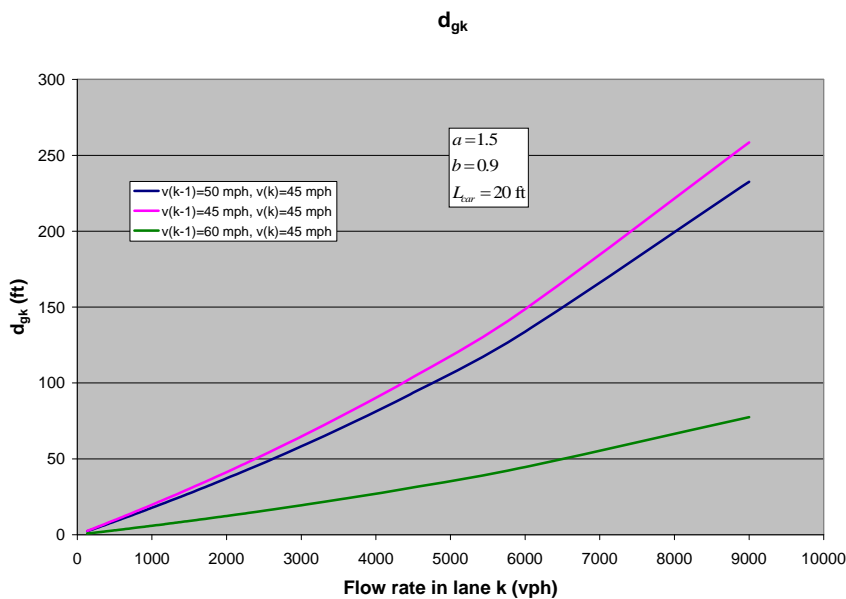


Figure 3-10. Plot of d_{gk} for the set of “reasonable” parameter values: $a = 1.5$

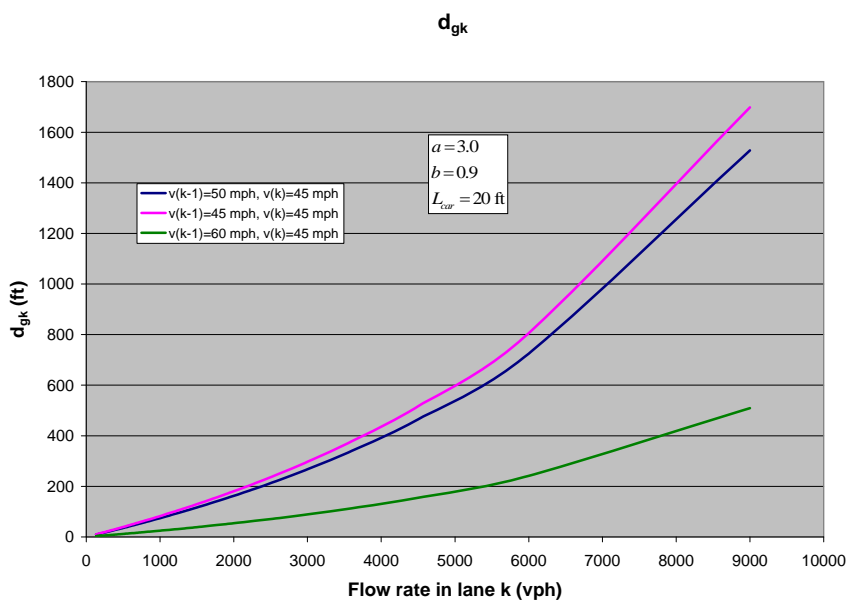


Figure 3-11. Plot of d_{gk} for the set of “reasonable” parameter values: $a = 3.0$

Then, finally,

$$\begin{aligned} \widehat{P}_i^e &= P_i^e \cdot H \left[\bar{d}_i - (d_{g1} + d_{g2} + \dots + d_{g(n-1)}) \right] \\ &= \left(1 - \Phi \left[\frac{(V_{i+1}^e - V_i^e)}{(\sigma_{F_{i+1}}^2 - \sigma_{F_i}^2) + (\sigma_{H_i}^2 - \sigma_{H_{i+1}}^2)} \right] \right) \cdot \prod_{k=1}^{i-1} \Phi \left[\frac{(V_{k+1}^e - V_k^e)}{(\sigma_{F_{k+1}}^2 - \sigma_{F_k}^2) + (\sigma_{H_k}^2 - \sigma_{H_{k+1}}^2)} \right] \cdot H \left[\bar{d}_i - (d_{g1} + d_{g2} + \dots + d_{g(n-1)}) \right] \end{aligned} \quad (51)$$

The procedure would be to compute \widehat{P}_i^e for each HOV vehicle based on a random draw from the distribution of P_i^e to determine the preferred entry point, and then determine if it is feasible for the vehicle to act on that preference by computing $H \left[\bar{d}_i - (d_{g1} + d_{g2} + \dots + d_{g(n-1)}) \right]$. If entry point i is preferred and $H[\cdot] = 1$, then assign the vehicle to a route that accesses the HOV lane at i . If entry point i is preferred and $H[\cdot] = 0$, then reject i as the access point, and repeat the random draw until $H[\cdot] = 1$ for a preferred access point.

4. Paramics Buffer-separated HOV Access API Development

4.1 Paramics Buffer-separated HOV Access API Schematic

A schematic of the buffer-separated HOV access plugin development based on the preceding behavioral model is displayed in Figure 4-1. This plugin can control one HOV route given multiple origin and destination zones, and multiple HOV vehicle types. The route is divided into several subsections by taking ingress/egress points as boundaries; each subsection may contain more than two Paramics nodes. The modeling procedure can be divided into three stages:

1. Traffic information update
2. Choice probability of entering HOV lane update
3. Choice probability of leaving HOV lane update

In the traffic information update stage, three variables: 1) section travel time, 2) lane density and 3) lane speed per section, are re-calculated based on most recent data obtained during the preceding time interval. Since the behavioral model assumes that the HOV drivers are fully knowledgeable about the traffic conditions, the traffic information obtained most recently is applied as the estimate of the historical travel time that the HOV drivers experienced as well as the perceived traffic condition at present. Furthermore, the choice/preference probability of accessing the HOV facility is computed for a HOV-eligible vehicle when it first enters the freeway section. The choice/preference probability of leaving HOV lane is computed after the HOV-eligible vehicle enters the HOV lane.

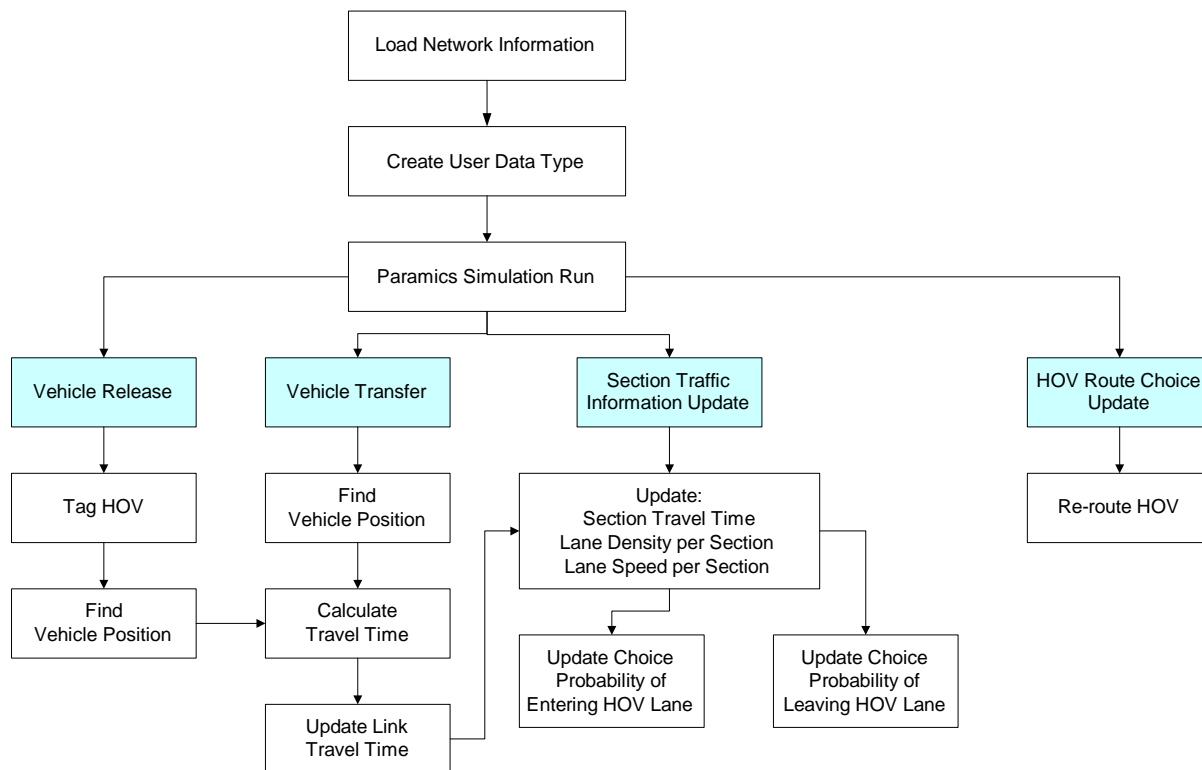


Figure 4-1. Paramics buffer-separated HOV access API Schematic

4.2 Sample Network

In order to test the “reasonableness” of the behavioral model, a sample network (as shown in Figures 4-2 and 4-3) was designed and coded in Paramics, as described below:

- Number of Lanes:
 - HOV lane: 1
 - Mainline: 4
- Number of Ramps:
 - On-ramp: 1 (2 lanes including one HOV lane)
 - Off-ramp: 1 (1 lane)
- Number of Zones:
 - Original: 2
 - Destination: 2
- Number of Ingress/egress points: 5 ingress and 5 egress points
- Distance between ingress/egress point: 2 km. ($\approx 1\frac{1}{4}$ mi.)
- Corridor length: ≈ 8 mile

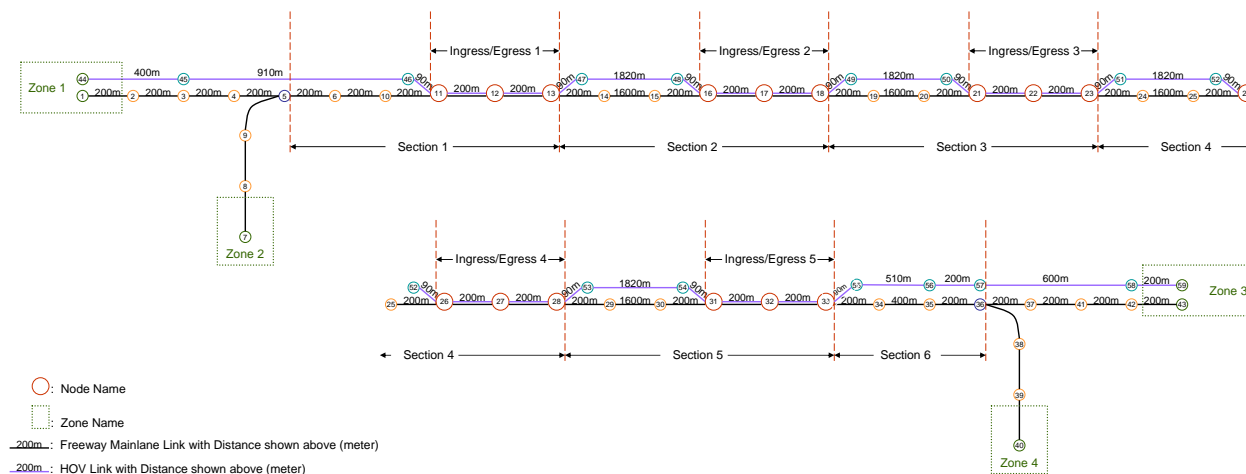


Figure 4-2. Paramics network skeleton

The link coding of this network in Paramics, as well as the distances between ingress/egress points, were designed to be compatible with Caltrans’ recommendations on minimum weave distances for buffer-separated HOV facilities (Caltrans, 2003), as shown in Figure 4-3.

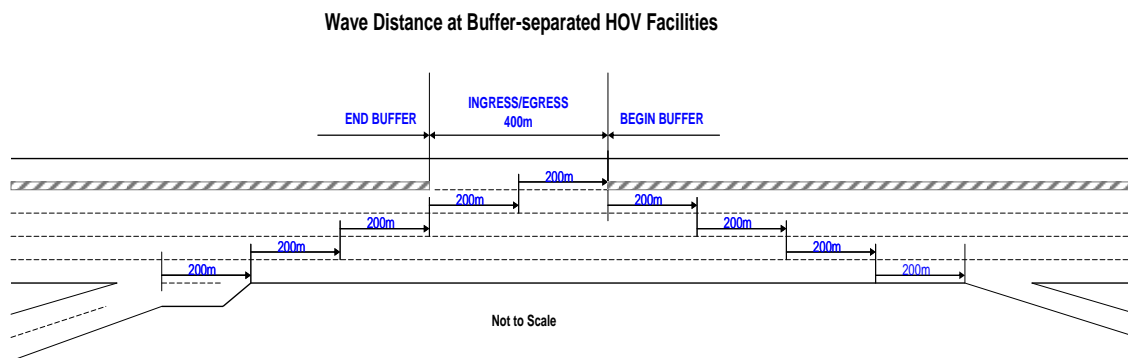


Figure 4-3. Weave distance at buffer-separated HOV facilities (Caltrans, 2003)

4.3 Implementation of Ingress Preference Model and Traffic Model

As described in section 3.5.2, for the proposed HOV driver behavioral model, the procedure of computing \hat{P}_i^e involves a sub-model for determining preferred HOV ingress/egress points (i.e., an ingress/egress choice/preference model) and a sub-model for determining the feasibilities of those ingress/egress points (i.e., a traffic-based lane changing model). The implementations of the choice/preference model (for both ingress and egress selection) and the traffic model are discussed below.

4.3.1 Ingress Preference Model

Recall:

$$\begin{aligned}
\widehat{P}_i^e &= P_i^e \cdot H \left[\bar{d}_i - (d_{g1} + d_{g2} + \dots + d_{g(n-1)}) \right] \\
&= \left(1 - \Phi \left[\frac{(V_{i+1}^e - V_i^e)}{\bar{\sigma}_i} \right] \right) \cdot \prod_{k=1}^{i-1} \Phi \left[\frac{(V_{k+1}^e - V_k^e)}{\bar{\sigma}_k} \right] \cdot H \left[\bar{d}_i - (d_{g1} + d_{g2} + \dots + d_{g(n-1)}) \right] \\
&= \left\{ \left(1 - \Phi \left[\frac{(V_{i+1}^e - V_i^e)}{(\sigma_{F_{i+1}}^2 - \sigma_{F_i}^2) + (\sigma_{H_i}^2 - \sigma_{H_{i+1}}^2)} \right] \right) \cdot \prod_{k=1}^{i-1} \Phi \left[\frac{(V_{k+1}^e - V_k^e)}{(\sigma_{F_{k+1}}^2 - \sigma_{F_k}^2) + (\sigma_{H_k}^2 - \sigma_{H_{k+1}}^2)} \right] \right\} \cdot H \left[\bar{d}_i - (d_{g1} + d_{g2} + \dots + d_{g(n-1)}) \right]
\end{aligned} \tag{51}$$

To find P_i^e :

Let $V_{\zeta_i^F}^e$ denote the travel time on freeway link i

$V_{\zeta_i^H}^e$ denote the travel time on HOV link i

$$V_{i+1}^e - V_i^e \Rightarrow$$

$$V_{i+1}^e \approx V_{\zeta_1^F}^e + V_{\zeta_2^F}^e + \dots + V_{\zeta_{i-1}^F}^e + V_{\zeta_i^F}^e + V_{\zeta_{i+1}^F}^e + V_{\zeta_{i+2}^H}^e + V_{\zeta_{i+3}^H}^e + \dots + V_{\zeta_j^H}^e$$

$$V_i^e \approx V_{\zeta_1^F}^e + V_{\zeta_2^F}^e + \dots + V_{\zeta_{i-1}^F}^e + V_{\zeta_i^F}^e + V_{\zeta_{i+1}^H}^e + V_{\zeta_{i+2}^H}^e + V_{\zeta_{i+3}^H}^e + \dots + V_{\zeta_j^H}^e$$

$$\therefore V_{i+1}^e - V_i^e \approx \left(V_{\zeta_{i+1}^F}^e - V_{\zeta_{i+1}^H}^e \right)$$

Let $\sigma_{\zeta_i^F}^2$ denote the variance of travel time on freeway link i

$\sigma_{\zeta_i^H}^2$ denote the variance of travel time on HOV link i

$$\sigma_{F_{i+1}}^2 - \sigma_{F_i}^2 \Rightarrow$$

$$\sigma_{F_{i+1}}^2 \approx \text{Var} \left(\zeta_1^F + \zeta_2^F + \dots + \zeta_i^F + \zeta_{i+1}^F \right)$$

$$= \text{Var} \left(\zeta_1^F \right) + \text{Var} \left(\zeta_2^F \right) + \dots + \dots + \text{Var} \left(\zeta_i^F \right) + \text{Var} \left(\zeta_{i+1}^F \right)$$

$$\sigma_{F_i}^2 \approx \text{Var} \left(\zeta_1^F + \zeta_2^F + \dots + \zeta_i^F \right)$$

$$= \text{Var} \left(\zeta_1^F \right) + \text{Var} \left(\zeta_2^F \right) + \dots + \dots + \text{Var} \left(\zeta_i^F \right)$$

$$\therefore \sigma_{F_{i+1}}^2 - \sigma_{F_i}^2 \approx \text{Var} \left(\zeta_{i+1}^F \right) = \sigma_{\zeta_{i+1}^F}^2$$

Similarly,

$$\begin{aligned}
\sigma_{H_i}^2 - \sigma_{H_{i+1}}^2 &\Rightarrow \\
\sigma_{H_i}^2 &\approx \text{Var}\left(\xi_{i+1}^{HOV} + \xi_{i+2}^{HOV} + \dots + \xi_j^{HOV}\right) \\
&= \text{Var}\left(\xi_{i+1}^{HOV}\right) + \text{Var}\left(\xi_{i+2}^{HOV}\right) + \text{Var}\left(\xi_{i+3}^{HOV}\right) + \dots + \text{Var}\left(\xi_j^{HOV}\right) \\
\sigma_{H_{i+1}}^2 &\approx \text{Var}\left(\xi_{i+2}^{HOV} + \dots + \xi_j^{HOV}\right) \\
&= \text{Var}\left(\xi_{i+2}^{HOV}\right) + \text{Var}\left(\xi_{i+3}^{HOV}\right) + \dots + \text{Var}\left(\xi_j^{HOV}\right) \\
\therefore \sigma_{H_i}^2 - \sigma_{H_{i+1}}^2 &\approx \text{Var}\left(\xi_{i+1}^{HOV}\right) = \sigma_{\xi_{i+1}^{HOV}}^2 \\
\therefore \frac{(V_{i+1}^e - V_i^e)}{\hat{\sigma}_i} &\approx \frac{(V_{i+1}^e - V_i^e)}{(\sigma_{F_{i+1}}^2 - \sigma_{F_i}^2) + (\sigma_{H_i}^2 - \sigma_{H_{i+1}}^2)} = \frac{V_{\xi_{i+1}^{HF}}^e - V_{\xi_{i+1}^{HV}}^e}{\sigma_{\xi_{i+1}^{HF}}^2 + \sigma_{\xi_{i+1}^{HOV}}^2} \\
\Rightarrow \frac{(V_{i+1}^e - V_i^e)}{\hat{\sigma}_i} &= \alpha \cdot \frac{V_{\xi_{i+1}^{HF}}^e - V_{\xi_{i+1}^{HV}}^e}{\sigma_{\xi_{i+1}^{HF}}^2 + \sigma_{\xi_{i+1}^{HOV}}^2} \quad \alpha < 0
\end{aligned}$$

where α is a scale parameter that specifies the relationship between travel time and utility to enter/exit HOV lane.

Substituting into Equation (51), we get:

$$\begin{aligned}
\hat{P}_i^e &= P_i^e \cdot H\left[\bar{d}_i - (d_{g1} + d_{g2} + \dots + d_{g(n-1)})\right] \\
&= \left(1 - \Phi\left[\frac{(V_{i+1}^e - V_i^e)}{\hat{\sigma}_i}\right]\right) \cdot \prod_{k=1}^{i-1} \Phi\left[\frac{(V_{k+1}^e - V_k^e)}{\hat{\sigma}_k}\right] \cdot H\left[\bar{d}_i - (d_{g1} + d_{g2} + \dots + d_{g(n-1)})\right] \\
&= \left\{ \left(1 - \Phi\left[\alpha \cdot \frac{(V_{i+1}^e - V_i^e)}{(\sigma_{F_{i+1}}^2 - \sigma_{F_i}^2) + (\sigma_{H_i}^2 - \sigma_{H_{i+1}}^2)}\right]\right) \cdot \prod_{k=1}^{i-1} \Phi\left[\alpha \cdot \frac{(V_{k+1}^e - V_k^e)}{(\sigma_{F_{k+1}}^2 - \sigma_{F_k}^2) + (\sigma_{H_k}^2 - \sigma_{H_{k+1}}^2)}\right] \right\} \cdot H\left[\bar{d}_i - (d_{g1} + d_{g2} + \dots + d_{g(n-1)})\right] \\
&= \left\{ \left(1 - \Phi\left[\alpha \cdot \frac{V_{\xi_{i+1}^{HF}}^e - V_{\xi_{i+1}^{HV}}^e}{\sigma_{\xi_{i+1}^{HF}}^2 + \sigma_{\xi_{i+1}^{HOV}}^2}\right]\right) \cdot \prod_{k=1}^{i-1} \Phi\left[\alpha \cdot \frac{V_{\xi_{k+1}^{HF}}^e - V_{\xi_{k+1}^{HV}}^e}{\sigma_{\xi_{k+1}^{HF}}^2 + \sigma_{\xi_{k+1}^{HOV}}^2}\right] \right\} \cdot H\left[\bar{d}_i - (d_{g1} + d_{g2} + \dots + d_{g(n-1)})\right]
\end{aligned}$$

It is assumed that the P_i^e is updated at a regular time interval (e.g. every 30 second). In the Paramics plugin, there is a three-step process to use P_i^e to determine the preferred ingress point for each HOV-eligible vehicle:

- (1) Update four parameters, $V_{\xi_{i+1}^{HF}}^e$, $V_{\xi_{i+1}^{HV}}^e$, $\sigma_{\xi_{i+1}^{HF}}^2$, and $\sigma_{\xi_{i+1}^{HOV}}^2$ every interval;
- (2) Compute P_i^e using the above formula;
- (3) Determine the preferred ingress point from a random draw based on the distribution of P_i^e .

It is noted that the updates of P_i^e and the four parameters can be executed at different times.

Therefore, for the event $\bar{d}_i \geq (d_{g1} + d_{g2} + \dots + d_{g(n-1)})$, we get:

$$P_i^e = \left(1 - \Phi \left[\alpha \cdot \frac{V_{\xi_{i+1}}^e - V_{\xi_{i+1}}^e}{\sigma_{\xi_{i+1}}^2 + \sigma_{\xi_{i+1}}^{eHOV}} \right] \right) \cdot \prod_{k=1}^{i-1} \Phi \left[\alpha \cdot \frac{V_{\xi_{k+1}}^e - V_{\xi_{k+1}}^e}{\sigma_{\xi_{k+1}}^2 + \sigma_{\xi_{k+1}}^{eHOV}} \right] \quad (52)$$

And, the values for P_i^e expand to:

$$P_1^e = \left[1 - \Phi \left(\alpha \cdot \frac{V_{\xi_2}^e - V_{\xi_2}^e}{\sigma_{\xi_2}^2 + \sigma_{\xi_2}^{eHOV}} \right) \right]$$

$$\begin{aligned} P_2^e &= \left(1 - \Phi \left[\alpha \cdot \frac{V_{\xi_3}^e - V_{\xi_3}^e}{\sigma_{\xi_3}^2 + \sigma_{\xi_3}^{eHOV}} \right] \right) \cdot \prod_{k=1}^1 \Phi \left[\alpha \cdot \frac{V_{\xi_{k+1}}^e - V_{\xi_{k+1}}^e}{\sigma_{\xi_{k+1}}^2 + \sigma_{\xi_{k+1}}^{eHOV}} \right] \\ &= \left[1 - \Phi \left(\alpha \cdot \frac{V_{\xi_3}^e - V_{\xi_3}^e}{\sigma_{\xi_3}^2 + \sigma_{\xi_3}^{eHOV}} \right) \right] \cdot \Phi \left(\alpha \cdot \frac{V_{\xi_2}^e - V_{\xi_2}^e}{\sigma_{\xi_2}^2 + \sigma_{\xi_2}^{eHOV}} \right) \end{aligned}$$

$$\begin{aligned} P_3^e &= \left(1 - \Phi \left[\alpha \cdot \frac{V_{\xi_4}^e - V_{\xi_4}^e}{\sigma_{\xi_4}^2 + \sigma_{\xi_4}^{eHOV}} \right] \right) \cdot \prod_{k=1}^2 \Phi \left[\alpha \cdot \frac{V_{\xi_{k+1}}^e - V_{\xi_{k+1}}^e}{\sigma_{\xi_{k+1}}^2 + \sigma_{\xi_{k+1}}^{eHOV}} \right] \\ &= \left[1 - \Phi \left(\alpha \cdot \frac{V_{\xi_4}^e - V_{\xi_4}^e}{\sigma_{\xi_4}^2 + \sigma_{\xi_4}^{eHOV}} \right) \right] \cdot \Phi \left(\alpha \cdot \frac{V_{\xi_3}^e - V_{\xi_3}^e}{\sigma_{\xi_3}^2 + \sigma_{\xi_3}^{eHOV}} \right) \cdot \Phi \left(\alpha \cdot \frac{V_{\xi_2}^e - V_{\xi_2}^e}{\sigma_{\xi_2}^2 + \sigma_{\xi_2}^{eHOV}} \right) \end{aligned}$$

$$\begin{aligned} P_4^e &= \left(1 - \Phi \left[\alpha \cdot \frac{V_{\xi_5}^e - V_{\xi_5}^e}{\sigma_{\xi_5}^2 + \sigma_{\xi_5}^{eHOV}} \right] \right) \cdot \prod_{k=1}^3 \Phi \left[\alpha \cdot \frac{V_{\xi_{k+1}}^e - V_{\xi_{k+1}}^e}{\sigma_{\xi_{k+1}}^2 + \sigma_{\xi_{k+1}}^{eHOV}} \right] \\ &= \left[1 - \Phi \left[\alpha \cdot \frac{V_{\xi_5}^e - V_{\xi_5}^e}{\sigma_{\xi_5}^2 + \sigma_{\xi_5}^{eHOV}} \right] \right] \cdot \Phi \left(\alpha \cdot \frac{V_{\xi_4}^e - V_{\xi_4}^e}{\sigma_{\xi_4}^2 + \sigma_{\xi_4}^{eHOV}} \right) \cdot \Phi \left(\alpha \cdot \frac{V_{\xi_3}^e - V_{\xi_3}^e}{\sigma_{\xi_3}^2 + \sigma_{\xi_3}^{eHOV}} \right) \cdot \Phi \left(\alpha \cdot \frac{V_{\xi_2}^e - V_{\xi_2}^e}{\sigma_{\xi_2}^2 + \sigma_{\xi_2}^{eHOV}} \right) \end{aligned}$$

$$\begin{aligned} P_5^e &= \left(1 - \Phi \left[\alpha \cdot \frac{V_{\xi_6}^e - V_{\xi_6}^e}{\sigma_{\xi_6}^2 + \sigma_{\xi_6}^{eHOV}} \right] \right) \cdot \prod_{k=1}^4 \Phi \left[\alpha \cdot \frac{V_{\xi_{k+1}}^e - V_{\xi_{k+1}}^e}{\sigma_{\xi_{k+1}}^2 + \sigma_{\xi_{k+1}}^{eHOV}} \right] \\ &= \left[1 - \Phi \left[\alpha \cdot \frac{V_{\xi_6}^e - V_{\xi_6}^e}{\sigma_{\xi_6}^2 + \sigma_{\xi_6}^{eHOV}} \right] \right] \cdot \Phi \left(\alpha \cdot \frac{V_{\xi_5}^e - V_{\xi_5}^e}{\sigma_{\xi_5}^2 + \sigma_{\xi_5}^{eHOV}} \right) \cdot \Phi \left(\alpha \cdot \frac{V_{\xi_4}^e - V_{\xi_4}^e}{\sigma_{\xi_4}^2 + \sigma_{\xi_4}^{eHOV}} \right) \cdot \Phi \left(\alpha \cdot \frac{V_{\xi_3}^e - V_{\xi_3}^e}{\sigma_{\xi_3}^2 + \sigma_{\xi_3}^{eHOV}} \right) \cdot \Phi \left(\alpha \cdot \frac{V_{\xi_2}^e - V_{\xi_2}^e}{\sigma_{\xi_2}^2 + \sigma_{\xi_2}^{eHOV}} \right) \end{aligned}$$

⋮

etc.

4.3.2 Egress Preference Model

Similarly, for the choice/preference egress decision we have:

$$\begin{aligned}
 \widehat{P}_{i+k}^x &= P_{i+k}^x \cdot H \left[\bar{d}_{i+k} - (d_{g1} + d_{g2} + \dots + d_{g(n-1)}) \right] \\
 &= \left(1 - \Phi \left[\frac{(V_{i+k+1}^x - V_{i+k}^x)}{\bar{\sigma}_{i+k}} \right] \right) \cdot \prod_{l=1}^{k-1} \Phi \left[\frac{(V_{i+l+1}^x - V_{i+l}^x)}{\bar{\sigma}_{i+l}} \right] \cdot H \left[\bar{d}_{i+k} - (d_{g1} + d_{g2} + \dots + d_{g(n-1)}) \right] \\
 &= \left\{ \left(1 - \Phi \left[\frac{(V_{i+k+1}^x - V_{i+k}^x)}{(\sigma_{H_{i+k+1}}^2 - \sigma_{H_{i+k}}^2) + (\sigma_{F_{i+k}}^2 - \sigma_{F_{i+k+1}}^2)} \right] \right) \cdot \prod_{l=1}^{k-1} \Phi \left[\frac{(V_{i+l+1}^x - V_{i+l}^x)}{(\sigma_{H_{i+l+1}}^2 - \sigma_{H_{i+l}}^2) + (\sigma_{F_{i+l}}^2 - \sigma_{F_{i+l+1}}^2)} \right] \right\} \cdot H \left[\bar{d}_{i+k} - (d_{g1} + d_{g2} + \dots + d_{g(n-1)}) \right]
 \end{aligned} \tag{53}$$

To find P_{i+k}^x :

Let $V_{\xi_i^F}^x$ denote the travel time on freeway link i

$V_{\xi_i^H}^x$ denote the travel time on HOV link i

$$V_{i+k+1}^x - V_{i+k}^x \Rightarrow$$

$$V_{i+k+1}^x \approx V_{\xi_1^F}^x + \dots + V_{\xi_{i-1}^F}^x + V_{\xi_i^F}^x + V_{\xi_{i+1}^H}^x + \dots + V_{\xi_{i+k}^H}^x + V_{\xi_{i+k+1}^H}^x + V_{\xi_{i+k+2}^F}^x + \dots + V_{\xi_n^F}^x$$

$$V_{i+k}^x \approx V_{\xi_1^F}^x + \dots + V_{\xi_{i-1}^F}^x + V_{\xi_i^F}^x + V_{\xi_{i+1}^H}^x + \dots + V_{\xi_{i+k}^H}^x + V_{\xi_{i+k+1}^F}^x + V_{\xi_{i+k+2}^F}^x + \dots + V_{\xi_n^F}^x$$

$$\therefore V_{i+k+1}^x - V_{i+k}^x \approx V_{\xi_{i+k+1}^H}^x - V_{\xi_{i+k+1}^F}^x$$

Let $\sigma_{\xi_i^F}^2$ denote the variance of travel time on freeway link i

$\sigma_{\xi_i^H}^2$ denote the variance of travel time on HOV link i

$$\sigma_{H_{i+k+1}}^2 - \sigma_{H_{i+k}}^2 \Rightarrow$$

$$\begin{aligned}
 \sigma_{H_{i+k+1}}^2 &\approx \text{Var}(\xi_{i+1}^{HOV} + \xi_{i+2}^{HOV} + \dots + \xi_{i+k}^{HOV} + \xi_{i+k+1}^{HOV}) \\
 &= \text{Var}(\xi_{i+1}^{HOV}) + \text{Var}(\xi_{i+2}^{HOV}) + \dots + \text{Var}(\xi_{i+k}^{HOV}) + \text{Var}(\xi_{i+k+1}^{HOV})
 \end{aligned}$$

$$\begin{aligned}
 \sigma_{H_{i+k}}^2 &\approx \text{Var}(\xi_{i+1}^{HOV} + \xi_{i+2}^{HOV} + \dots + \xi_{i+k}^{HOV}) \\
 &= \text{Var}(\xi_{i+1}^{HOV}) + \text{Var}(\xi_{i+2}^{HOV}) + \dots + \text{Var}(\xi_{i+k-1}^{HOV}) + \text{Var}(\xi_{i+k}^{HOV})
 \end{aligned}$$

$$\therefore \sigma_{H_{i+k+1}}^2 - \sigma_{H_{i+k}}^2 \approx \text{Var}(\xi_{i+k+1}^{HOV}) = \sigma_{\xi_{i+k+1}^{HOV}}^2$$

$$\begin{aligned}
\sigma_{F_{i+k}}^2 - \sigma_{F_{i+k+1}}^2 &\Rightarrow \\
\sigma_{F_{i+k}}^2 &\approx \text{Var}(\xi_{i+k+1}^F + \xi_{i+k+2}^F + \dots + \xi_n^F) \\
&= \text{Var}(\xi_{i+k+1}^F) + \text{Var}(\xi_{i+k+2}^F) + \dots + \text{Var}(\xi_n^F) \\
\sigma_{F_{i+k+1}}^2 &\approx \text{Var}(\xi_{i+k+2}^F + \dots + \xi_n^F) \\
&= \text{Var}(\xi_{i+k+2}^F) + \dots + \text{Var}(\xi_n^F) \\
\therefore \sigma_{F_{i+k}}^2 - \sigma_{F_{i+k+1}}^2 &\approx \text{Var}(\xi_{i+k+1}^F) = \sigma_{\xi_{i+k+1}^F}^2 \\
\therefore \frac{(V_{i+k+1}^x - V_{i+k}^x)}{\bar{\sigma}_{i+k}} &\approx \frac{(V_{i+k+1}^x - V_{i+k}^x)}{(\sigma_{H_{i+k+1}}^2 - \sigma_{H_{i+k}}^2) + (\sigma_{F_{i+k}}^2 - \sigma_{F_{i+k+1}}^2)} = \frac{V_{\xi_{i+k+1}^H}^x - V_{\xi_{i+k+1}^F}^x}{\sigma_{\xi_{i+k+1}^H}^2 + \sigma_{\xi_{i+k+1}^F}^2} \\
\Rightarrow \frac{(V_{i+k+1}^x - V_{i+k}^x)}{\bar{\sigma}_{i+k}} &= \alpha \cdot \frac{V_{\xi_{i+k+1}^H}^x - V_{\xi_{i+k+1}^F}^x}{\sigma_{\xi_{i+k+1}^H}^2 + \sigma_{\xi_{i+k+1}^F}^2} \quad \alpha < 0
\end{aligned}$$

Substituting into Equation (53), we get:

$$\begin{aligned}
\bar{P}_{i+k}^x &= P_{i+k}^x \cdot H[\bar{d}_{i+k} - (d_{g1} + d_{g2} + \dots + d_{g(n-1)})] \\
&= \left[1 - \Phi \left[\alpha \cdot \frac{(V_{i+k+1}^x - V_{i+k}^x)}{\bar{\sigma}_{i+k}} \right] \right] \cdot \prod_{l=1}^{k-1} \Phi \left[\alpha \cdot \frac{(V_{i+l+1}^x - V_{i+l}^x)}{\bar{\sigma}_{i+l}} \right] \cdot H[\bar{d}_{i+k} - (d_{g1} + d_{g2} + \dots + d_{g(n-1)})] \\
&= \left\{ \left[1 - \Phi \left[\alpha \cdot \frac{(V_{i+k+1}^x - V_{i+k}^x)}{(\sigma_{H_{i+k+1}}^2 - \sigma_{H_{i+k}}^2) + (\sigma_{F_{i+k}}^2 - \sigma_{F_{i+k+1}}^2)} \right] \right] \cdot \prod_{l=1}^{k-1} \Phi \left[\alpha \cdot \frac{(V_{i+l+1}^x - V_{i+l}^x)}{(\sigma_{H_{i+l+1}}^2 - \sigma_{H_{i+l}}^2) + (\sigma_{F_{i+l}}^2 - \sigma_{F_{i+l+1}}^2)} \right] \right\} \cdot H[\bar{d}_{i+k} - (d_{g1} + d_{g2} + \dots + d_{g(n-1)})] \\
&= \left\{ \left[1 - \Phi \left[\alpha \cdot \frac{V_{\xi_{i+k+1}^H}^x - V_{\xi_{i+k+1}^F}^x}{\sigma_{\xi_{i+k+1}^H}^2 + \sigma_{\xi_{i+k+1}^F}^2} \right] \right] \cdot \prod_{l=1}^{k-1} \Phi \left[\alpha \cdot \frac{V_{\xi_{i+l+1}^H}^x - V_{\xi_{i+l+1}^F}^x}{\sigma_{\xi_{i+l+1}^H}^2 + \sigma_{\xi_{i+l+1}^F}^2} \right] \right\} \cdot H[\bar{d}_{i+k} - (d_{g1} + d_{g2} + \dots + d_{g(n-1)})]
\end{aligned}$$

Similarly, it is assumed that the P_{i+k}^x are updated at a regular time interval (e.g., every 30 second).

In the Paramics plugin, there is a three-step process to use P_{i+k}^x to determine the preferred egress point for each HOV-eligible vehicle that is already on HOV lane:

- (1) Update four parameters, $V_{\xi_{i+k+1}^F}^x$, $V_{\xi_{i+k+1}^H}^x$, $\sigma_{\xi_{i+k+1}^F}^2$, and $\sigma_{\xi_{i+k+1}^{HOV}}^2$ every interval;
- (2) Compute P_{i+k}^x using the above formula;
- (3) Determine the preferred egress point from a random draw based on the distribution of P_{i+k}^x .

It is noted that the updates of P_{i+k}^x and the four parameters can be executed at different times.

Then, for $\bar{d}_{i+k} \geq (d_{g1} + d_{g2} + \dots + d_{g(n-1)})$, we get:

$$P_{i+k}^x = \left(1 - \Phi \left[\alpha \cdot \frac{V_{\xi_{i+k+1}^H}^x - V_{\xi_{i+k+1}^F}^x}{\sigma_{\xi_{i+k+1}^H}^2 + \sigma_{\xi_{i+k+1}^F}^2} \right] \right) \cdot \prod_{l=1}^{k-1} \Phi \left[\alpha \cdot \frac{V_{\xi_{i+l+1}^H}^x - V_{\xi_{i+l+1}^F}^x}{\sigma_{\xi_{i+l+1}^H}^2 + \sigma_{\xi_{i+l+1}^F}^2} \right] \quad (54)$$

And, the values for P_{i+k}^x expand to:

$$P_{i+1}^x = \left(1 - \Phi \left[\alpha \cdot \frac{V_{\xi_{i+2}}^x - V_{\xi_{i+2}}^F}{\sigma_{\xi_{i+2}}^2 + \sigma_{\xi_{i+2}}^F} \right] \right)$$

$$\begin{aligned} P_{i+2}^x &= \left(1 - \Phi \left[\alpha \cdot \frac{V_{\xi_{i+3}}^x - V_{\xi_{i+3}}^F}{\sigma_{\xi_{i+3}}^2 + \sigma_{\xi_{i+3}}^F} \right] \right) \cdot \prod_{l=1}^1 \Phi \left[\alpha \cdot \frac{V_{\xi_{i+l+1}}^x - V_{\xi_{i+l+1}}^F}{\sigma_{\xi_{i+l+1}}^2 + \sigma_{\xi_{i+l+1}}^F} \right] \\ &= \left(1 - \Phi \left[\alpha \cdot \frac{V_{\xi_{i+3}}^x - V_{\xi_{i+3}}^F}{\sigma_{\xi_{i+3}}^2 + \sigma_{\xi_{i+3}}^F} \right] \right) \cdot \Phi \left[\alpha \cdot \frac{V_{\xi_{i+2}}^x - V_{\xi_{i+2}}^F}{\sigma_{\xi_{i+2}}^2 + \sigma_{\xi_{i+2}}^F} \right] \end{aligned}$$

$$\begin{aligned} P_{i+3}^x &= \left(1 - \Phi \left[\alpha \cdot \frac{V_{\xi_{i+4}}^x - V_{\xi_{i+4}}^F}{\sigma_{\xi_{i+4}}^2 + \sigma_{\xi_{i+4}}^F} \right] \right) \cdot \prod_{l=1}^2 \Phi \left[\alpha \cdot \frac{V_{\xi_{i+l+1}}^x - V_{\xi_{i+l+1}}^F}{\sigma_{\xi_{i+l+1}}^2 + \sigma_{\xi_{i+l+1}}^F} \right] \\ &= \left(1 - \Phi \left[\alpha \cdot \frac{V_{\xi_{i+4}}^x - V_{\xi_{i+4}}^F}{\sigma_{\xi_{i+4}}^2 + \sigma_{\xi_{i+4}}^F} \right] \right) \cdot \Phi \left[\alpha \cdot \frac{V_{\xi_{i+3}}^x - V_{\xi_{i+3}}^F}{\sigma_{\xi_{i+3}}^2 + \sigma_{\xi_{i+3}}^F} \right] \cdot \Phi \left[\alpha \cdot \frac{V_{\xi_{i+2}}^x - V_{\xi_{i+2}}^F}{\sigma_{\xi_{i+2}}^2 + \sigma_{\xi_{i+2}}^F} \right] \end{aligned}$$

$$\begin{aligned} P_{i+4}^x &= \left(1 - \Phi \left[\alpha \cdot \frac{V_{\xi_{i+5}}^x - V_{\xi_{i+5}}^F}{\sigma_{\xi_{i+5}}^2 + \sigma_{\xi_{i+5}}^F} \right] \right) \cdot \prod_{l=1}^3 \Phi \left[\alpha \cdot \frac{V_{\xi_{i+l+1}}^x - V_{\xi_{i+l+1}}^F}{\sigma_{\xi_{i+l+1}}^2 + \sigma_{\xi_{i+l+1}}^F} \right] \\ &= \left(1 - \Phi \left[\alpha \cdot \frac{V_{\xi_{i+5}}^x - V_{\xi_{i+5}}^F}{\sigma_{\xi_{i+5}}^2 + \sigma_{\xi_{i+5}}^F} \right] \right) \cdot \Phi \left[\alpha \cdot \frac{V_{\xi_{i+4}}^x - V_{\xi_{i+4}}^F}{\sigma_{\xi_{i+4}}^2 + \sigma_{\xi_{i+4}}^F} \right] \cdot \Phi \left[\alpha \cdot \frac{V_{\xi_{i+3}}^x - V_{\xi_{i+3}}^F}{\sigma_{\xi_{i+3}}^2 + \sigma_{\xi_{i+3}}^F} \right] \cdot \Phi \left[\alpha \cdot \frac{V_{\xi_{i+2}}^x - V_{\xi_{i+2}}^F}{\sigma_{\xi_{i+2}}^2 + \sigma_{\xi_{i+2}}^F} \right] \end{aligned}$$

$$\begin{aligned} P_{i+5}^x &= \left(1 - \Phi \left[\alpha \cdot \frac{V_{\xi_{i+6}}^x - V_{\xi_{i+6}}^F}{\sigma_{\xi_{i+6}}^2 + \sigma_{\xi_{i+6}}^F} \right] \right) \cdot \prod_{l=1}^4 \Phi \left[\alpha \cdot \frac{V_{\xi_{i+l+1}}^x - V_{\xi_{i+l+1}}^F}{\sigma_{\xi_{i+l+1}}^2 + \sigma_{\xi_{i+l+1}}^F} \right] \\ &= \left(1 - \Phi \left[\alpha \cdot \frac{V_{\xi_{i+6}}^x - V_{\xi_{i+6}}^F}{\sigma_{\xi_{i+6}}^2 + \sigma_{\xi_{i+6}}^F} \right] \right) \cdot \Phi \left[\alpha \cdot \frac{V_{\xi_{i+5}}^x - V_{\xi_{i+5}}^F}{\sigma_{\xi_{i+5}}^2 + \sigma_{\xi_{i+5}}^F} \right] \cdot \Phi \left[\alpha \cdot \frac{V_{\xi_{i+4}}^x - V_{\xi_{i+4}}^F}{\sigma_{\xi_{i+4}}^2 + \sigma_{\xi_{i+4}}^F} \right] \cdot \Phi \left[\alpha \cdot \frac{V_{\xi_{i+3}}^x - V_{\xi_{i+3}}^F}{\sigma_{\xi_{i+3}}^2 + \sigma_{\xi_{i+3}}^F} \right] \cdot \Phi \left[\alpha \cdot \frac{V_{\xi_{i+2}}^x - V_{\xi_{i+2}}^F}{\sigma_{\xi_{i+2}}^2 + \sigma_{\xi_{i+2}}^F} \right] \end{aligned}$$

⋮

etc.

4.3.3 Traffic Model: Acceptable Gap Calculation

Recall:

$$d_{gk} = \frac{v_k v_k \left[\exp \left(\frac{aL_{car}}{v_k v_k} \right) - 1 - \frac{aL_{car}}{v_k v_k} \right]}{\max(|v_k - v_{k-1}|, |v_k - bv_{k-1}|)} \cdot v_k \quad ; k = 1, 2, \dots, n_l - 1 \quad ; a \geq 1 \quad ; b \leq 1 \quad (50)$$

For a multiple-lane freeway, a HOV-eligible vehicle on mixed-flow lanes may execute lane changes toward the road median several times in order to enter the HOV lane. Similarly, a HOV-eligible vehicle on the HOV lane may execute lane changes toward the road curb several times in order to leave the HOV lane and then exit the freeway. As a result, the lane speeds and densities applied in Equation (50) have to be taken into consideration. In addition, the number of lanes within a road section between two consecutive HOV ingress/egress points may not be the same due to geometric design. A simple way to address these issues is to assume that, when computing d_{gk} , the number of lanes is defined based on the current location of the HOV-eligible vehicle. We further assume that the traffic condition is similar within a road section, so the lane speeds and densities collected at the last link of the road section are applied.

5. Model Sensitivity Analysis and Validation

For model development purposes, it is important to ascertain the reasonableness of the proposed model. What is of interest is whether or not the model is capable of modeling different HOV driver behaviors under different scenarios. Sensitivity analysis is performed for this purpose.

5.1 Calibration Parameters and Control Parameters

As shown in Equations (50), (52), and (54), L_{car} , a , b , and α are the calibration parameters of the proposed HOV driver behavioral model. :

$$d_{gk} = \frac{v_k \nu_k \left[\exp\left(\frac{aL_{car}}{v_k \nu_k}\right) - 1 - \frac{aL_{car}}{v_k \nu_k} \right]}{\max(|v_k - v_{k-1}|, |v_k - bv_{k-1}|)} \cdot v_k \quad ; k = 1, 2, \dots, n_l - 1 \quad ; a \geq 1 \quad ; b \leq 1 \quad (50)$$

$$P_i^e = \left(1 - \Phi \left[\alpha \cdot \frac{V_{\xi_{i+1}}^e - V_{\xi_{i+1}}^e}{\sigma_{\xi_{i+1}}^2 + \sigma_{\xi_{i+1}}^{HOV}} \right] \right) \cdot \prod_{k=1}^{i-1} \Phi \left[\alpha \cdot \frac{V_{\xi_{k+1}}^e - V_{\xi_{k+1}}^e}{\sigma_{\xi_{k+1}}^2 + \sigma_{\xi_{k+1}}^{HOV}} \right] \quad (52)$$

$$P_{i+k}^x = \left(1 - \Phi \left[\alpha \cdot \frac{V_{\xi_{i+k+1}}^x - V_{\xi_{i+k+1}}^x}{\sigma_{\xi_{i+k+1}}^2 + \sigma_{\xi_{i+k+1}}^2} \right] \right) \cdot \prod_{l=1}^{k-1} \Phi \left[\alpha \cdot \frac{V_{\xi_{i+l+1}}^x - V_{\xi_{i+l+1}}^x}{\sigma_{\xi_{i+l+1}}^2 + \sigma_{\xi_{i+l+1}}^2} \right] \quad (54)$$

The definition of each calibration parameter is described in the following:

1. Parameter L_{car} : The average vehicle length, which is typically assumed to be on the order of 20 ft.

2. Parameter b : The tolerable speed decrease fraction when a driver makes a lane change, which is less than or equal to 1 ($b \leq 1$), but should not be smaller than 0.9 (Stuster and Coffman, 1998) due to safety concerns.
3. Parameter a : Applied to estimate the spatial gap for a vehicle to change lane, which is a multiplier of L_{car} and is greater than or equal to 1 ($a \geq 1$). The greater the value of a , the longer the spatial gap required for a vehicle to make a lane change.
4. Parameter α : A scalar to reflect the mapping of travel time savings to the utility to enter/exit HOV lane, and should be less than 0 ($\alpha < 0$).

We firstly tested the sample network with a set of a values to exam the “reasonableness” of the HOV driver behavioral model. A freeway network is also selected for sensitivity analysis to validate the proposed model.

In addition to the calibration parameters noted above, four “implementation” parameters are added to extend the capability of the theoretical buffer-separated HOV ingress/egress model to application in real-world implementation:

1. Ingress Priority: This parameter is used to reflect the extent of the choice set for selecting favorable ingress points and the proportion of the drivers that will follow this rule. For example, it could be specified that 80% of HOV drivers will consider only the first three possible ingress points to enter a HOV lane given a specified route.
2. Egress Persistency: This parameter is used to reflect the persistency of staying in the HOV lane before considering exiting at a favorable egress point, and the proportion of the drivers that will follow this rule. For example, it could be specified that 90% of HOV drivers will consider only the last two egress points prior to their assigned freeway exit to leave current HOV lane given a specified route.
3. Preference Probability Threshold (PV_TH): The values of P_i^e and P_{i+k}^x must be greater than PV_TH to be considered as a candidate ingress/egress point.
4. Update Time Interval (PV_TIME): The time interval (seconds) to update the traffic information.

5.2 Sensitivity Analysis of the Sample Network

As described in Section 4.2 (see Figure 4-2), the sample network contains five ingress/egress points, six sections, and four zones. Four case scenarios are applied for sensitivity analysis:

- Case 1: Ramp to Ramp (Zone 2 to Zone 4)
- Case 2: Mainline to Ramp (Zone 1 to Zone 4)
- Case 3: Ramp to Mainline (Zone 2 to Zone 3)
- Case 4: Mainline to Mainline (Zone 1 to Zone 3)

and the OD tables for the four cases are shown in Tables 5-1 and 5-2:

Table 5-1 OD table for Case 1 and Case 2.

Zone	1	2	3	4	Total
1	0	0	6249	551	6800
2	0	0	49	551	600
3	0	0	0	0	0
4	0	0	0	0	0
Total	0	0	6298	1102	7400

Table 5-2 OD table for Case 3 and Case 4.

Zone	1	2	3	4	Total
1	0	0	6249	551	6800
2	0	0	551	49	600
3	0	0	0	0	0
4	0	0	0	0	0
Total	0	0	6800	600	7400

The simulation time is one hour, and the HOV proportion is 9%. The settings of calibration parameters are the same for each of the four cases, while the “implementation” parameters are set different for Case 3 and Case 4 as shown below:

- Calibration parameters:
 - Parameter a : $1.5 \leq a \leq 1000$
 - Parameter b : $b = 0.9$
 - Parameter L_{car} : $L_{car} = 20 \text{ ft}$
 - Parameter α : $\alpha = -1$
- Implementation parameters:
 - Ingress Priority: No control.
 - Egress Persistency: No control for Case 1 and Case 2; for Case 3 and Case 4, all of the HOV vehicles will stay in HOV lane after entering HOV lane.
 - Preference Probability Threshold: $PV_TH > 0.01$
 - Update Time Interval: $PV_TIME = 30$

5.2.1 Case 1 Results: Ramp to Ramp

For the Case 1 scenario, HOV vehicles can enter the HOV lane via taking ingress points 1 to 4, and leave the HOV lane via taking egress points 2 to 5. It is expected that HOV vehicles choose farther ingress points or may be even less likely to enter the HOV lane at all, if a becomes larger. The summary of Case 1 results is shown in Figure 5-1. The total number of HOV nodes, HOV_TN, indicates the overall usage of the HOV route, and can be formulated as:

$$HOV_TN = \sum_{i=1}^n HOV_SN, \quad n = \text{number of HOV sections} \quad (105)$$

where HOV_SN is the number of HOV vehicles traveling on the n th HOV section, and HOV_TN is the total number of vehicles observed traveling on any of the HOV sections; i.e., HOV_TN multiplied by the section length equals the total VMT on the HOV facility.

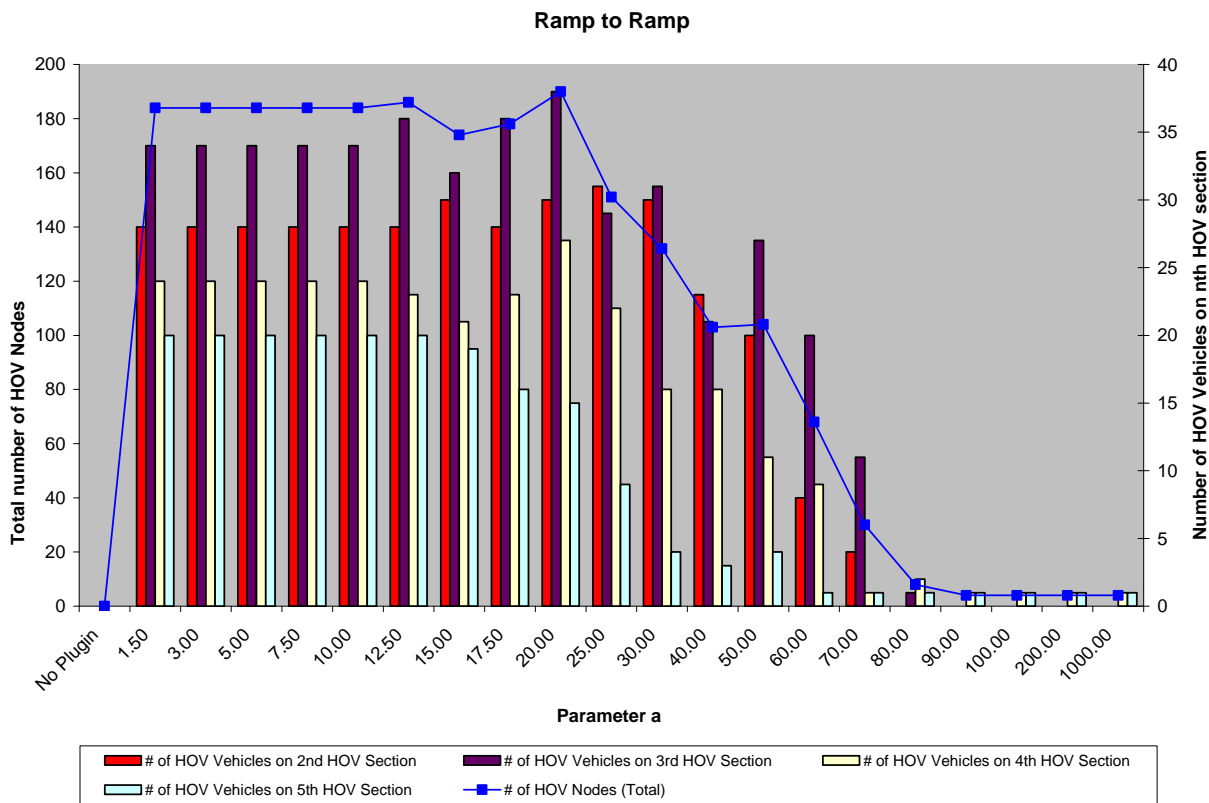


Figure 5-1. Summary of Case 1 results: Ramp to Ramp

It can be seen from Figure 5-1 that, with the HOV plugin disabled, no HOV vehicle took HOV lane. When the plugin was enabled, identical results were obtained for parameter a ranged from 1.5 to 10.0. The usage of each HOV sections varies when parameter a varies between 12.5 and 80.0. In addition, the HOV_TN decreased while a increased, which is as expected.

The distribution of HOV ingress/egress decisions for selected values of the calibration parameter a are listed in Figure 5-2. The figure shows that the usages of ingress point 1 is larger when parameter a is smaller than 30. As the value of parameter a increases, the usage of ingress point 2 increases while the usage of ingress point 1 decreases, which is as expected. It is also noted that the usages of egress point 3 and 4 also increase as a increases, since the HOV driver generally requires a longer distance for the required weaving maneuvers to reach the target ramp after departing from current HOV lane with larger values of a .

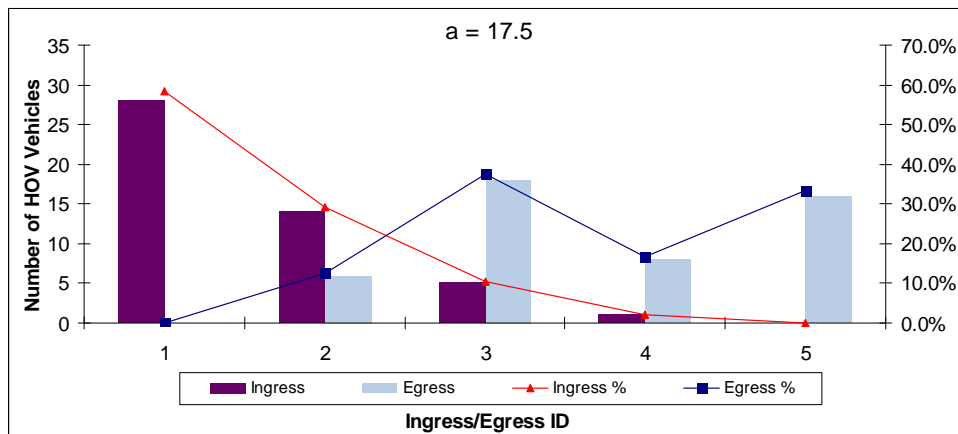
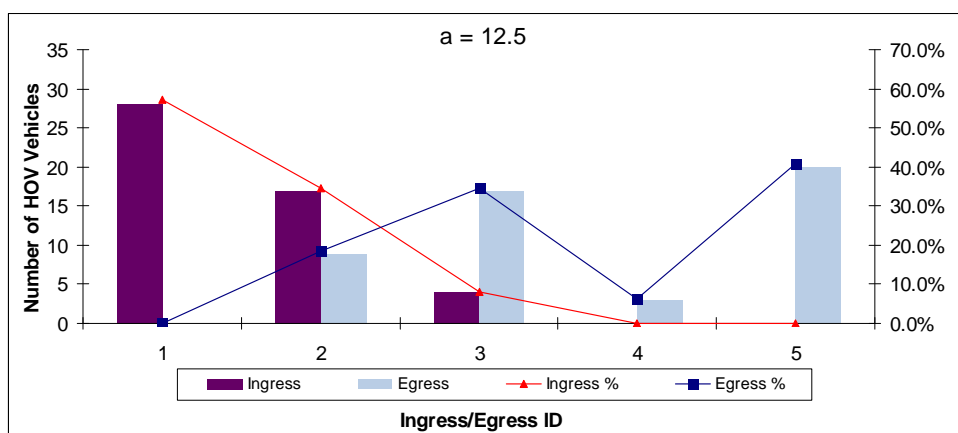
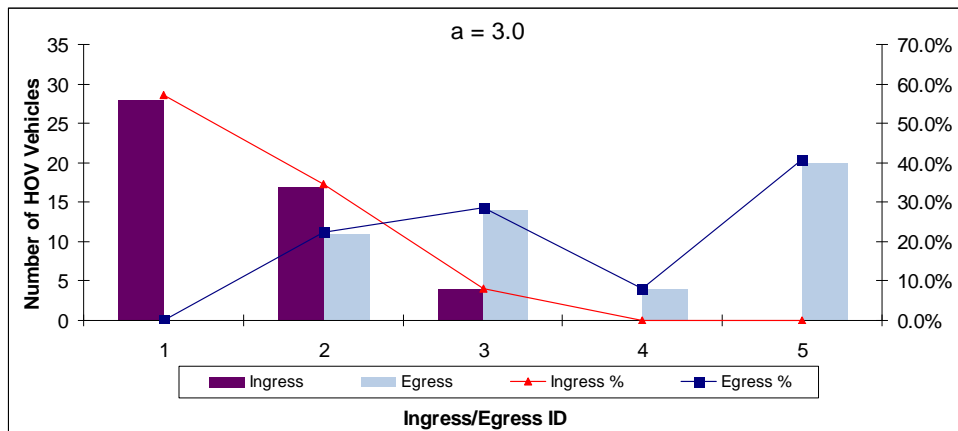


Figure 5-2. Case 1 results variation with parameter *a*

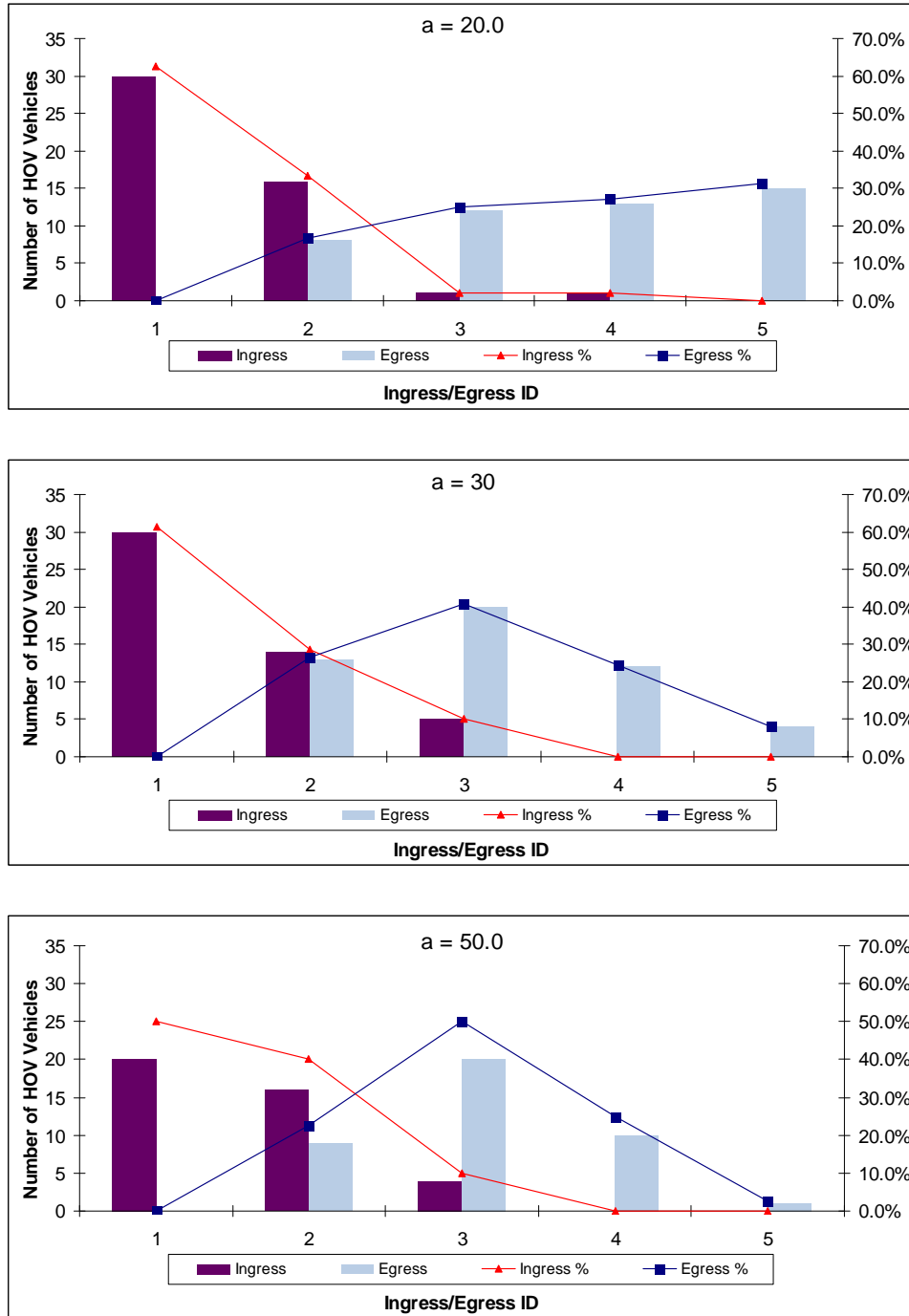


Figure 5-3. Case 1 results variation with parameter a (cont.)

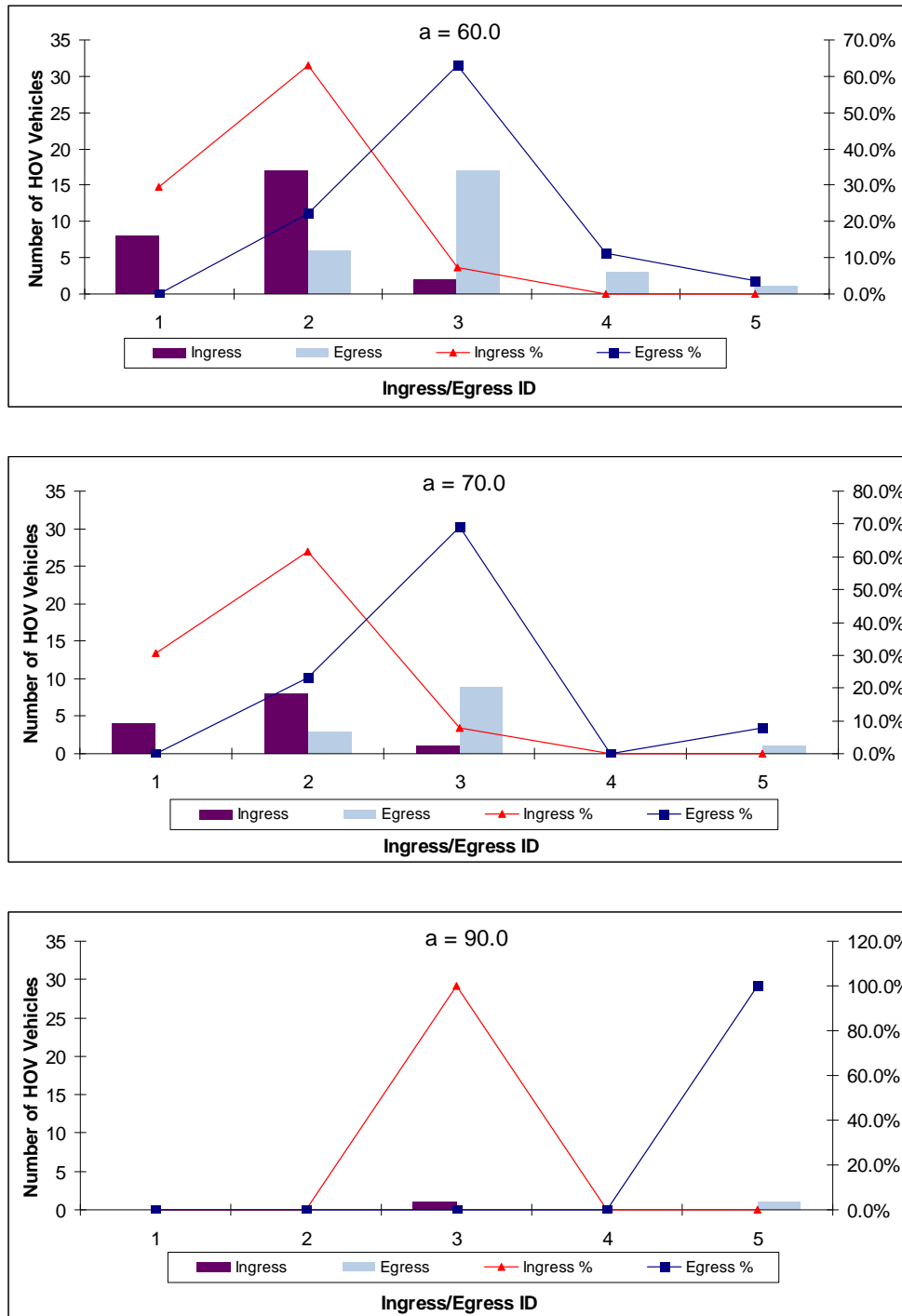


Figure 5-4. Case 1 results variation with parameter a (cont.)

To investigate the usage distribution of ingress/egress points under congestion, another simulation run was performed to demonstrate a congestion scenario. The settings of the calibration and implementation parameters were the same (i.e. $a = 3.0$), while the network coding was modified to generate congestion at freeway sections 1, 5, and 6 without changing geometries. The changes of travel times at each section are shown in Figure 5-3:

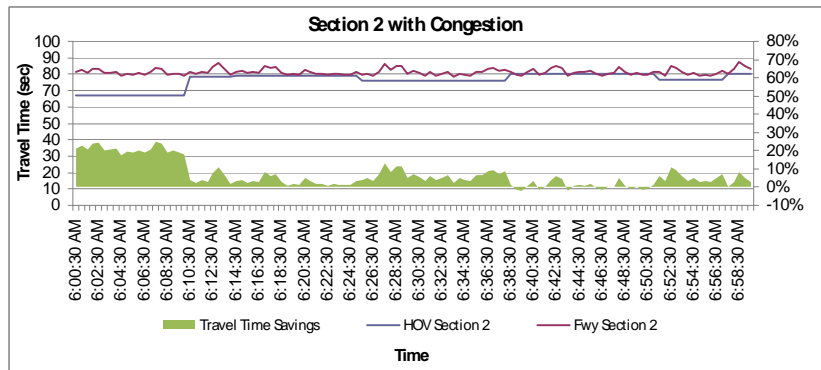
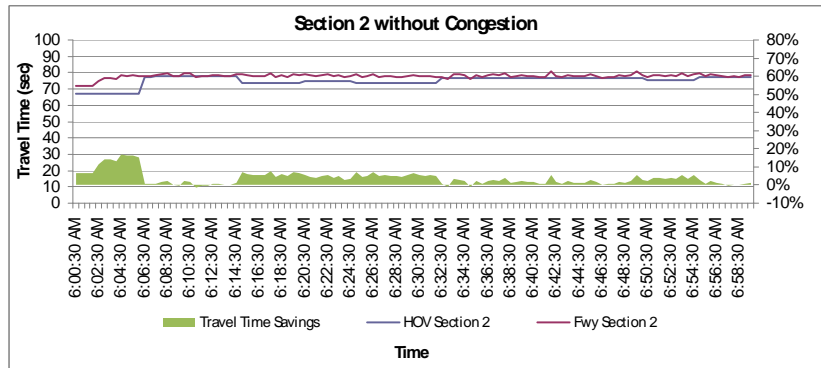
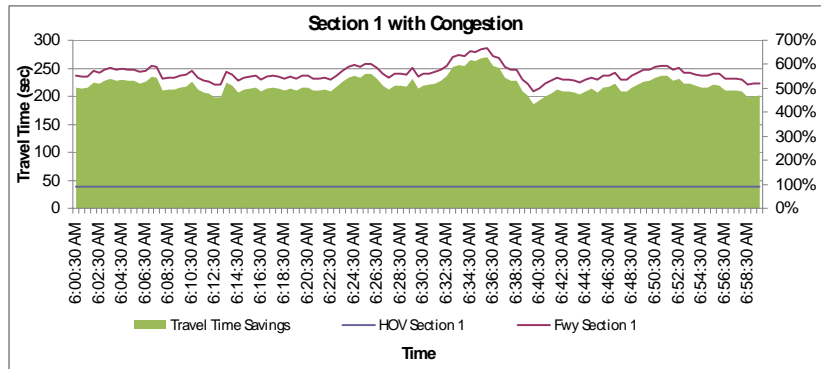
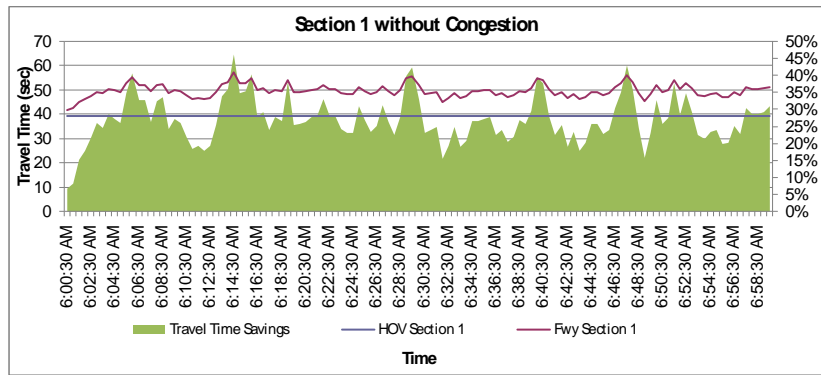


Figure 5-5. The differences of travel time at each section

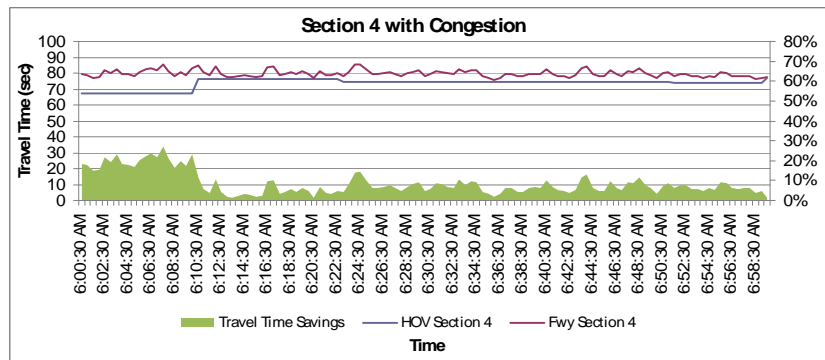
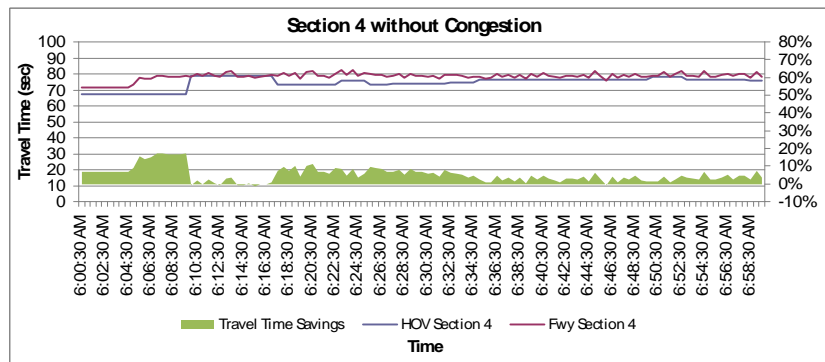
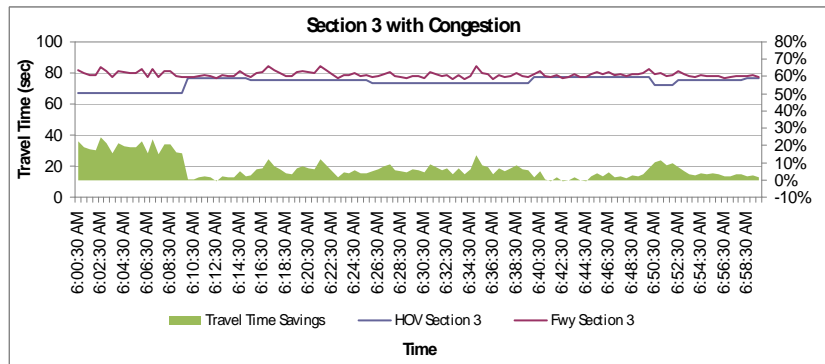
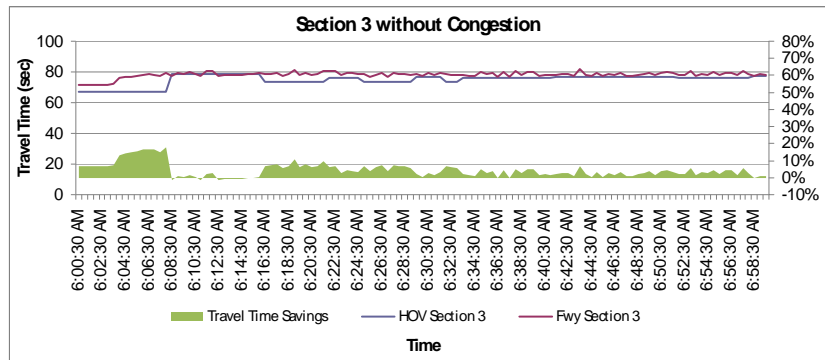


Figure 5-6. The differences of travel time at each section (cont.)

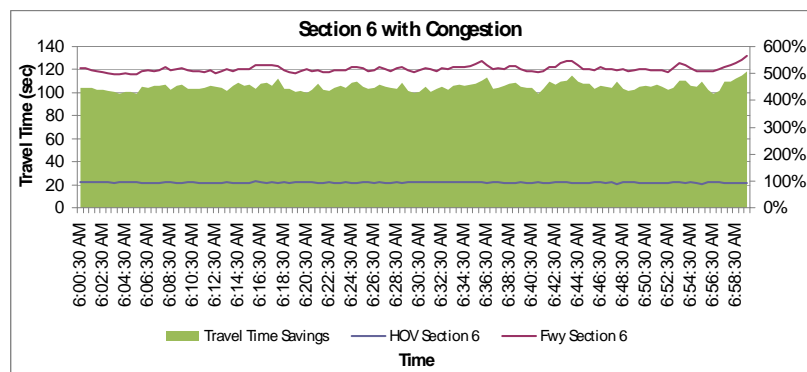
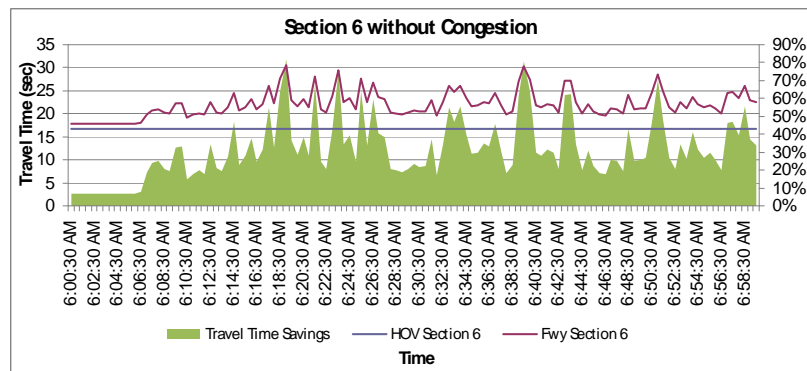
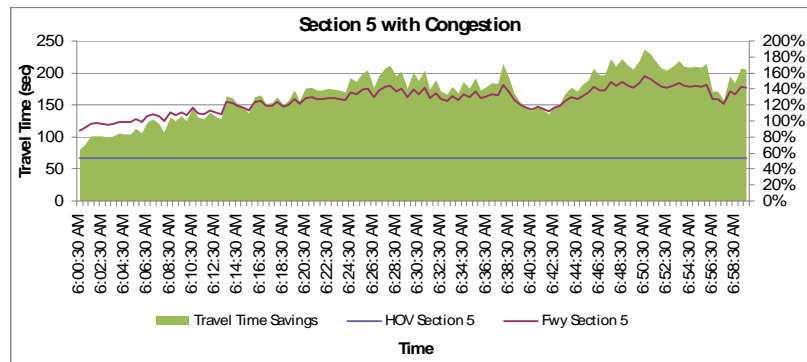
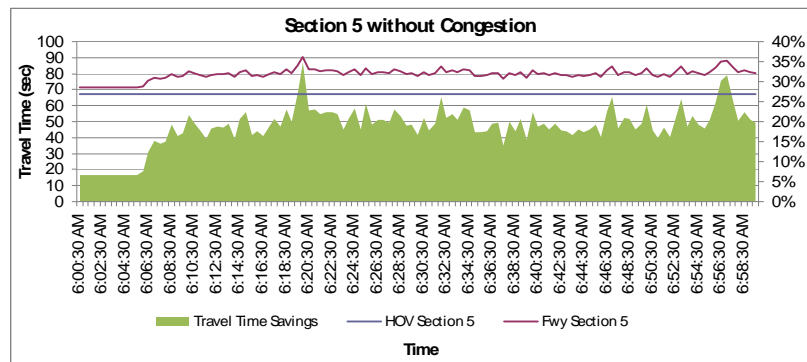


Figure 5-7. The differences of travel time at each section (cont.)

Since the congestion occurred only on the mainline mixed-flow lanes of the freeway sections, the savings of travel time associated with travel on the HOV sections are more significant. The usage distribution of ingress/egress points without congestion is compared with congestion scenario, as shown in Figure 5-4. As expected, the congestion case shifts the pattern of ingress usage to the right due to the weaving difficulties, and the egress pattern to the left due to the potential difficulties in making the exit.

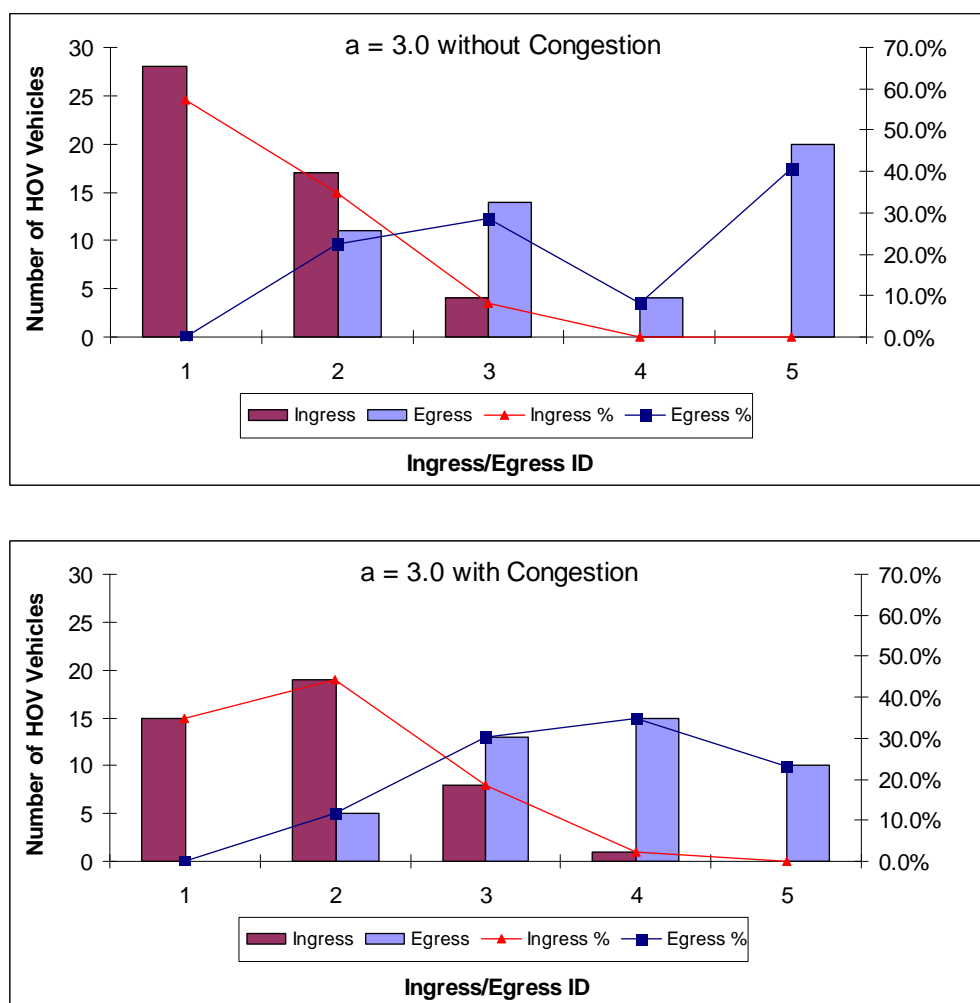


Figure 5-8. Comparison of non-congestion and congestion scenarios

5.2.2 Case 2 Results: Mainline to Ramp

For the Case 2 scenario, HOV vehicles can enter HOV lane via taking ingress points 1 to 4, and leave HOV lane via taking egress points 2 to 5. It is expected that, as in Case 1, HOV vehicles choose farther ingress points, or may even be less likely to enter HOV lane, if a becomes larger. In addition, compared to the Case 1 scenario, the usage of ingress point 1 should be greater since in this case the HOV vehicles are initially distributed across the lanes on the mainline resulting in

fewer lane changing maneuvers being required to enter an ingress point. The summary of Case 2 results is shown in Figure 5-5.

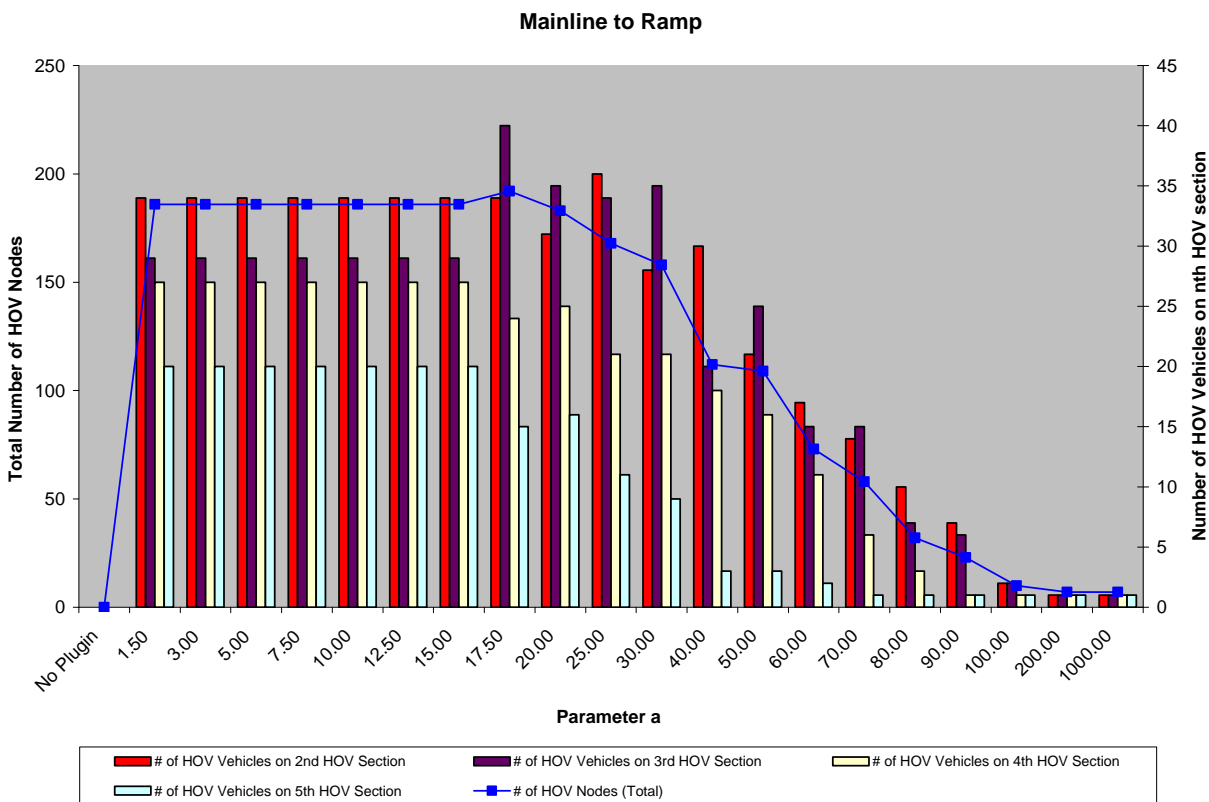


Figure 5-9. Summary of Case 2 results: Mainline to Ramp

As in the Case 1 scenario, with the HOV plugin disabled, no HOV vehicle takes HOV lane. When the plugin is enabled, identical results are obtained for parameter a ranging from 1.5 to 15.0. The usage of each HOV sections varied when parameter a varies between 17.5 and 100.0. In addition, the HOV_TN decreases while a increases, which agreed with the expectation.

The distribution of HOV ingress/egress decisions for selected values of the calibration parameter a are listed in Figure 5-6. As shown in Figure 5-4, higher usage of ingress point 1 ($> 60\%$) is observed when the value of parameter a is less than 25. The usages of ingress points 2 and 3 are increased with parameter a ranging from 17.5 to 50. Relative to the usage of egress points, egress points 2 and 3 are preferred with larger values of parameter a .

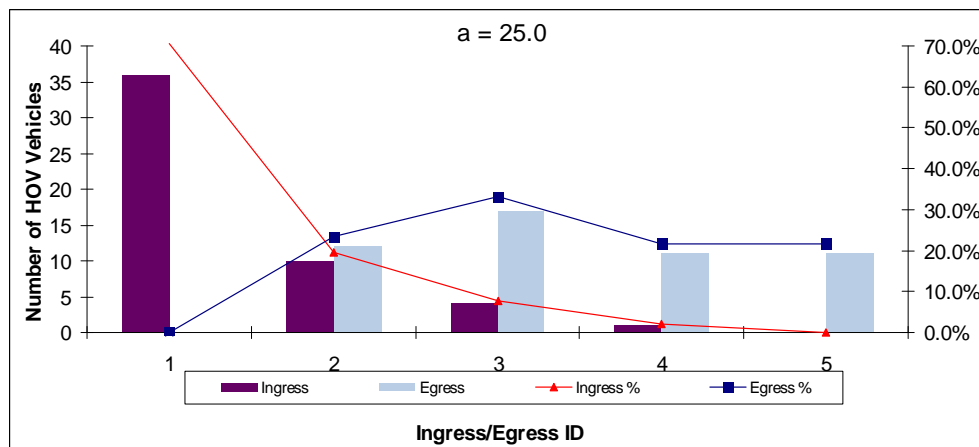
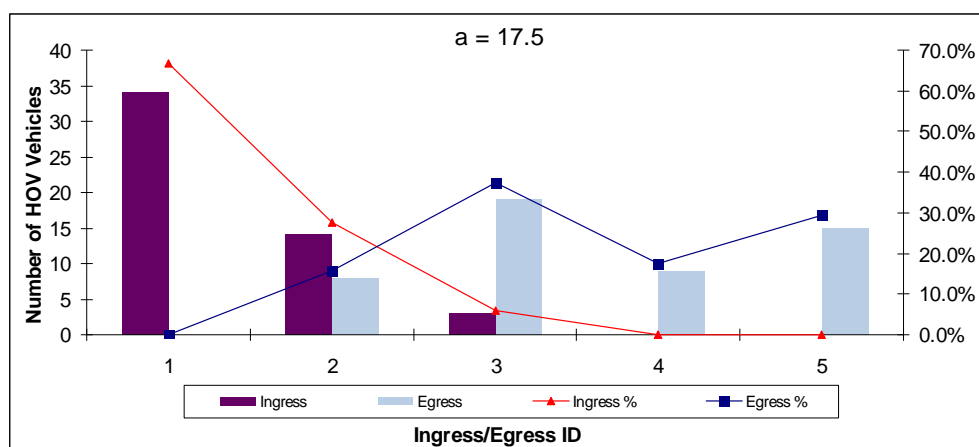
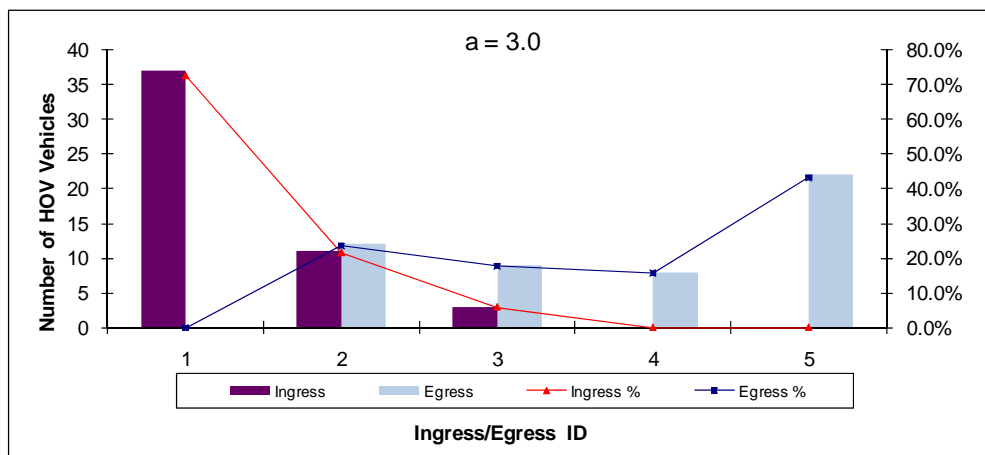


Figure 5-10. Case 2 results variation with parameter *a*

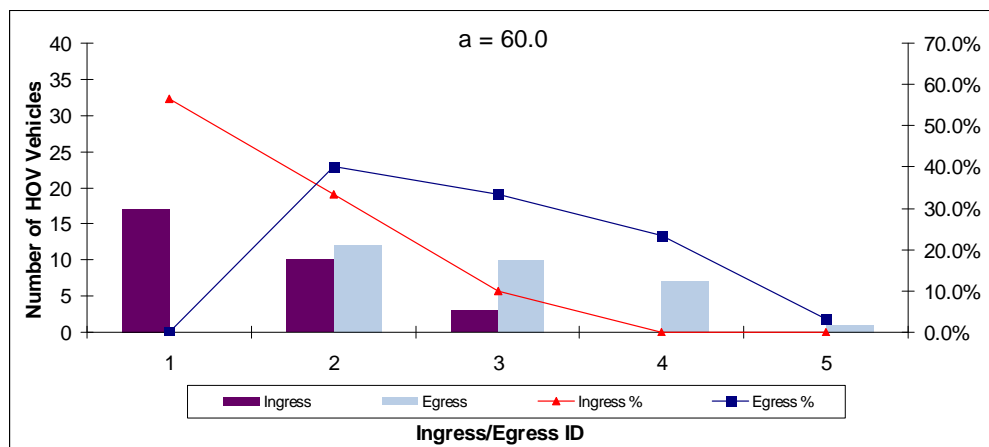
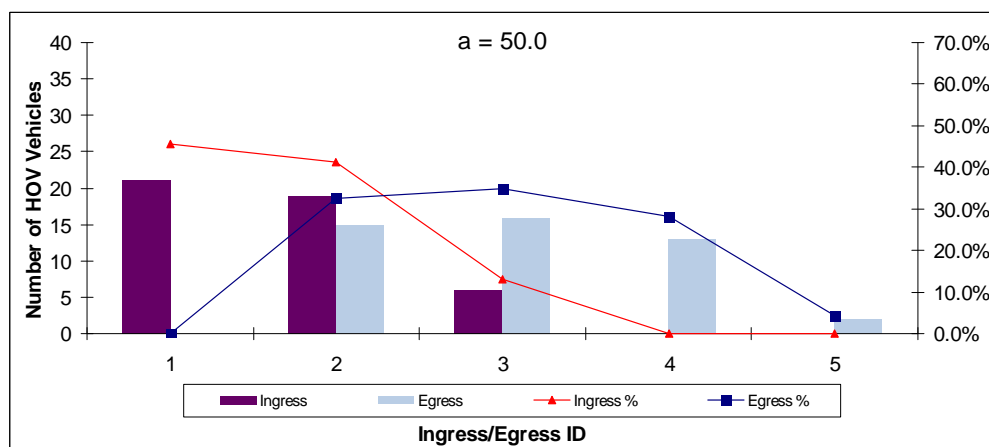
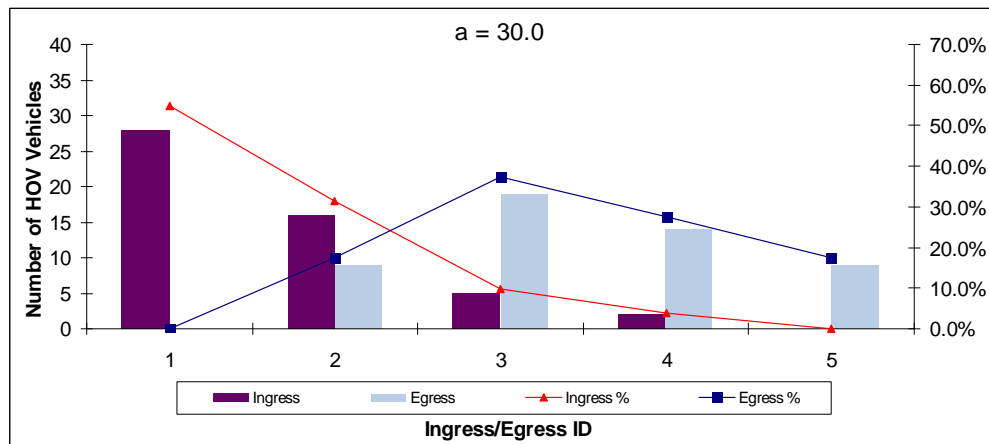


Figure 5-11. Case 2 results variation with parameter *a* (cont.)

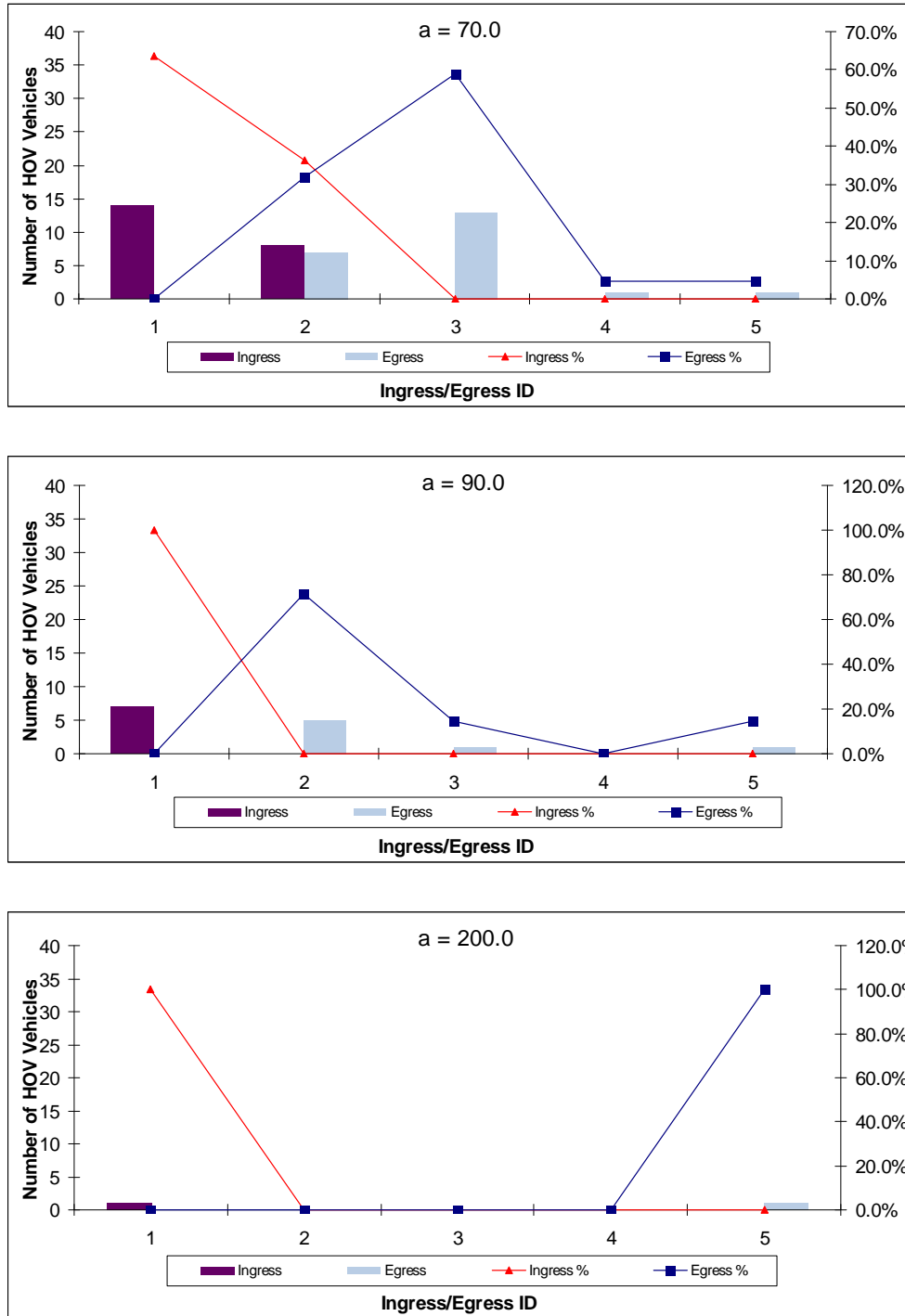


Figure 5-12. Case 2 results variation with parameter a (cont.)

5.2.3 Case 3 Results: Ramp to Mainline

For the Case 3 scenario, HOV vehicles can enter HOV lane via ingress points 1 to 4, and remain in the HOV lane to the end of the test network. It is expected that, as in Case 1, HOV vehicles

choose farther ingress points or even be less likely to enter HOV lane at all, if the value of parameter a becomes larger. In addition, the usages of each HOV sections may be similar with smaller parameter a and the usage of the last HOV section should be high since the HOV vehicles are committed to stay in the HOV lane. The summary of Case 3 results is shown in Figure 5-7.

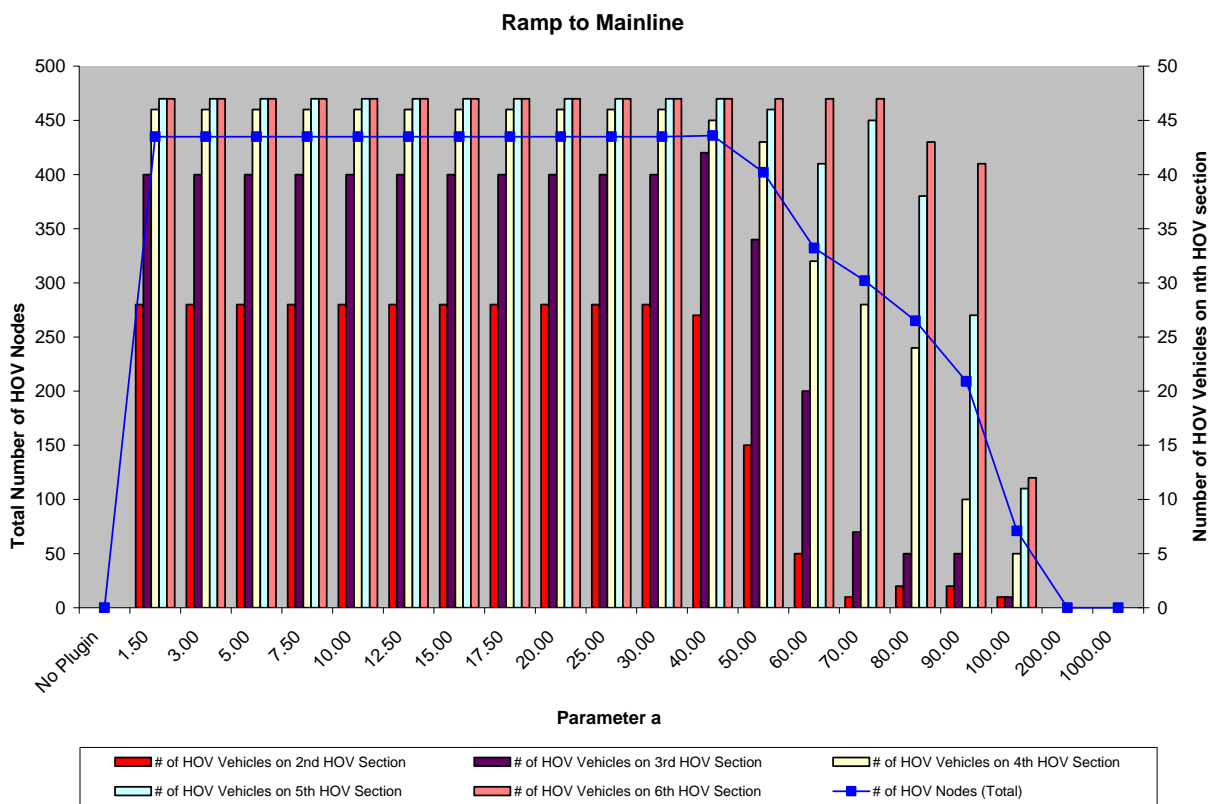


Figure 5-13. Summary of Case 3 results: Ramp to Mainline

It is found that no HOV vehicle takes HOV lane when the HOV plugin is disabled. When the plugin is enabled, identical results are obtained as expected for parameter a values ranging from 1.5 to 30.0. The usage of each HOV section varies when parameter a is set between 40.0 and 100.0. The usage of the last HOV section (6th HOV section) remains high when parameter a is smaller than 90.0, but it decreases dramatically when parameter a is greater than 90.0. In addition, similar to Case 1, HOV_TN decreases as the value of a increases and no HOV vehicle takes the HOV lane when the value of the parameter is greater than 40.0.

The distribution of HOV ingress decisions (in this case, there are no egress decisions) for selected values of the calibration parameter a are listed in Figure 5-8. As shown in Figure 5-6, higher usages of ingress point 1 (> 50%) are observed for values of parameter a less than 40.0. As the value of the parameter a increases, the distribution of ingress decisions shifts toward ingress point farther downstream, as expected, with an increasing percentage of HOV-eligible vehicles foregoing use of the HOV facility altogether.

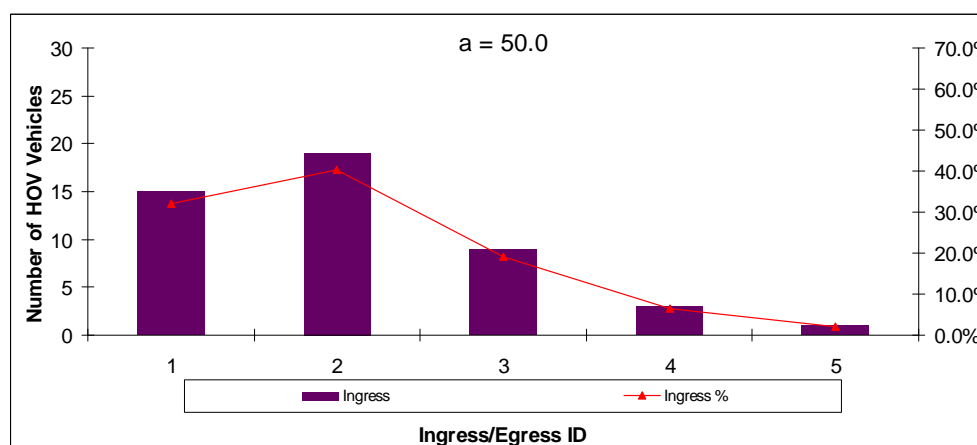
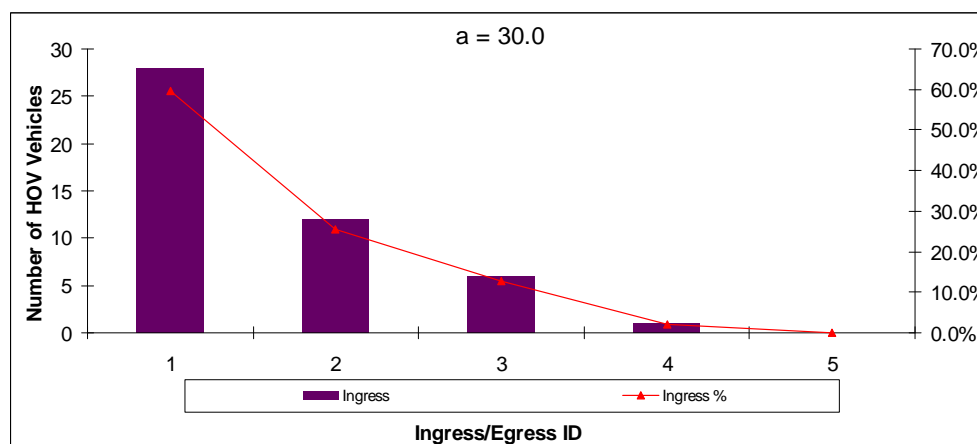
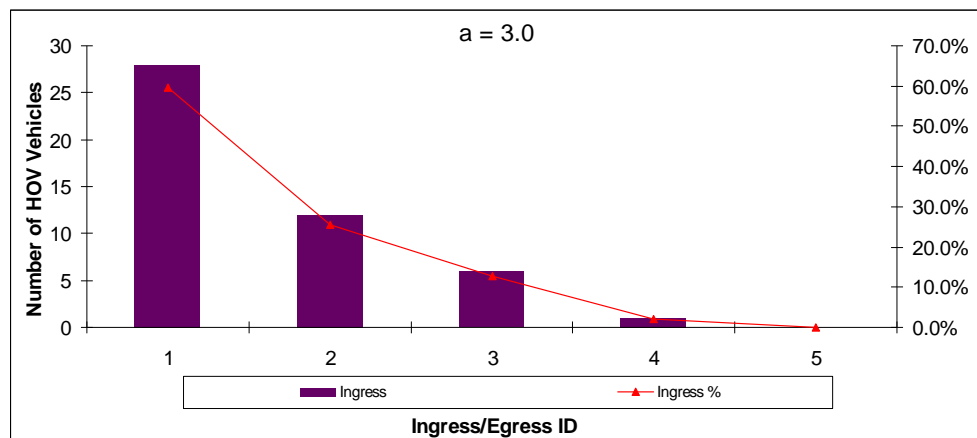


Figure 5-14. Case 3 results variation with parameter *a*

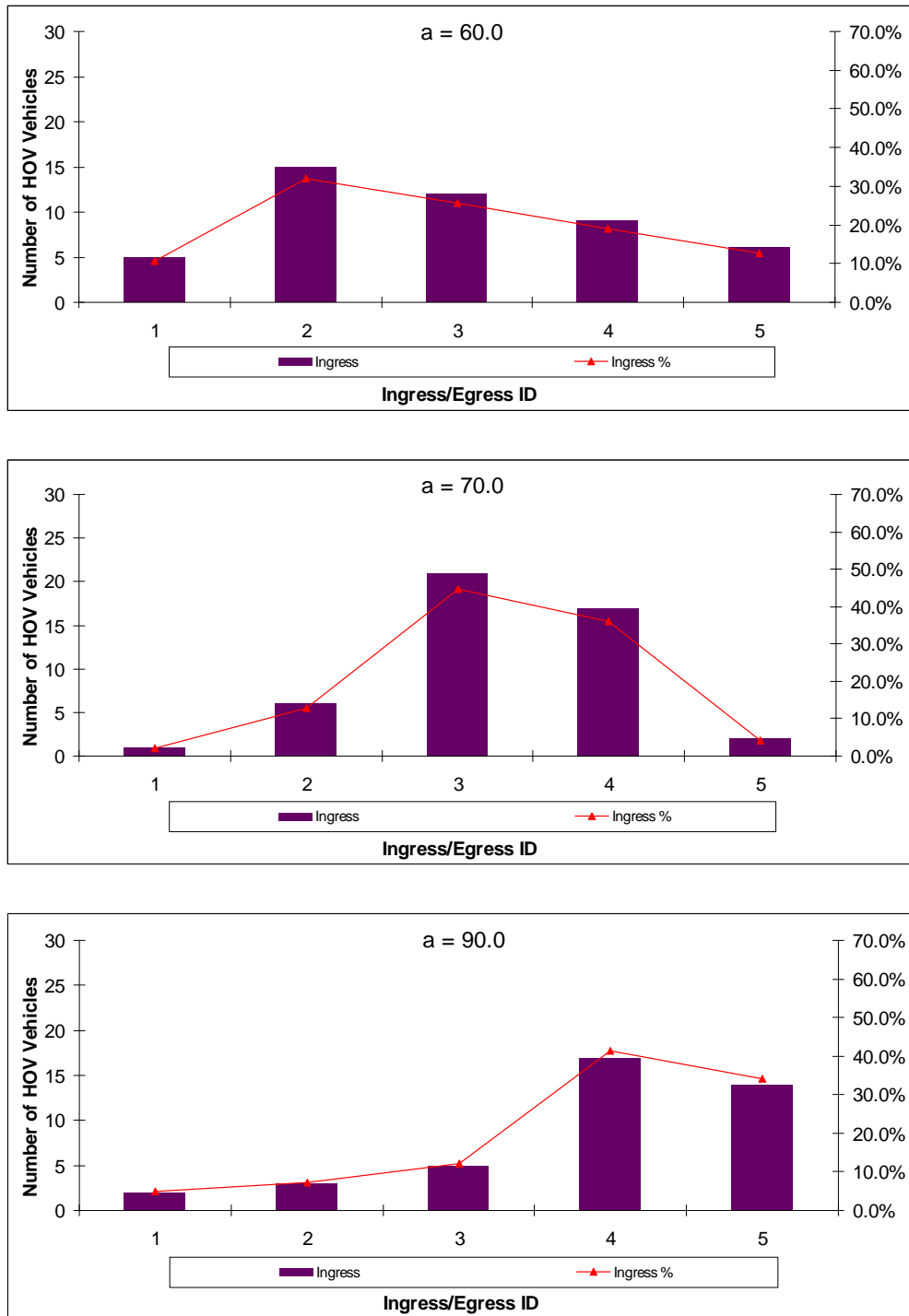


Figure 5-15. Case 3 results variation with parameter a (cont.)

5.2.4 Case 4 Results: Mainline to Mainline

For the Case 4 scenario, HOV vehicles can enter HOV lane via ingress points 1 to 4, and remain in the HOV lane to the end of the test network. The expectation is that, as in previous cases,

HOV vehicles choose farther ingress points or even be less likely to enter HOV lane at all, as values of parameter a become larger. As in Case 3, the usages of each HOV sections may be similar with smaller parameter a and the usage of the last HOV section should be high since the HOV vehicles are committed to stay in the HOV lane. In addition, the usage of ingress point 1 should be greater than that observed in Case 2, since the initial positions of the HOV-eligible vehicles are distributed across all lanes on the mainline and fewer lane changing maneuvers are required to enter an ingress point. The summary of Case 4 results is shown in Figure 5-9.

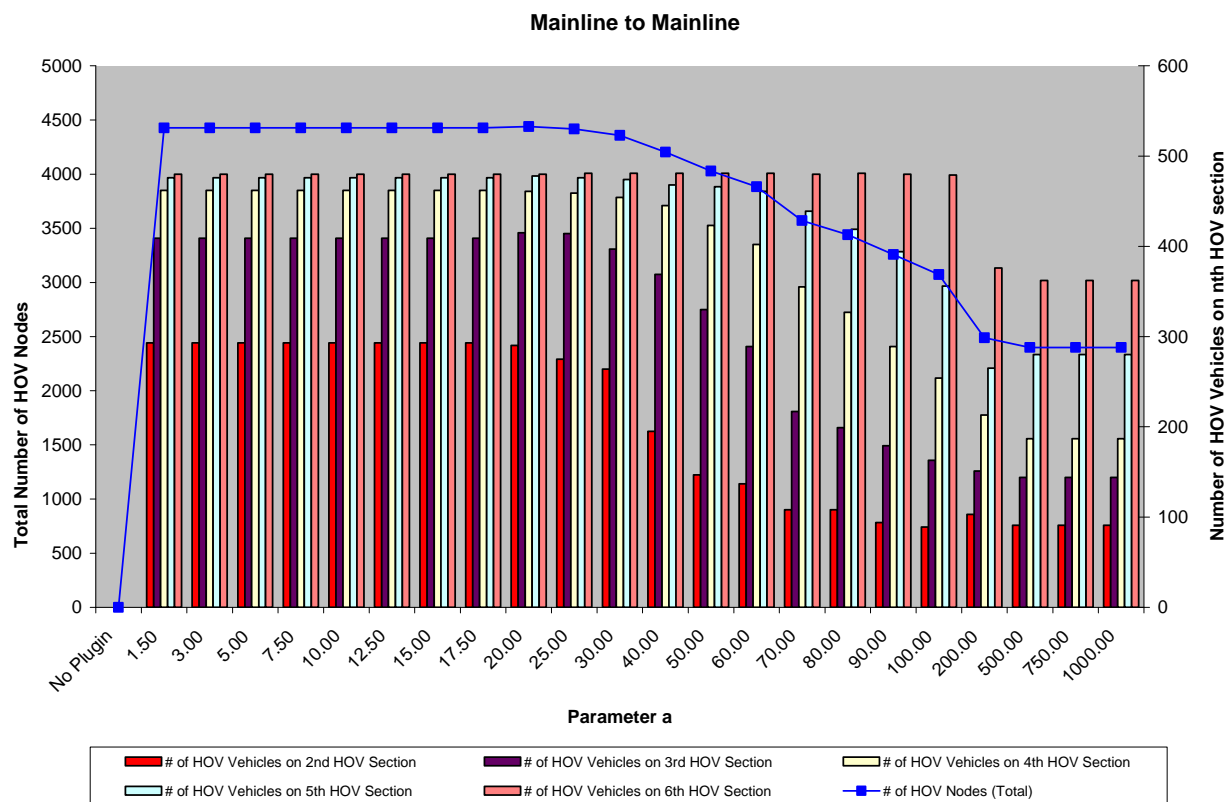


Figure 5-16. Summary of Case 4 results: Mainline to Mainline

With the plugin enabled, identical results were obtained (as expected) for values of parameter a ranging from 1.5 to 17.5. The usage of each HOV section varied when parameter a was set between 20.0 and 200.0. As observed in Case 3, the usage of the last HOV section (6th HOV section) remained high for values of parameter a less than 100.0 and began to decrease when a was greater than 200.0. In addition, similar to Case 1, the HOV_TN decreased as a increased.

As shown in Figure 5-10, higher usages of ingress point 1 (> 50%) are observed when parameter a is less than 30.0. The usage of the last two egress points (4 and 5) increases as the value of parameter a increases, which is as expected. It is also found that the ingress points 2 and 3 are preferred only when the value of parameter a is within the range 40 to 70. When parameter a becomes larger, usage of the HOV facility decreases for all ingress points, with ingress point 1 being more favorable than ingress points 2 and 3.

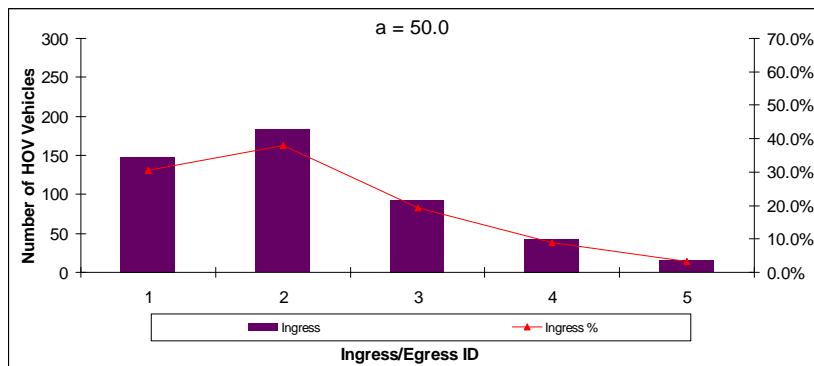
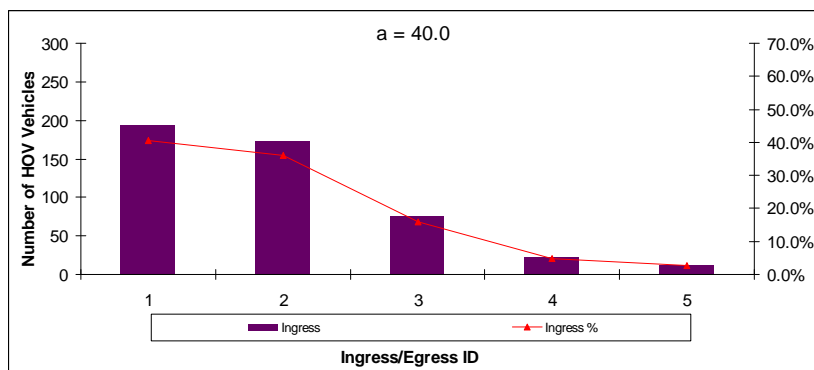
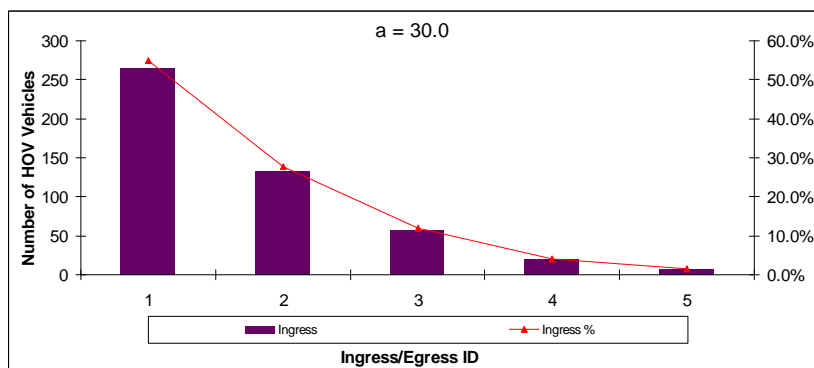
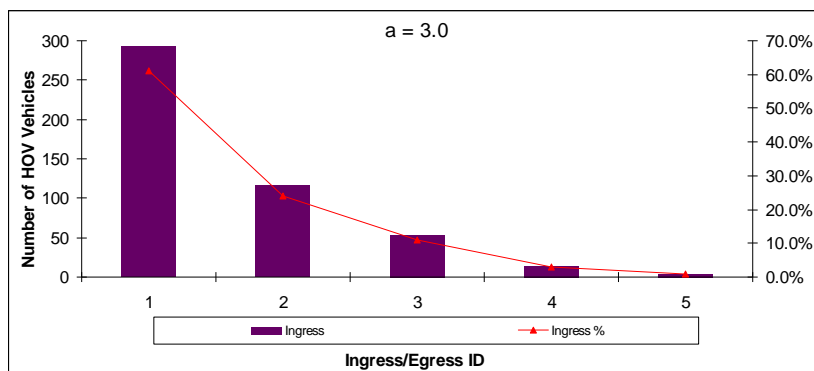


Figure 5-17. Case 4 results variation with parameter a

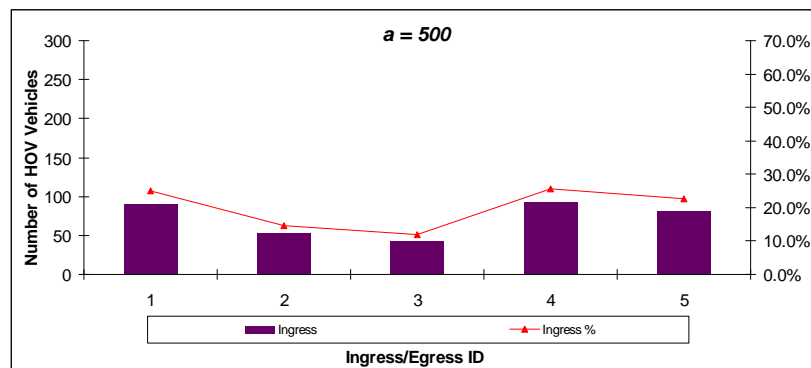
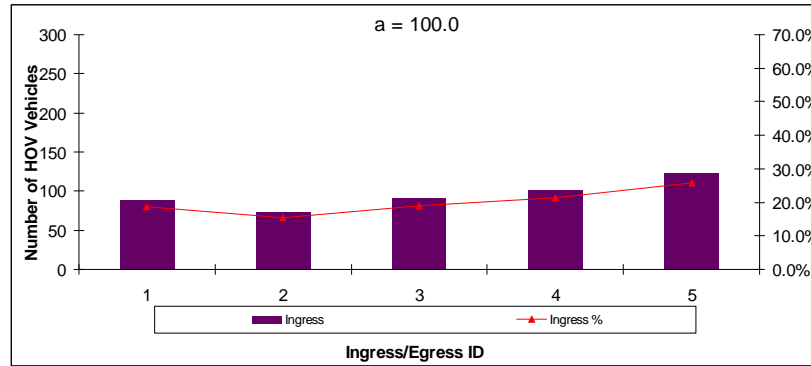
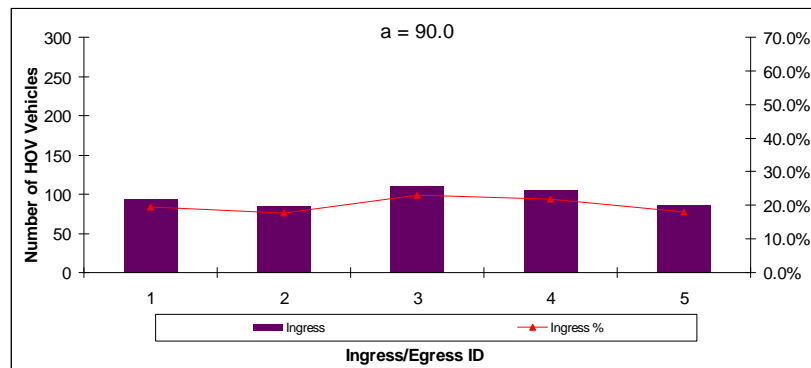
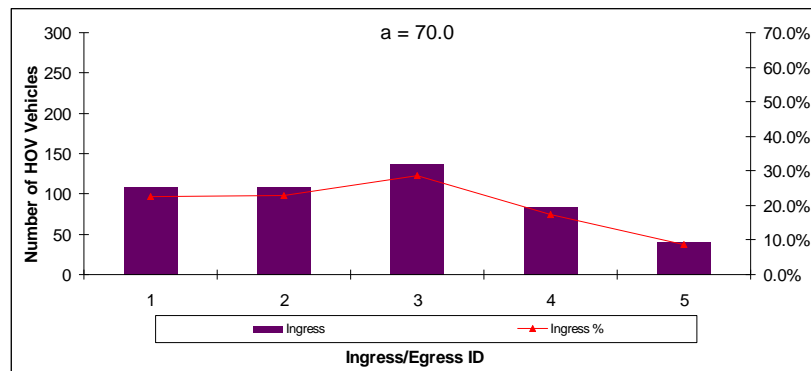


Figure 5-18. Case 4 results variation with parameter *a* (cont.)

5.3 Sensitivity Analysis using the SR-57 Network

The freeway network selected for sensitivity analysis is SR-57 SB network in Orange County, California. The HOV-eligible vehicles traveling from Lambert Rd to Chapman Ave via SR-57 (about 9.6 mi, as shown in Figure 5-11) are controlled by the buffer-separated HOV access plugin. There are eight ingress/egress points in the network, and the number of lanes varies from four lanes to seven lanes. The simulation time is 1.25 hour, during which the traffic begins with free flow conditions and shifts to stop-and-go congested conditions.

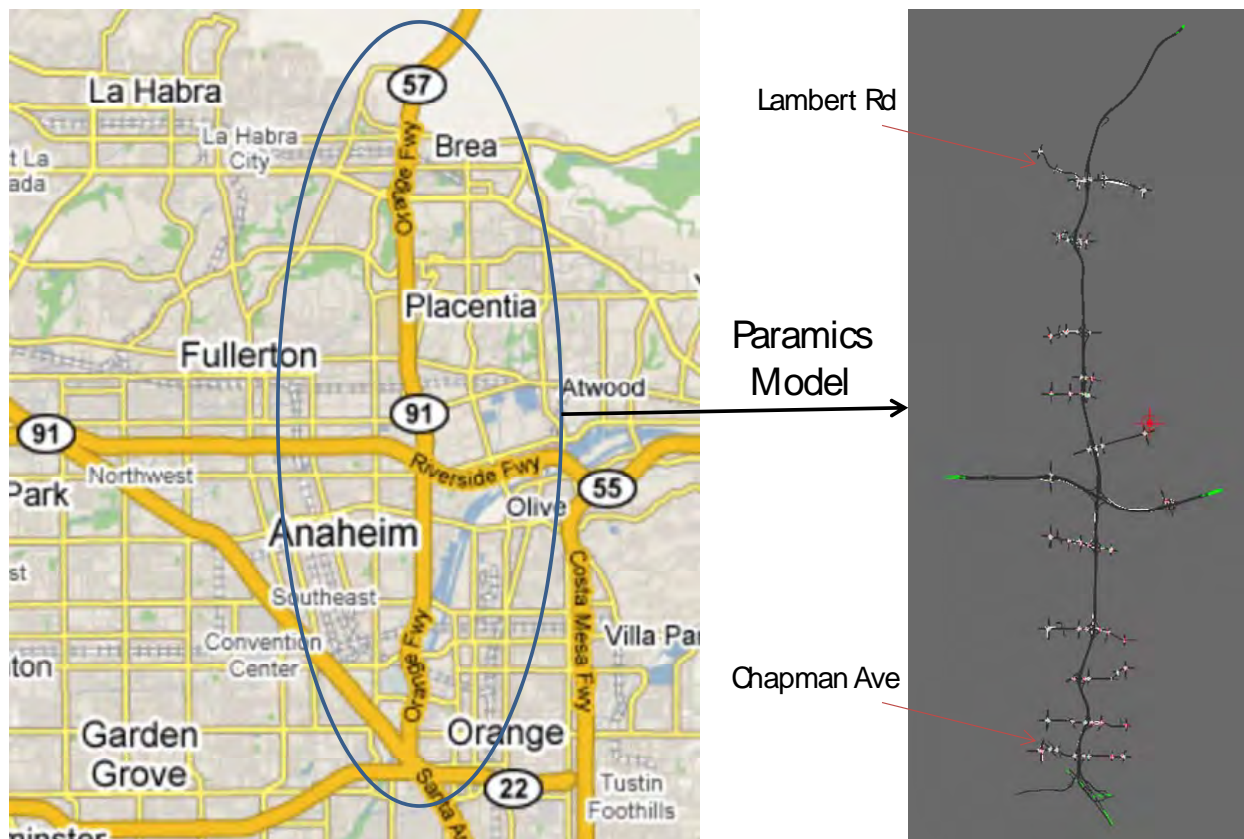


Figure 5-19. Freeway Network for Sensitivity Analysis: SR-57 Network

Because the SR-57 network involves various traffic conditions during the simulation time period, we first run tests on the parameter α to examine how the travel time savings affect the proposed model. The settings of calibration parameters and the implementation parameters are as shown below:

- Calibration parameters:
 - Parameter a : $a = 3.0$
 - Parameter b : $b = 0.9$
 - Parameter L_{car} : $L_{car} = 20\text{ ft}$
 - Parameter α : $-0.5 \leq \alpha \leq -10$

- Implementation parameters:
 - Ingress Priority: 80% HOV vehicles will only consider the first 4 ingress points (i.e. ingress points 1 to 4) to enter the HOV lane.
 - Egress Persistency: after entering the HOV lane, 80% HOV vehicles will only consider the last 3 egress points (i.e. egress points 6 to 8) to leave current HOV lane.
 - Preference Probability Threshold: $PV_TH > 0.01$
 - Update Time Interval: $PV_TIME = 30$

First, we analyzed the sensitivity of parameter α . As shown in Figure 5-12, it is found that more HOV vehicles take the first access and the last access as the ingress and egress points respectively with larger settings of parameter α . This is because larger values of parameter α imply that the HOV drivers derive greater benefit from any travel time savings associated with travel on the HOV lane. Therefore, the HOV drivers enter the HOV lane as soon as possible and stay in HOV lane until as close to their destination as possible.

Next, we performed sensitivity analysis for parameter a by assuming $\alpha = -7.0$. The settings of calibration parameters and the implementation parameters are as shown below:

- Calibration parameters:
 - Parameter a : $3.0 \leq a \leq 50$
 - Parameter b : $b = 0.9$
 - Parameter L_{car} : $L_{car} = 20\text{ft}$
 - Parameter α : $\alpha = -7.0$
- Implementation parameters:
 - Ingress Priority: 80% HOV vehicles will only consider the first 4 ingress points (i.e. ingress points 1 to 4) to enter the HOV lane.
 - Egress Persistency: after entering the HOV lane, 80% HOV vehicles will only consider the last 3 egress points (i.e. egress points 6 to 8) to leave current HOV lane.
 - Preference Probability Threshold: $PV_TH > 0.01$
 - Update Time Interval: $PV_TIME = 30$

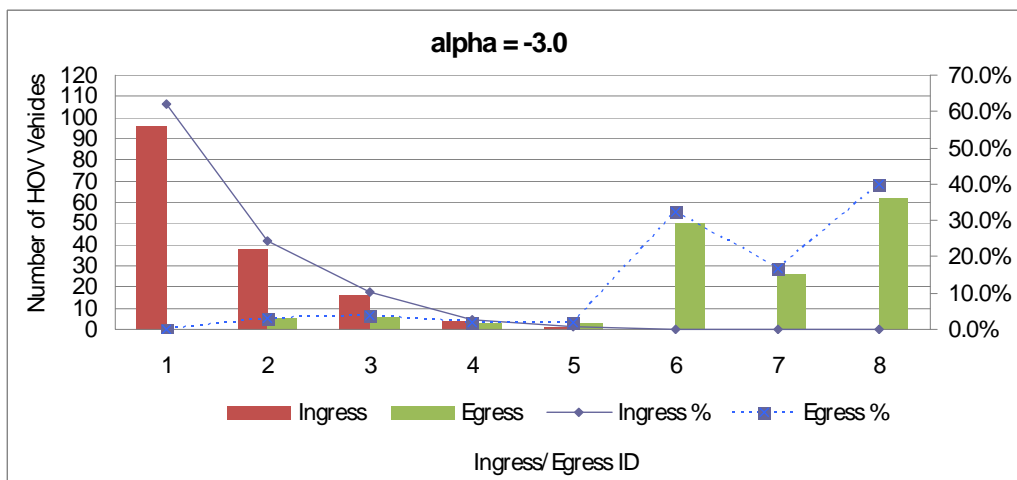
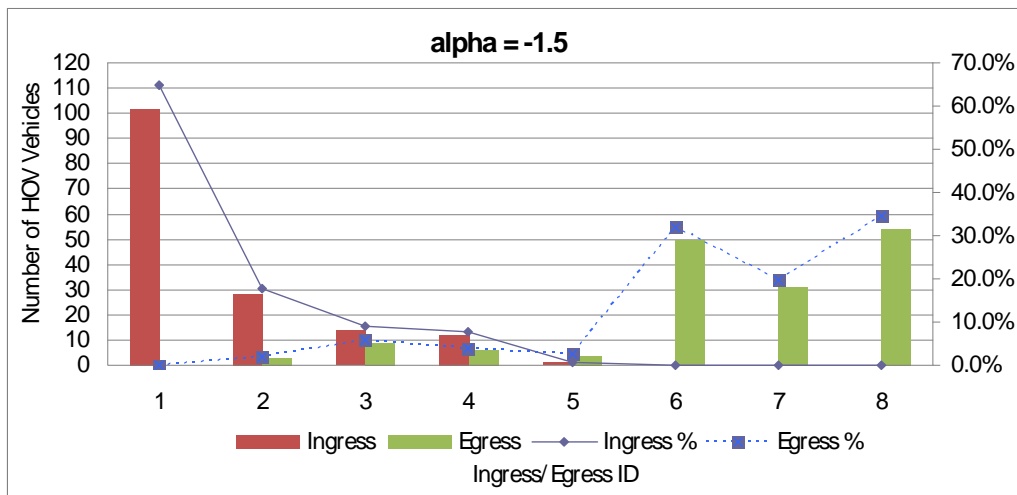
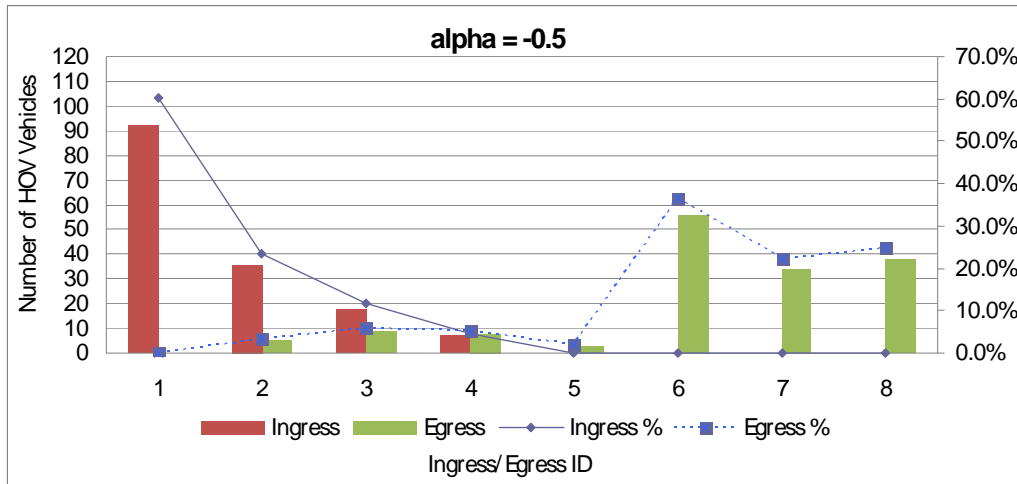


Figure 5-20. SR-57 Network sensitivity analysis results for different values of α

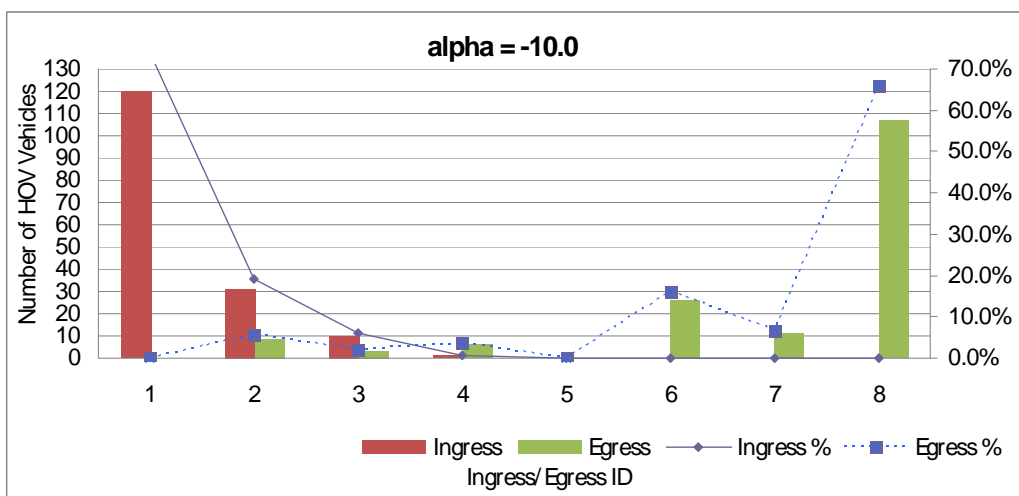
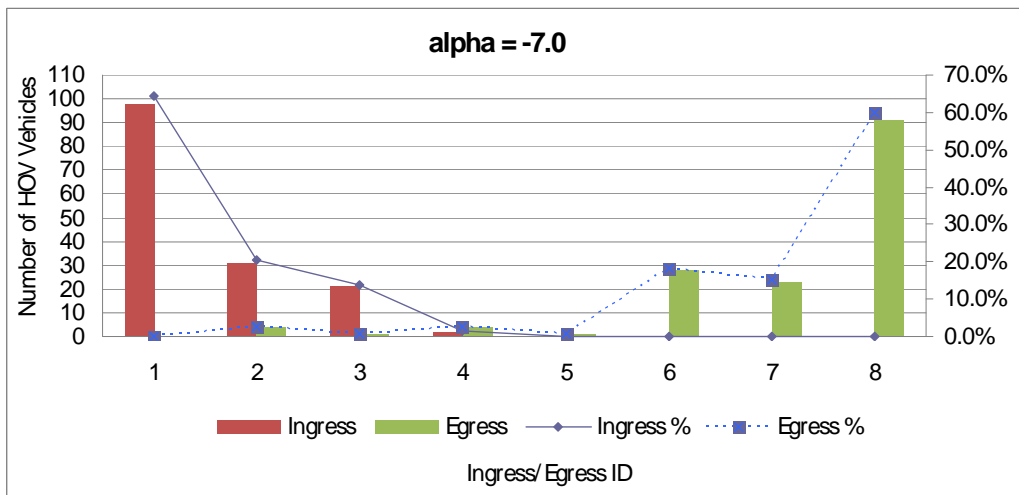
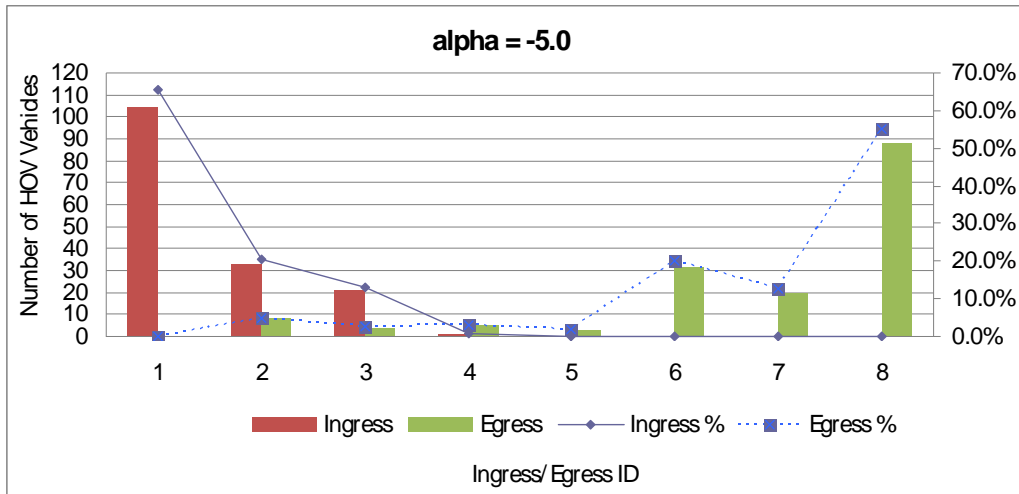


Figure 5-21. SR-57 Network sensitivity analysis results for different values of α (cont.)

As shown in Figure 5-13, it is found that high usages of ingress point 1 (> 65%) are observed for all scenarios. The usage of the egress point 6 increases as the value of parameter a increases, due to the setting of the egress persistency implementation parameter.

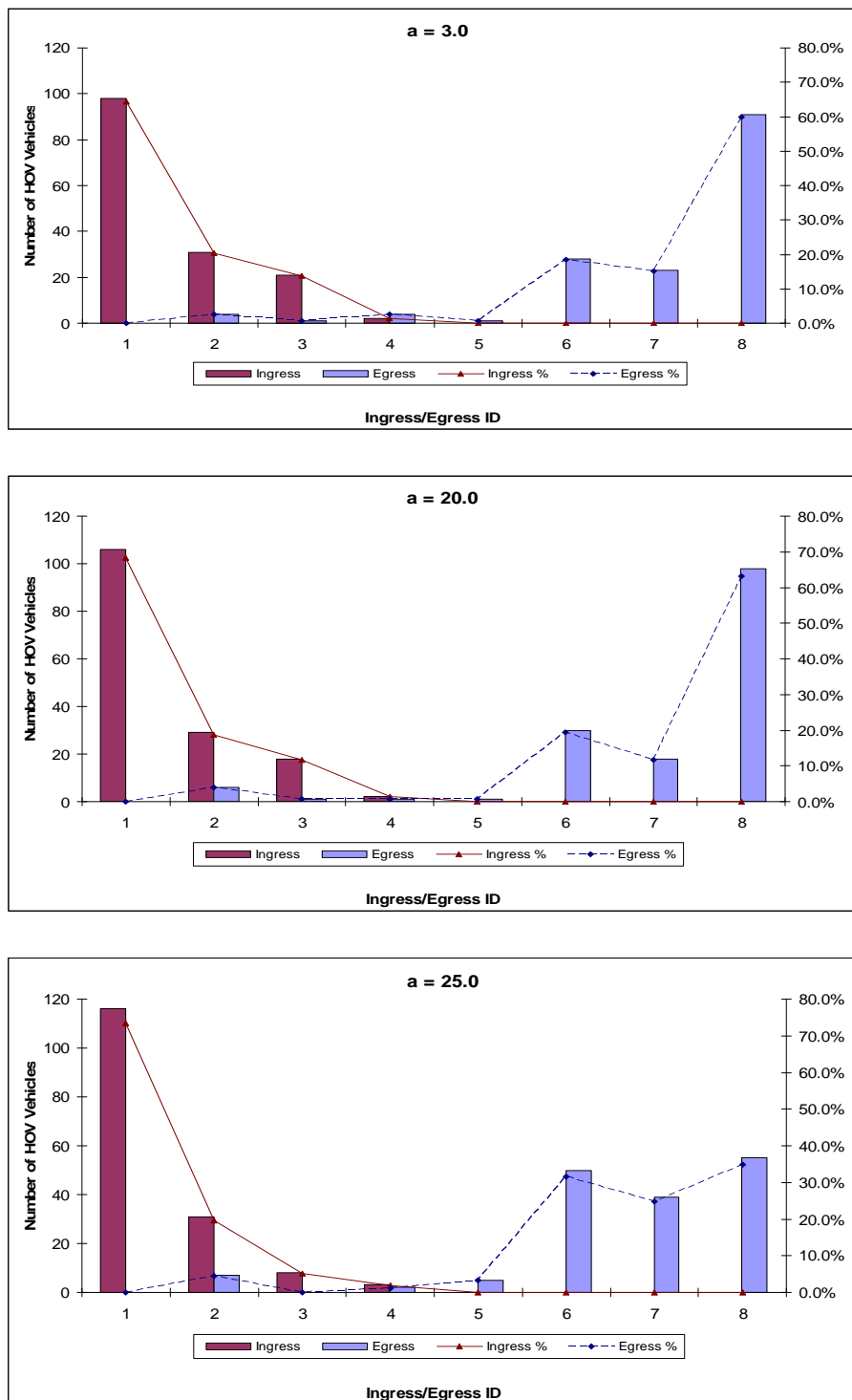


Figure 5-22. SR-57 Network sensitivity analysis results for different values of a

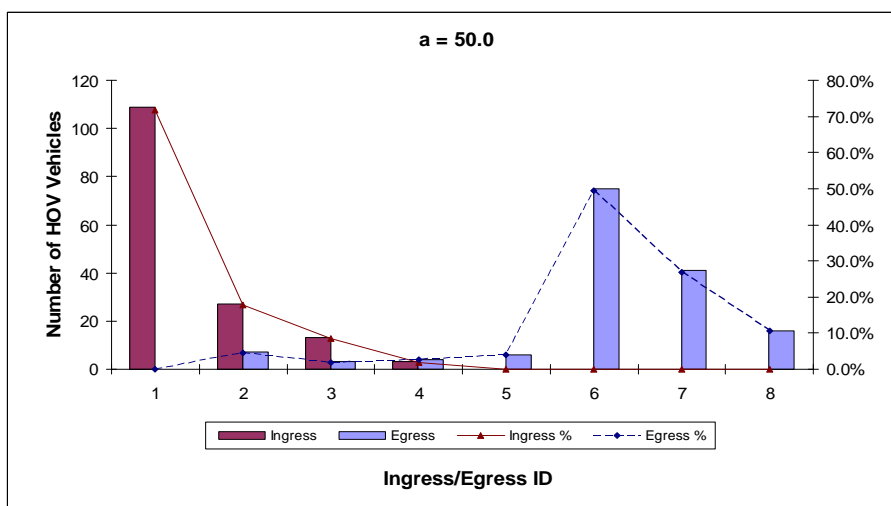
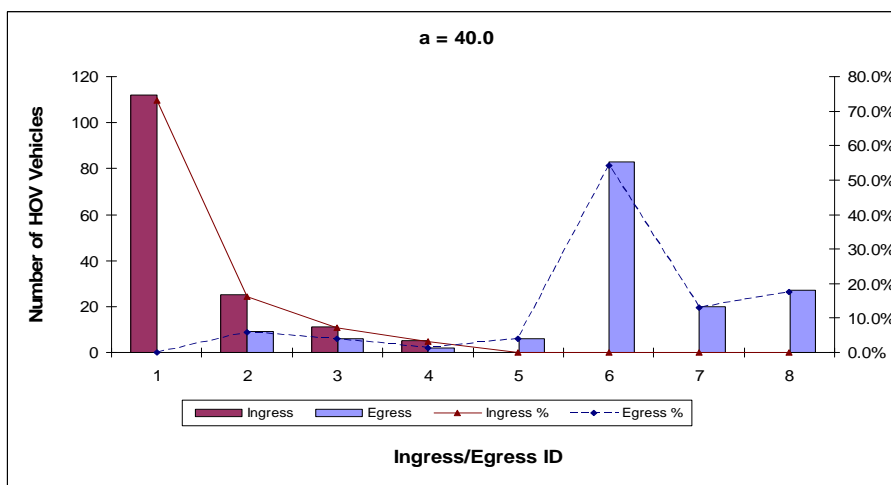
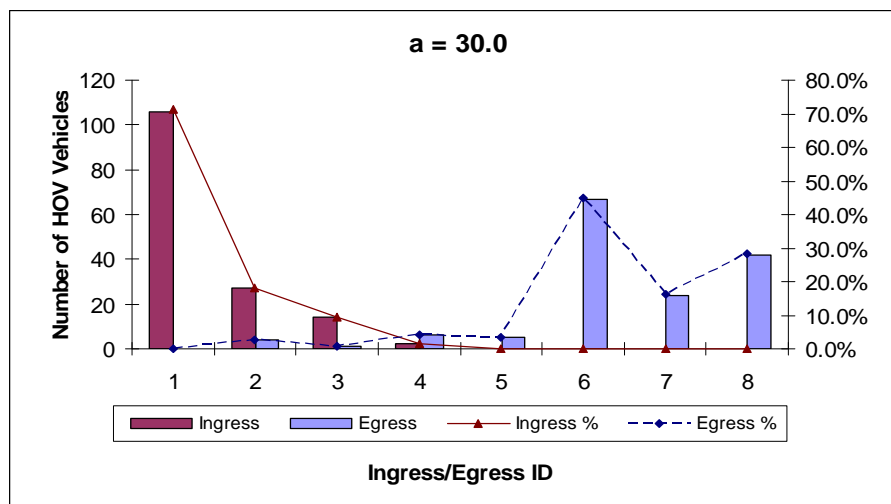


Figure 5-23. SR-57 Network sensitivity analysis results for different values of *a* (cont.)

5.4 Model Validation and Discussion

In Section 5.3, we analyzed and discussed the sensitivities of the results relative to the calibration parameters and implementation parameters. To validate the proposed HOV driver behavioral model, we further investigated the results collected at ingress point 1. This location is selected because based on the nature of the proposed model, HOV drivers should prefer to take the first available ingress point to enter the HOV lane as long as they can benefit from the travel time savings and there are traffic conditions that permit the weaving necessary to access the HOV facility.

Based on the results described in Figure 5-13, it is assumed that the case with parameter $a = 25.0$ can accurately replicate the real world scenario. Under the condition, the usages at ingress point 1 are compared against flow and travel time, as shown in Figure 5-14, Figure 5-15, and Figure 5-16. It must be noted that only the HOV vehicles that completed their trips within the simulation time are discussed here.

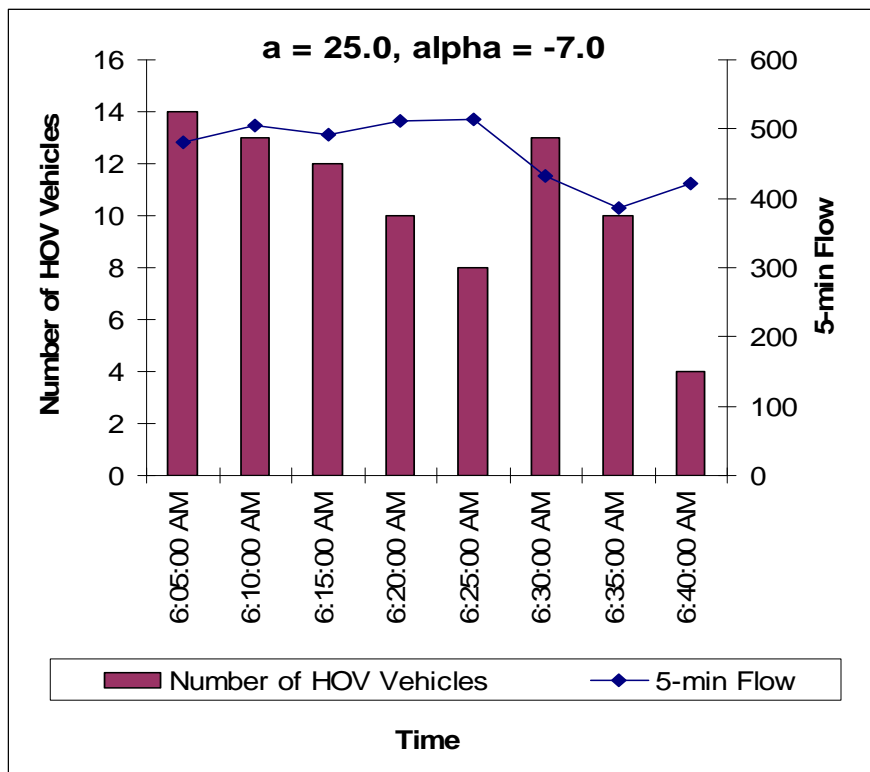


Figure 5-24. Model validation: Usage of ingress point 1 vs 5-min flow

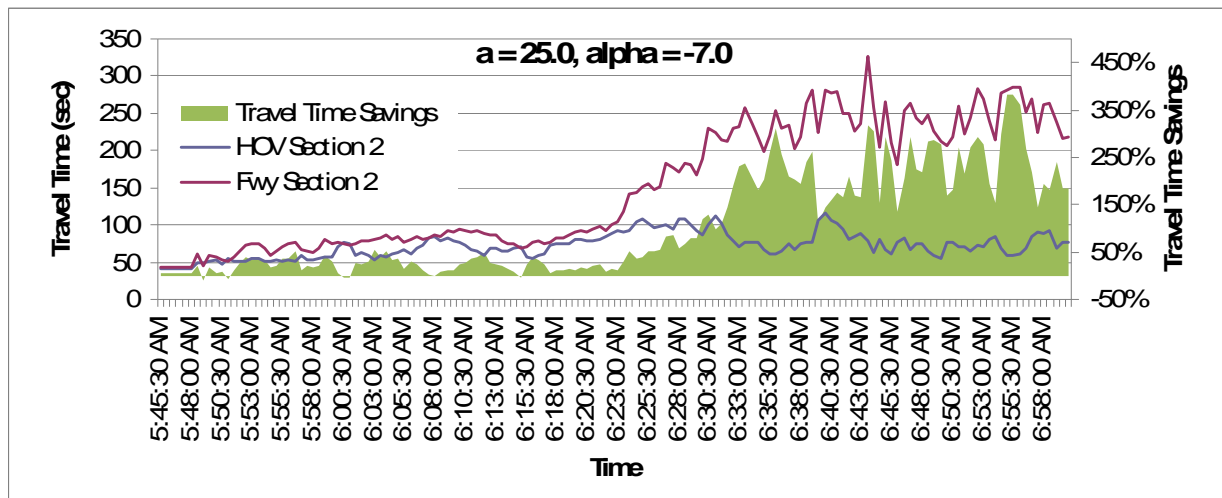


Figure 5-25. Model Validation: Travel time savings at ingress point 1

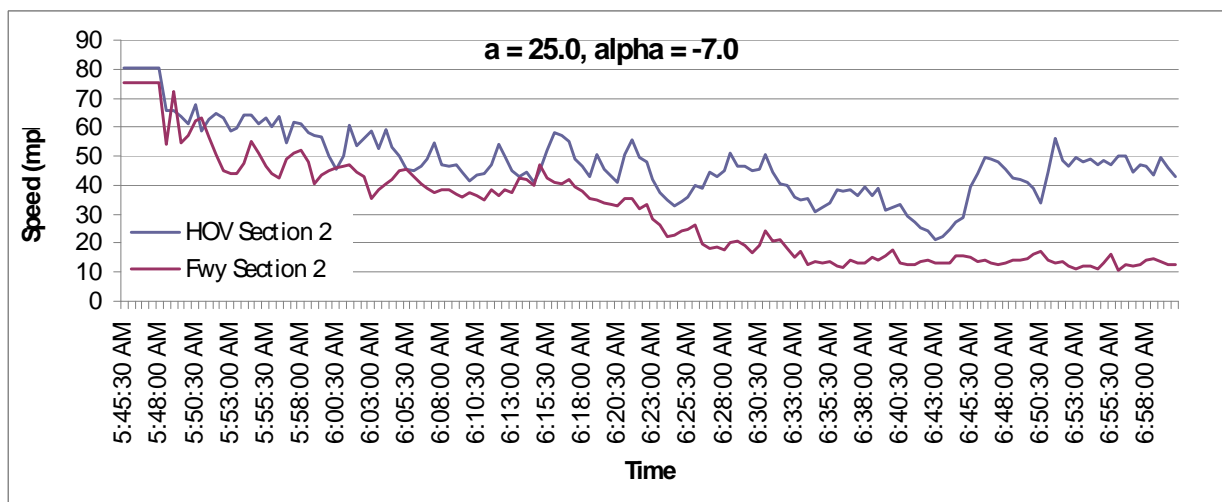


Figure 5-26. Model Validation: Speed at ingress point 1

According to Figure 5-14, Figure 5-15, and Figure 5-16, it is found that the HOV ingress point usage drops at 6:10am as the savings of travel time decreases. As the flow increases from 6:10am to 6:25am, the usage of the ingress point 1 continues to decrease due to insignificant travel time savings. Note that traffic conditions become very congested around 6:25am. In addition, the freeway travel time starts increasing around 6:25am and reaches the peak around 6:35am, while the 5-min flow starts decreasing after 6:25am and the speed starts decreasing after 6:20am. Although, as expected, the usage of ingress point 1 also increases while the congestion forms, it drops again after 6:35am, ostensibly because the speed on the freeway mainline is low and the traffic is very congested, thus decreasing the opportunity for the HOV-eligible vehicles to execute the lane-changing maneuvers required to take the first ingress point to enter the HOV lane.

To examine the usage of ingress point 1 under free flow condition, a demand scalar is applied to reduce the freeway mainline demand. The scalar is set to 0.8. The results are shown in Figure 5-17, Figure 5-18, and Figure 5-19.

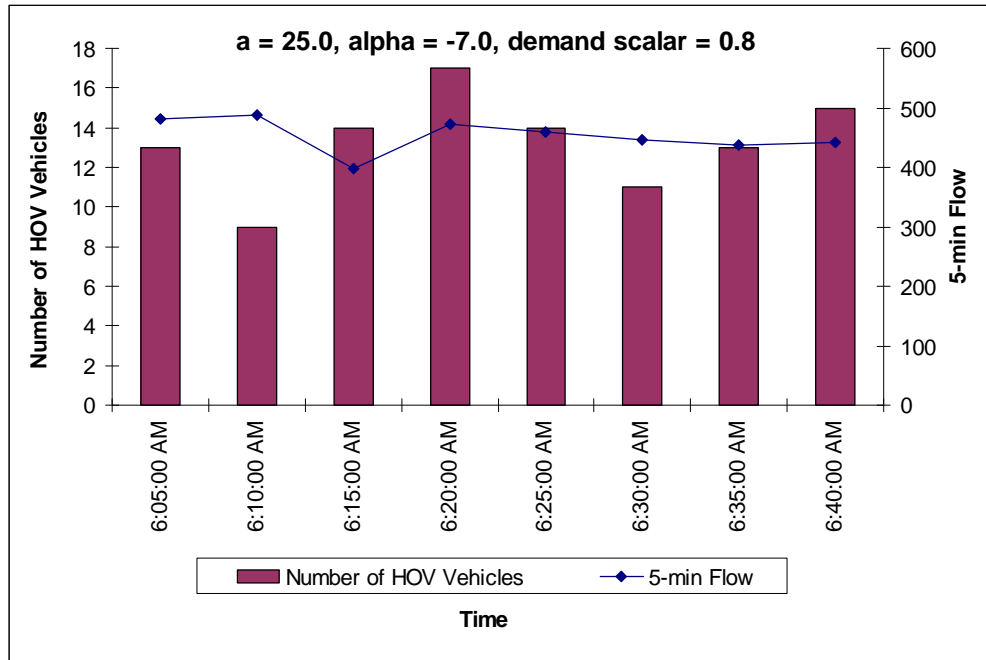


Figure 5-27. Model Validation under free flow conditions: Usage of ingress point 1

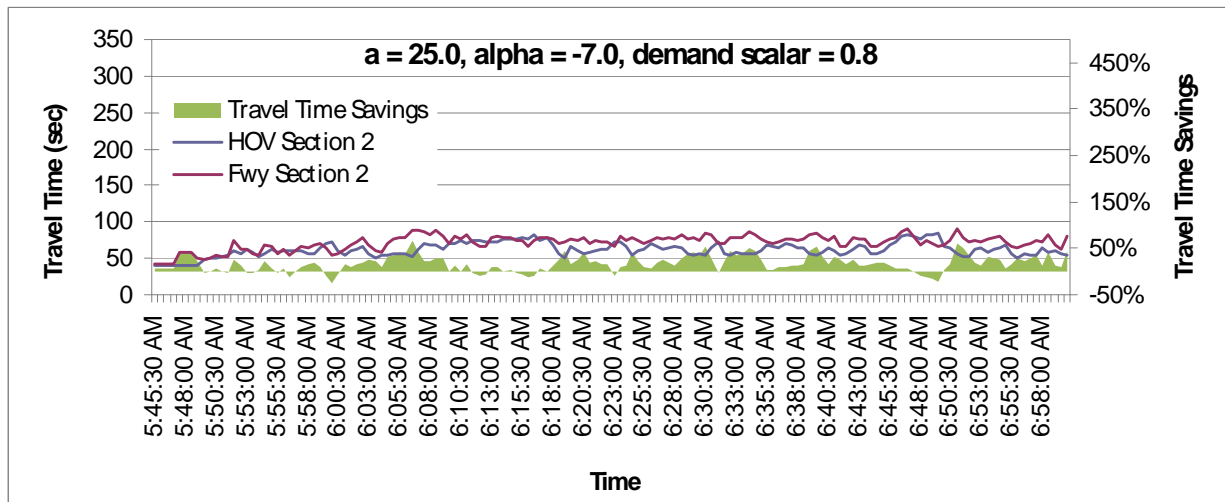


Figure 5-28. Model Validation under free flow conditions: Travel Time Savings

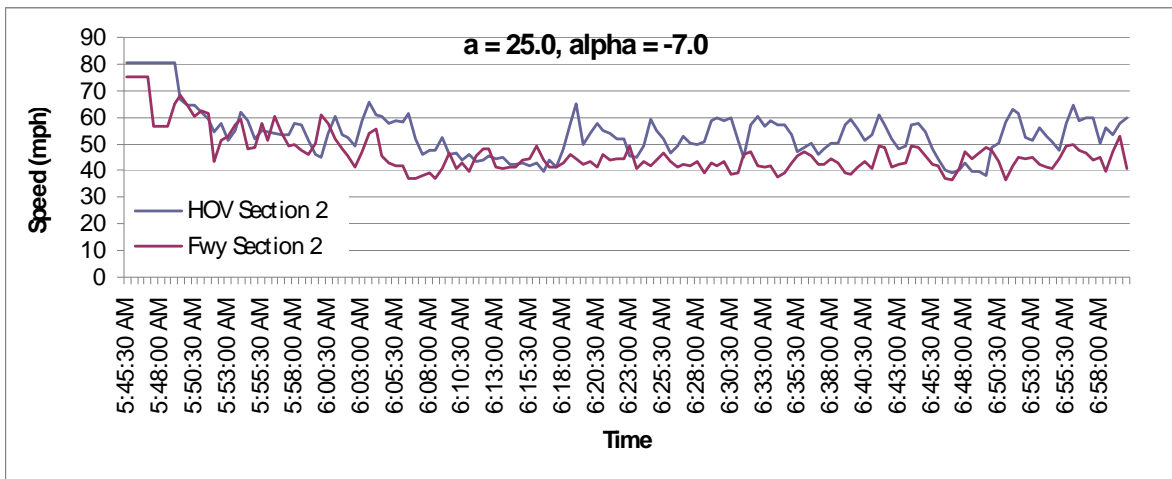


Figure 5-29. Model Validation under free flow conditions: Speed

It can be observed that usage of ingress point 1 drops as the savings of travel time decreases. However, the relationship between ingress point usages and 5-min flow is not strong. In addition, and consistent with the model formulation, with the demand of the mainline freeway scaled down, usage of ingress point 1 is greater than that in the case without applying demand scalar.

Another simulation run without applying the plugin was performed for comparison. In this case, the demand was not scaled. In addition, the dynamic feed back function in Paramics was enabled and was set to 2 minutes, so that the HOV-eligible vehicles would prefer to use HOV lane if the travel cost is lower on HOV lane. It must be noted that about 15% HOV-eligible vehicles re-entered the HOV lane after leaving it, and only the first action was considered here. Furthermore, all HOV-eligible vehicles in the network were affected by the dynamic feedback control; in other words, the travel time savings on HOV lane may become less significant, since the HOV-eligible vehicles would stick to HOV lane as long as the travel cost is lower on HOV lane. The results are shown in Figure 5-20 and 5-21.

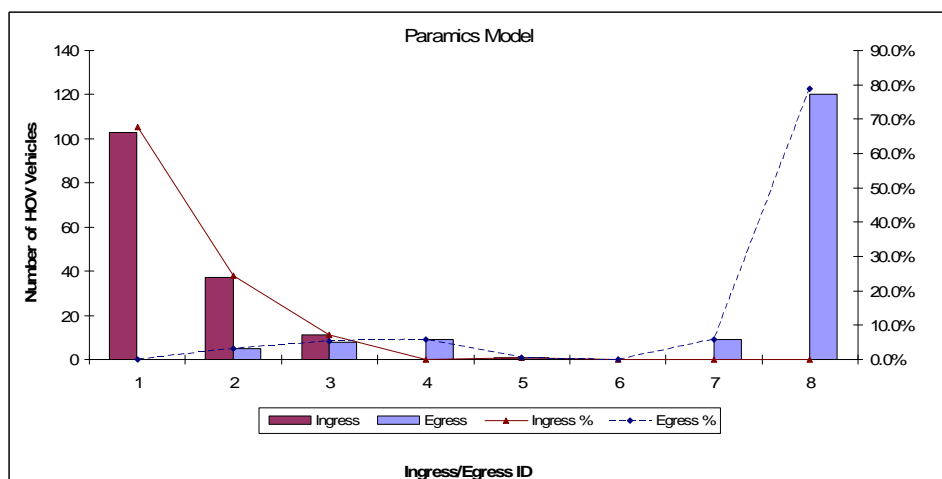


Figure 5-30. Ingress/egress point usages with dynamic feedback control

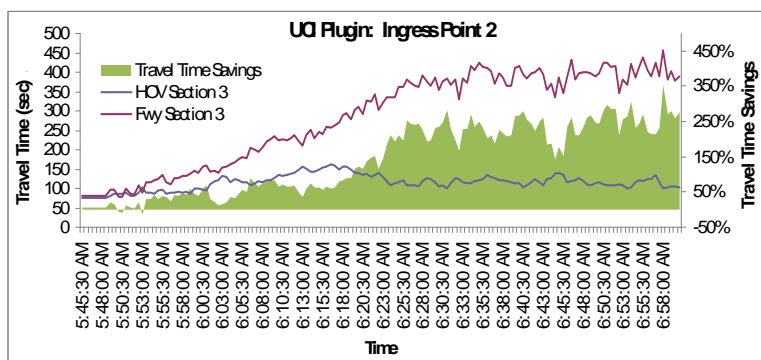
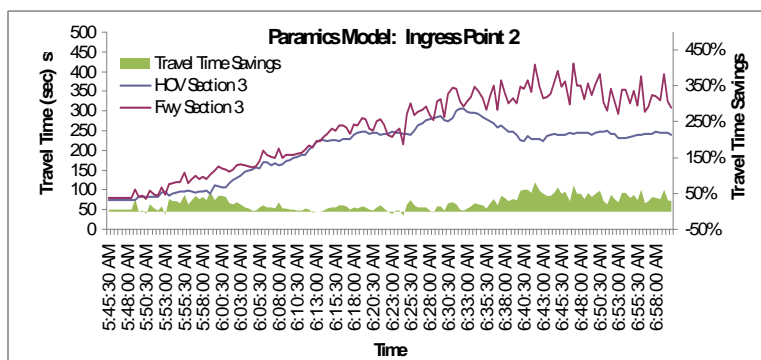
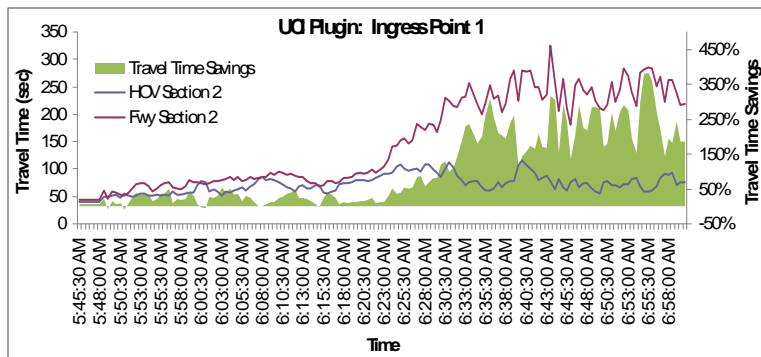
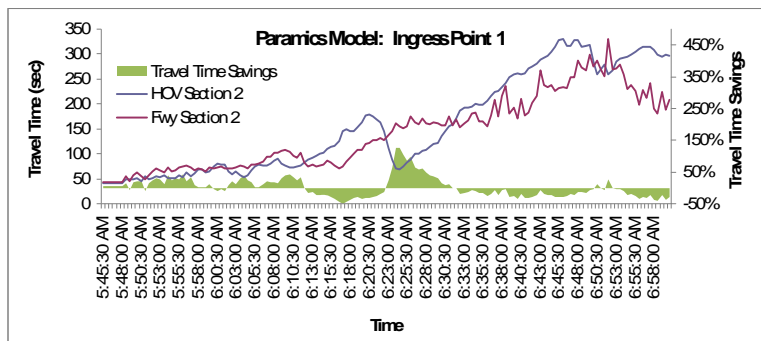


Figure 5-31. Travel time saving comparison

It can be seen from Figure 5-20 that high usage occurred at the first ingress point and at the last egress point. The travel time savings at ingress point 1 and 2 are decreased dramatically as shown in Figure 5-21. The results of travel time savings from the proposed model are also displayed to compare with the Paramics model. It is obvious that less congestion effects are found with the proposed model. The speeds and densities in the vicinities of these two HOV ingress/egress points for the current Paramics Model against the proposed plugin are shown in Figure 5-22. At ingress point 1, more vehicles traveled at higher speeds and lower densities in the case of our plugin, while at ingress point 2, more vehicles traveled at higher densities with speeds around 10 mph compared with Paramics model.

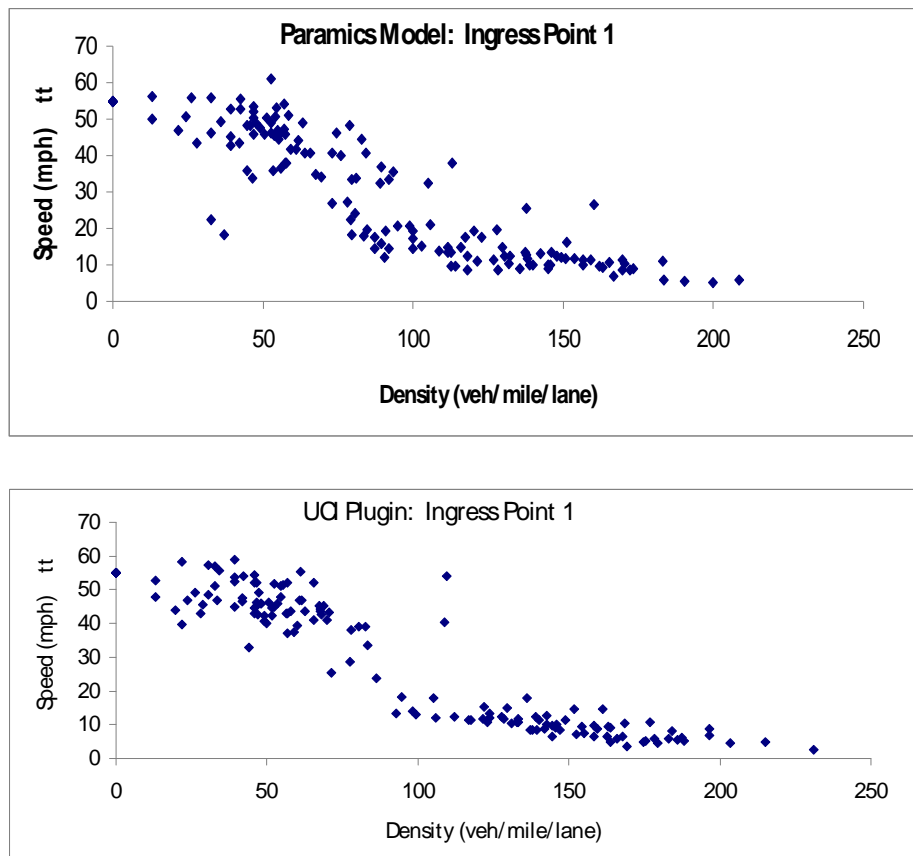


Figure 5-32. Speed-Density comparison at ingress point 1

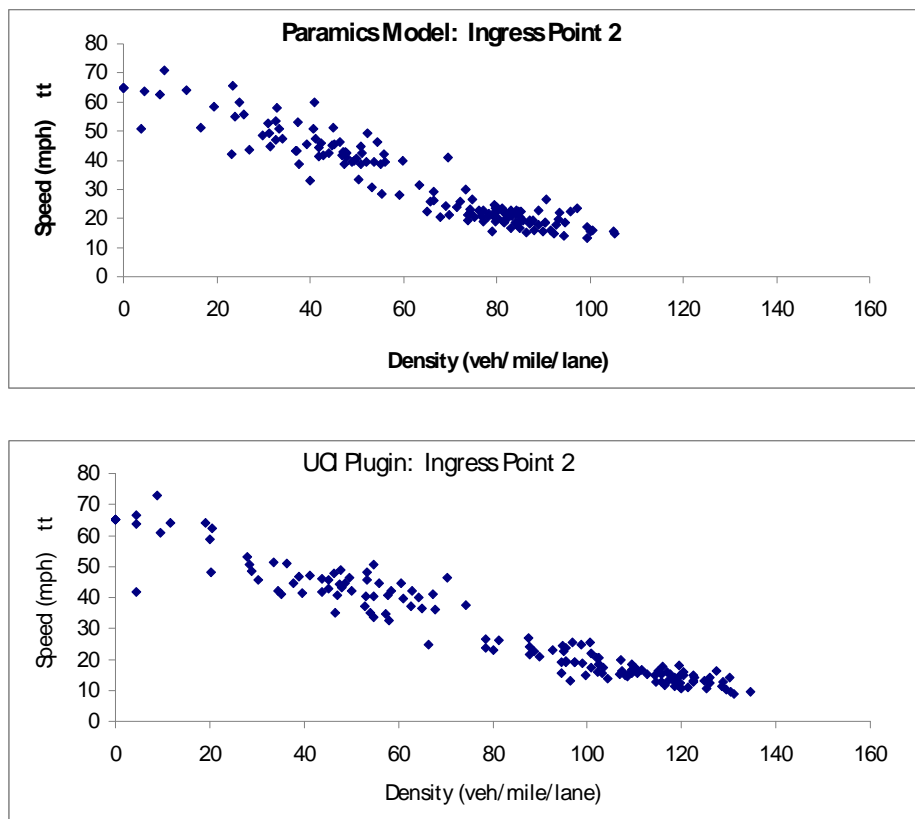


Figure 5-33. Speed-Density comparison at ingress point 2

6. Conclusions

This project proposed a new HOV driver behavioral model that incorporates an access preference/choice model for examining travel time savings and a traffic model for calculating the acceptable gap to get in/out of the HOV lane. A buffer-separated HOV access plugin was also developed using a micro-simulation tool, Paramics, based on the proposed model. In order to extend its capability for implementation, additional parameters were applied during the model development process, including ingress and egress points selection control, and traffic information update. The plugin was applied to a sample network and a real-world freeway network for analyzing the reasonableness of the model through sensitivity analysis. The freeway network was further investigated for model validation purposes.

The results have shown the reasonableness of the proposed model under various traffic conditions. The proposed model also demonstrated its feasibility and applicability via setting various calibration parameters and control parameters. It is recommended that detailed HOV ingress/egress point usage data and HOV path information should be obtained from real world to further calibrate and validate the proposed model.

References

- Breiland, C., L. Chu, and H. Benouar (2006). "Operational Effect of Allowing Single Occupant Hybrid Vehicles into High Occupancy Vehicle Lanes," *Transportation Research Record 1959*, pp. 151-158.
- Brownstone, D., L. Chu, T. Golob, K. S. Nesamani, and W. Recker (2007). *Evaluation Of Incorporating Hybrid Vehicle Use of HOV Lanes*. California PATH Research Report for Task Order 5315, UCB-ITS-PRR-2008-26, University of California, Berkeley.
- California Department of Transportation (Caltrans), Division of Traffic Operations (2003). *High-Occupancy Vehicle Guidelines*. Accessed on June 15, 2009: http://www.dot.ca.gov/hq/traffops/systemops/hov/hov_sys/guidelines/
- Choudhury, C. F. (2005). *Modeling Lane-changing Behavior in Presence of Exclusive Lanes*. MS Thesis, Massachusetts Institute of Technology.
- Chu, X. (1993). *Trip Scheduling and Economic Analysis of Transportation Policies*. Ph.D. Dissertation, University of California, Irvine.
- Dahlgren, J. (2002). "High-occupancy/toll lanes: where should they be implemented," *Transportation Research Part A 36(3)*, pp. 239-255.
- Giuliano, G., D. W. Levine, and R. F. Teal (1990). "Impact of high occupancy vehicle lanes on carpooling behavior," *Transportation*, Vol. 17, No. 2, pp. 159-177.
- Hill, E. G. (2000). *HOV Lanes in California: Are They Achieving Their Goals?* Legislative Analyst Office, California. Accessed on June 23, 2009: http://www.lao.ca.gov/2000/010700_hov/010700_hov_lanes.pdf
- Kostyniuk, L. P. (1982), "Demand Analysis for Ridesharing: State-of-the-Art Review," *Transportation Research Record 876*, pp. 17-26.
- McDonald, N. C., and R. B. Noland (2001), "Simulated Travel Impacts of High Occupancy Vehicle Lane Conversion Alternatives," *Transportation Research Record 1765*, pp. 1-7.
- Rodier, C. J., and R. A. Johnston (2000). "A Comparison of High Occupancy Vehicle, High Occupancy Toll, and Truck-Only Lanes in the Sacramento Region." *University of California Transportation Center Report, No. 422*, Berkeley, California.
- Small, K. A. (1977). "Priority Lanes on Urban Radial Freeways: An Economic-simulation Model," *Transportation Research Record 637*, pp. 8-13.
- Stuster, J. and Z. Coffman (1998). *Synthesis of Safety Research Related to Speed and Speed Limits*. FHWB-RD-98-154, Federal Highway Administration. Accessed on June 22, 2009: www.tfhr.gov/safety/speed/speed.htm and www.tfhr.gov/safety/speed/speed.htm

Teal, R. F. (1987). "Carpooling: who, how and why," *Transportation Research Part A* 21(3), pp. 203–214.

Ungemah, D. and M. Swisher (2006). "So You Want to Make a High-Occupancy Toll Lane?" *Transportation Research Record* 1960, pp.94-98.

Varaiya, P. (2007). *Effectiveness of California's High Occupancy Vehicle (HOV) System*. California PATH Research Report, UCB-ITS-PRR-2007-5, University of California, Berkeley.

Wellander, C., and K. Leotta (2000). "Are High-Occupancy Vehicle Lanes Effective? Overview of High-Occupancy Vehicle Facilities Across North America," *Transportation Research Record* 1711, pp. 23-30.

Appendix A: Plugin Input Specifications and Plugin Pseudo Code

Input files:

File name: HOV_p_control.txt

Parameters:

- PV_TIME (Update Time Interval): $PV_TIME > 0$; the time interval (seconds) to update the traffic information.
- V_EST_A (α , Scale Parameter): $V_EST_A < 0$; to specify the relationship between travel time and utility to enter/exit HOV lane.
- PV_TH (Preference Probability Threshold): $PV_TH > 0$; the values of P_i^e and P_{i+k}^x must be greater than PV_TH to be considered as a candidate ingress/egress point.
- H_EST_A (a , Lane Changing Control Parameter): $H_EST_A \geq 1$; a vehicle will need at least a spatial gap $> a \cdot L_{car}$.
- H_EST_B (b , Lane Changing Control Parameter): $H_EST_B \leq 1$; a vehicle can decrease its speed by some fraction b in order to make a lane change.
- H_EST_L (L_{car} , Vehicle Length): Vehicle length in feet.

File name: hov_info.txt

Parameters:

- Number of Origin Zone: The number of origin zones that the target HOV-eligible vehicles are released from.
- Origin: Origin Zone Index; separated by space while input more than one index.
- Number of Destination Zone: The number of destination zones that the target HOV-eligible vehicles will arrive at.
- Destination: Destination Zone Index; separated by space while input more than one index.
- Number of HOV vehicle type: The number of HOV vehicle types in the network.
- HOV vehicle type: HOV Vehicle Type Index.
- Ingress priority and percentage: This parameter is used to reflect the extent of the choice set for selecting favorable ingress points and the proportion of the drivers that will follow this rule; separated by space.
- Egress persistency and percentage: This parameter is used to reflect the persistency of staying in the HOV lane before considering exiting at a favorable egress point, and the proportion of the drivers that will follow this rule; separated by space.

File name: fwy_route.txt

Format:

- First line: Total number of freeway sections on a given route
- Second line: The first section index and the number of node within this section; separated by space.
- Third line: Node name of each node in the first section from upstream to downstream; separated by space.

- Fourth line: The second section index and the number of node within this section; separated by space.
- Fifth line: Node name of each node in the second section from upstream to downstream; separated by space.
- ...

File name: hov_route.txt

Format:

- First line: Total number of HOV sections on a given route
- Second line: The first section index and the number of node within this section; separated by space.
- Third line: Node name of each node in the first section from upstream to downstream; separated by space.
- Fourth line: The second section index and the number of node within this section; separated by space.
- Fifth line: Node name of each node in the second section from upstream to downstream; separated by space.
- ...

File name: hov_ingress.txt

Format:

- First line: Total number of ingress sections on a given route
- Second line: The first section index and the number of node within this section; separated by space.
- Third line: Node name of each node in the first section from upstream to downstream; separated by space.
- Fourth line: The second section index and the number of node within this section; separated by space.
- Fifth line: Node name of each node in the second section from upstream to downstream; separated by space.
- ...

File name: hov_egress.txt

Format:

- First line: Total number of egress sections on a given route
- Second line: The first section index and the number of node within this section; separated by space.
- Third line: Node name of each node in the first section from upstream to downstream; separated by space.
- Fourth line: The second section index and the number of node within this section; separated by space.
- Fifth line: Node name of each node in the second section from upstream to downstream; separated by space.
- ...

Output files:File name: `_H_EST_A_veh_route.txt`

Variable name:

- Vehicle release time: Release time of a target HOV-eligible vehicle.
- Preferred ingress point: Ingress index of preferred ingress point.
- Preferred egress point: Egress index of preferred egress point.
- Vehicle index: Vehicle's unique index in the network
- Vehicle type: Vehicle type index
- Origin Zone: Original zone index.
- Destination Zone: Destination zone index.
- Node name: Name of each node (in order) that the vehicle visited

File name: `_H_EST_A_TT.txt`

Variable name:

- SectionID: Section ID
- Timestamp: Current simulation time.
- HOV_Sp: Averaged HOV section Speed.
- HOV_AvgTT: Averaged HOV section travel time.
- HOV_AvgVar: Variance of HOV section travel time
- HOV_Cnt: Number of HOV vehicles traveling over the section within the time interval.
- Fwy_Sp: Averaged freeway section Speed.
- Fwy_AvgTT: Averaged freeway section travel time.
- Fwy_AvgVar: Variance of freeway section travel time
- Fwy_Cnt: Number of freeway vehicles traveling over the section within the time interval.
- Avg_Fwy_LinkSpd: Weighted average freeway link speed.
- Avg_Fwy_LinkDty: Weighted average freeway link density.

Plugin Pseudo:

Step 1:

- Load the following inputs when open a network:
 - HOV plugin implementation parameters info
 - HOV network settings info
 - Freeway route info
 - HOV route info
 - Ingress info
 - Egress info

Step 2:

- Tag the target HOV-eligible vehicle when it is released to the network

- Output route information of the target HOV-eligible vehicle when it arrives at its destination

Step 3:

- When a vehicle is transferring to next section, update its travel time of current section
- At each time interval, update:
 - HOV section travel time
 - Freeway section travel time
 - Preferences probability of each ingress and egress points

Step 4:

- When a tagged vehicle first enters the pre-defined route segment:
 - Compute acceptable gap to get in the HOV lane for each ingress point
 - Compute the probabilities of choosing each ingress point (P_i^e)
 - Determine the preferred ingress point from a random draw from the distribution of P_i^e
- Once a tagged vehicle enters the HOV lane from its preferred ingress point:
 - Compute acceptable gap to get out the HOV lane for each egress point
 - Compute the probabilities of choosing each egress point (P_{i+k}^x)
 - Determine the preferred egress point from a random draw from the distribution of P_{i+k}^x

Step 5:

- Re-route tagged vehicles by assigned ingress and egress points

Appendix B: Derivation of Preference to Enter HOV Lane at Ingress/Egress (i/e) i

Consider a driver's choice (or preference) to enter the HOV facility at entry point (i/e) i , conditioned on the decision to exit the facility at exit point (i/e) j . Consistent with standard random utility assumptions, let the utility of this choice be denoted by:

$$U_i^e = \sum_{q=1}^i U_q^F + \sum_{l=i+1}^j U_l^{HOV} ; i < j \leq n \quad (\text{B-1})$$

where U_i^e denotes the travel time utility of entering the HOV lane at i/e point i (under the presumption of exiting at i/e point j). Or, in matrix form

$$\mathbf{U}^e = \begin{bmatrix} U_1^e \\ U_2^e \\ U_3^e \\ \vdots \\ U_i^e \\ \vdots \\ U_j^e \end{bmatrix} = \begin{bmatrix} 1 & 0 & 0 & \cdots & 0 & 0 & 0 \\ 1 & 1 & 0 & \cdots & 0 & 0 & 0 \\ 1 & 1 & 1 & \cdots & 0 & 0 & 0 \\ \vdots & \vdots & \vdots & \ddots & \vdots & \vdots & \vdots \\ 1 & 1 & 1 & \cdots & 1 & 0 & 0 \\ \vdots & \vdots & \vdots & \ddots & \vdots & \vdots & \vdots \\ 1 & 1 & 1 & \cdots & 1 & 1 & 1 \end{bmatrix} \begin{bmatrix} U_1^F \\ U_2^F \\ U_3^F \\ \vdots \\ U_i^F \\ \vdots \\ U_j^F \end{bmatrix} + \begin{bmatrix} 0 & 1 & 1 & \cdots & 1 & 1 & 1 \\ 0 & 0 & 1 & \cdots & 1 & 1 & 1 \\ 0 & 0 & 0 & \cdots & 1 & 1 & 1 \\ \vdots & \vdots & \vdots & \ddots & \vdots & \vdots & \vdots \\ 0 & 0 & 0 & \cdots & 0 & 1 & 1 \\ 0 & 0 & 0 & \cdots & 0 & 0 & 1 \\ 0 & 0 & 0 & \cdots & 0 & 0 & 0 \end{bmatrix} \begin{bmatrix} U_1^{HOV} \\ U_2^{HOV} \\ U_3^{HOV} \\ \vdots \\ U_i^{HOV} \\ \vdots \\ U_j^{HOV} \end{bmatrix} \quad (\text{B-2})$$

(Note: the decision to enter the HOV lane at $j = n$ is *de facto* the decision not to enter the HOV lane at all; i.e., to use only the mainline freeway between O and D.) Assume $U_i^e = V_i^e + \xi_i^e$, where V_i^e denotes the utility (actually a disutility) associated with the expected travel time (or, generalized cost in the case of HOT lanes) using entry point i and ξ_i^e denotes the random delay associated with unknown traffic effects. Assume ξ_i^e are multivariate normal distributed, i.e.,

$$\mathbf{U}^e = \text{MVN}(\mathbf{V}^e, \mathbf{\Sigma}^e) \quad (\text{B-3})$$

where $\mathbf{\Sigma}^e$ is the covariance matrix.

Assume that the covariance between any two alternatives is only in the links they share in common; i.e.,

$$\text{Cov}(U_i^e, U_k^e) = \text{Var}(\xi_1^F + \xi_2^F + \cdots + \xi_i^F + \xi_{k+1}^{HOV} + \xi_{k+2}^{HOV} + \cdots + \xi_j^{HOV}) = \sigma_{F_i H_k}^2 ; i, k = 1, \dots, j \quad (\text{B-4})$$

So, for example,

$$\mathbf{M} = [M_{ik}] \tag{B-7}$$

$$M_{ik} = \begin{cases} 1, & k-i=1 \\ 0, & i=k=j \\ -\delta_{ik}, & \text{otherwise} \end{cases}$$

$$\mathbf{M} = \begin{bmatrix} -1 & 1 & 0 & \cdots & 0 & 0 & 0 & 0 \\ 0 & -1 & 1 & \cdots & 0 & 0 & 0 & 0 \\ 0 & 0 & -1 & \cdots & 0 & 0 & 0 & 0 \\ \vdots & \vdots & \vdots & \ddots & \vdots & \vdots & \vdots & \vdots \\ 0 & 0 & & \cdots & -1 & 1 & 0 & 0 \\ \vdots & & & & & \ddots & & \vdots \\ 0 & 0 & 0 & \cdots & 0 & & -1 & 1 \\ 0 & 0 & 0 & \cdots & 0 & 0 & 0 & 0 \end{bmatrix}$$

$$\Delta \mathbf{U}^e = \begin{bmatrix} U_2^e - U_1^e \\ U_3^e - U_2^e \\ U_4^e - U_3^e \\ \vdots \\ U_{i+1}^e - U_i^e \\ \vdots \\ U_j^e - U_{j-1}^e \\ 0 \end{bmatrix} = \mathbf{M} \mathbf{U}^e = \begin{bmatrix} -1 & 1 & 0 & \cdots & 0 & 0 & 0 & 0 \\ 0 & -1 & 1 & \cdots & 0 & 0 & 0 & 0 \\ 0 & 0 & -1 & \cdots & 0 & 0 & 0 & 0 \\ \vdots & \vdots & \vdots & \ddots & \vdots & \vdots & \vdots & \vdots \\ 0 & 0 & & \cdots & -1 & 1 & 0 & 0 \\ \vdots & & & & & \ddots & & \vdots \\ 0 & 0 & 0 & \cdots & 0 & & -1 & 1 \\ 0 & 0 & 0 & \cdots & 0 & 0 & 0 & 0 \end{bmatrix} \begin{bmatrix} U_1^e \\ U_2^e \\ U_3^e \\ \vdots \\ U_i^e \\ \vdots \\ U_j^e \end{bmatrix} = \begin{bmatrix} \Delta U_{21}^e \\ \Delta U_{32}^e \\ \Delta U_{43}^e \\ \vdots \\ \Delta U_{i+1,i}^e \\ \vdots \\ \Delta U_{j,j-1}^e \\ 0 \end{bmatrix} \tag{B-8}$$

Then,

$$\Delta \mathbf{U}^e = \text{MVN}(\mathbf{M} \mathbf{V}^e, \mathbf{M} \boldsymbol{\Sigma}^e \mathbf{M}^T) \tag{B-9}$$

$$\mathbf{M}\Sigma^e\mathbf{M}^T = \begin{bmatrix} (\sigma_{F_2}^2 - \sigma_{F_1}^2) & 0 & 0 & \dots & 0 & \dots & 0 & 0 \\ 0 & (\sigma_{F_3}^2 - \sigma_{F_2}^2) & 0 & \dots & 0 & \dots & 0 & 0 \\ 0 & 0 & (\sigma_{F_4}^2 - \sigma_{F_3}^2) & 0 & 0 & \dots & 0 & 0 \\ \vdots & \vdots & \vdots & \ddots & & & \vdots & \vdots \\ 0 & 0 & 0 & \dots & (\sigma_{F_i}^2 - \sigma_{F_{i-1}}^2) & \dots & 0 & 0 \\ \vdots & \vdots & \vdots & & & \ddots & \vdots & \vdots \\ 0 & 0 & 0 & \dots & 0 & \dots & (\sigma_{F_j}^2 - \sigma_{F_{j-1}}^2) & 0 \\ 0 & 0 & 0 & \dots & 0 & \dots & 0 & 0 \end{bmatrix}$$

$$+ \begin{bmatrix} (\sigma_{H_1}^2 - \sigma_{H_2}^2) & 0 & 0 & \dots & 0 & \dots & 0 & 0 \\ 0 & (\sigma_{H_2}^2 - \sigma_{H_3}^2) & 0 & \dots & 0 & \dots & 0 & 0 \\ 0 & 0 & (\sigma_{H_3}^2 - \sigma_{H_4}^2) & \dots & 0 & \dots & 0 & 0 \\ \vdots & \vdots & \vdots & & \vdots & & \vdots & \vdots \\ 0 & 0 & 0 & \dots & (\sigma_{H_i}^2 - \sigma_{H_{i+1}}^2) & \dots & 0 & 0 \\ \vdots & \vdots & \vdots & & \vdots & & \vdots & \vdots \\ 0 & 0 & 0 & \dots & 0 & \dots & \sigma_{H_{j-1}}^2 & 0 \\ 0 & 0 & 0 & \dots & 0 & \dots & 0 & 0 \end{bmatrix}$$

Or,

$$\mathbf{M}\Sigma^e\mathbf{M}^T = \begin{bmatrix} (\sigma_{F_2}^2 - \sigma_{F_1}^2) + (\sigma_{H_1}^2 - \sigma_{H_2}^2) & 0 & 0 & \dots & 0 & \dots & 0 & 0 \\ 0 & (\sigma_{F_3}^2 - \sigma_{F_2}^2) + (\sigma_{H_2}^2 - \sigma_{H_3}^2) & 0 & \dots & 0 & \dots & 0 & 0 \\ 0 & 0 & (\sigma_{F_4}^2 - \sigma_{F_3}^2) + (\sigma_{H_3}^2 - \sigma_{H_4}^2) & 0 & 0 & \dots & 0 & 0 \\ \vdots & \vdots & \vdots & \ddots & & & \vdots & \vdots \\ 0 & 0 & 0 & \dots & (\sigma_{F_i}^2 - \sigma_{F_{i-1}}^2) + (\sigma_{H_{i-1}}^2 - \sigma_{H_i}^2) & \dots & 0 & 0 \\ \vdots & \vdots & \vdots & & \vdots & \ddots & \vdots & \vdots \\ 0 & 0 & 0 & \dots & 0 & \dots & (\sigma_{F_j}^2 - \sigma_{F_{j-1}}^2) + \sigma_{H_{j-1}}^2 & 0 \\ 0 & 0 & 0 & \dots & 0 & \dots & 0 & 0 \end{bmatrix} \quad (\text{B-10})$$

$$\mathbf{M}\Sigma^e\mathbf{M}^T = \begin{bmatrix} \hat{\sigma}_1^2 & 0 & 0 & \dots & 0 & \dots & 0 & 0 \\ 0 & \hat{\sigma}_2^2 & 0 & \dots & 0 & \dots & 0 & 0 \\ 0 & 0 & \hat{\sigma}_3^2 & 0 & 0 & \dots & 0 & 0 \\ \vdots & \vdots & \vdots & \ddots & & & \vdots & \vdots \\ 0 & 0 & 0 & \dots & \hat{\sigma}_i^2 & \dots & 0 & 0 \\ \vdots & \vdots & \vdots & & \vdots & \ddots & \vdots & \vdots \\ 0 & 0 & 0 & \dots & 0 & \dots & \hat{\sigma}_{j-1}^2 & 0 \\ 0 & 0 & 0 & \dots & 0 & \dots & 0 & 0 \end{bmatrix}$$

where

(B-11)

$$\hat{\sigma}_i^2 = (\sigma_{F_{i+1}}^2 - \sigma_{F_i}^2) - (\sigma_{H_{i+1}}^2 - \sigma_{H_i}^2); \sigma_{H_j}^2 \equiv 0$$

$\mathbf{M}\Sigma^e\mathbf{M}^T$ being a diagonal matrix implies that the $\Delta U_{i,i-1}^e = U_i^e - U_{i-1}^e$; $i = 2, \dots, j$ are independent random variables. Then

$$\Pr\left[U_{i+1}^e \geq U_i^e \text{ and } U_{k+1}^e \geq U_k^e\right] = \Pr\left[\Delta U_{i+1,i}^e \geq 0\right] \cdot \Pr\left[\Delta U_{k+1,k}^e \geq 0\right] \quad (\text{B-12})$$

Let P_i^e denote the probability that HOV lane entry i will be preferred for the trip from O to D. Then

$$P_i^e = \Pr\left[U_i^e \geq U_k^e ; \forall k \in \mathbf{R}\right] \quad (\text{B-13})$$

where

$$\mathbf{R} = \{1, 2, 3, \dots, i, \dots, j\} \quad (\text{B-14})$$

Define

$$\begin{aligned} \mathbf{R}' &= \{\forall k < i ; k \in \mathbf{R}\} \\ \mathbf{R}'' &= \{\forall k > i ; k \in \mathbf{R}\} \end{aligned} \quad (\text{B-15})$$

Then,

$$P_i^e = \Pr\left[U_i^e \geq U_k^e ; \forall k \in \mathbf{R}'\right] \cdot \Pr\left[U_i^e \geq U_k^e ; \forall k \in \mathbf{R}''\right] \quad (\text{B-16})$$

But, assuming completely myopic driver behavior: i.e., that the driver will enter the HOV lane at the first opportunity for which the decision to enter is better than the decision to enter the next available i/e point:

$$\begin{aligned} \Pr\left[U_i^e \geq U_k^e ; \forall k \in \mathbf{R}'\right] &= \Pr\left[U_i^e \geq U_{i-1}^e \mid U_{i-1}^e \geq U_{i-2}^e\right] \cdot \Pr\left[U_{i-1}^e \geq U_{i-2}^e \mid U_{i-2}^e \geq U_{i-3}^e\right] \cdot \dots \\ &\quad \cdot \Pr\left[U_3^e \geq U_2^e \mid U_2^e \geq U_1^e\right] \cdot \Pr\left[U_2^e \geq U_1^e\right] \end{aligned} \quad (\text{B-17})$$

Or,

$$\begin{aligned} \Pr\left[U_i^e \geq U_k^e ; \forall k \in \mathbf{R}'\right] &= \Pr\left[\Delta U_{i,i-1}^e \geq 0 \mid \Delta U_{i-1,i-2}^e \geq 0\right] \cdot \Pr\left[\Delta U_{i-1,i-2}^e \geq 0 \mid \Delta U_{i-2,i-3}^e \geq 0\right] \cdot \dots \\ &\quad \cdot \Pr\left[\Delta U_{3,2}^e \geq 0 \mid \Delta U_{2,1}^e \geq 0\right] \cdot \Pr\left[\Delta U_{2,1}^e \geq 0\right] \end{aligned} \quad (\text{B-18})$$

Or, since the $\Delta U_{k,k-1}^e$ are independent:

$$\Pr[U_i^e \geq U_k^e ; \forall k \in \mathbf{R}'] = \prod_{k=1}^{i-1} \Pr[\Delta U_{k+1,k}^e \geq 0] \quad (\text{B-19})$$

Then,

$$P_i^e = \prod_{k=1}^{i-1} \Pr[\Delta U_{k+1,k}^e \geq 0] \cdot \Pr[U_i^e \geq U_k^e ; \forall k \in \mathbf{R}''] \quad (\text{B-20})$$

Once again invoking the assumption of myopic behavior,

$$\Pr[U_i^e \geq U_k^e ; \forall k \in \mathbf{R}''] = \Pr[U_i^e \geq U_{i+1}^e] = 1 - \Pr[\Delta U_{i+1,i}^e \geq 0] \quad (\text{B-21})$$

Then,

$$P_i^e = \left(1 - \Pr[\Delta U_{i+1,i}^e \geq 0]\right) \cdot \prod_{k=1}^{i-1} \Pr[\Delta U_{k+1,k}^e \geq 0] \quad (\text{B-22})$$

But,

$$\Delta U_{k+1,k}^e \text{ is } N\left[(V_{k+1}^e - V_k^e), \hat{\sigma}_k^2\right]; k = 1, \dots, j-1 \quad (\text{B-23})$$

So,

$$\Pr[\Delta U_{k+1,k}^e \geq 0] = \Phi\left[\frac{(V_{k+1}^e - V_k^e)}{\hat{\sigma}_k}\right] \quad (\text{B-24})$$

where $\Phi[\cdot]$ is the cumulative normal distribution function. Then

$$P_i^e = \left(1 - \Phi\left[\frac{(V_{i+1}^e - V_i^e)}{\hat{\sigma}_i}\right]\right) \cdot \prod_{k=1}^{i-1} \Phi\left[\frac{(V_{k+1}^e - V_k^e)}{\hat{\sigma}_k}\right] \quad (\text{B-25})$$

Appendix C: Derivation of Preference to Exit HOV Lane at Ingress/Egress (i/e) j

Consider next a driver's choice (or preference) to exit the HOV facility at exit point (i/e) j , conditioned on the decision to enter the facility at entry point (i/e) i . Consistent with standard random utility assumptions, let the utility of this choice be denoted by:

$$U_j^x = \sum_{q=j+1}^n U_q^F + \sum_{l=i+1}^j U_l^{HOV} ; i < j \leq n; j = i+1, \dots, n \quad (C-1)$$

where U_j^x denotes the travel time utility of exiting the HOV lane at i/e point j (under the presumption of entering at i/e point i). Or, in matrix form

$$\mathbf{U}^x = \begin{bmatrix} U_{i+1}^x \\ U_{i+2}^x \\ U_{i+3}^x \\ \vdots \\ U_{j=i+k}^x \\ \vdots \\ U_n^x \end{bmatrix} = \begin{bmatrix} 1 & 0 & 0 & \cdots & 0 & 0 & 0 \\ 1 & 1 & 0 & \cdots & 0 & 0 & 0 \\ 1 & 1 & 1 & \cdots & 0 & 0 & 0 \\ \vdots & \vdots & \vdots & \ddots & \vdots & \vdots & \vdots \\ 1 & 1 & 1 & \cdots & 1 & 0 & 0 \\ \vdots & \vdots & \vdots & \cdots & \vdots & \vdots & \vdots \\ 1 & 1 & 1 & \cdots & 1 & 1 & 1 \end{bmatrix} \begin{bmatrix} U_{i+1}^{HOV} \\ U_{i+2}^{HOV} \\ U_{i+3}^{HOV} \\ \vdots \\ U_{j=i+k}^{HOV} \\ \vdots \\ U_n^{HOV} \end{bmatrix} + \begin{bmatrix} 0 & 1 & 1 & \cdots & 1 & 1 & 1 \\ 0 & 0 & 1 & \cdots & 1 & 1 & 1 \\ 0 & 0 & 0 & \cdots & 1 & 1 & 1 \\ \vdots & \vdots & \vdots & \ddots & \vdots & \vdots & \vdots \\ 0 & 0 & 0 & \cdots & 0 & 1 & 1 \\ 0 & 0 & 0 & \cdots & 0 & 0 & 1 \\ 0 & 0 & 0 & \cdots & 0 & 0 & 0 \end{bmatrix} \begin{bmatrix} U_{i+1}^F \\ U_{i+2}^F \\ U_{i+3}^F \\ \vdots \\ U_{i+k}^F \\ \vdots \\ U_n^F \end{bmatrix} \quad (C-2)$$

Assume $U_j^x = V_j^x + \xi_j^x$, where V_j^x denotes the disutility associated with the expected travel time using exit point j and ξ_j^x denotes the random delay associated with unknown traffic effects. Assume ξ_j^x are multivariate normal distributed, i.e.,

$$\mathbf{U}^x = \text{MVN}(\mathbf{V}^x, \mathbf{\Sigma}^x) \quad (C-3)$$

where $\mathbf{\Sigma}^x$ is the covariance matrix.

Assume that the covariance between any two alternatives is only in the links they share in common; i.e.,

$$\text{Cov}(U_k^x, U_j^x) = \text{Var}(\xi_{j+1}^F + \xi_{j+2}^F + \dots + \xi_n^F + \xi_{i+1}^{HOV} + \xi_{i+2}^{HOV} + \dots + \xi_k^{HOV}) = \sigma_{F_j H_k}^2 \quad (C-4)$$

Assume, for simplicity, that the mainline freeway variances are independent of the HOV lane variances, i.e.,

$$\begin{aligned} \sigma_{H_k F_j}^2 &= \text{Cov}(U_k^x, U_j^x) = \text{Var}(\xi_{i+1}^{HOV} + \xi_{i+2}^{HOV} + \dots + \xi_k^{HOV}) + \text{Var}(\xi_{j+1}^F + \xi_{j+2}^F + \dots + \xi_n^F); k = i+1, \dots, j; k \leq j \\ &= \sigma_{H_k}^2 + \sigma_{F_j}^2 \end{aligned} \quad (C-5)$$

Then,

$$\Sigma = \begin{matrix} U_{i+1}^x \\ U_{i+2}^x \\ U_{i+3}^x \\ \vdots \\ U_{i+k}^x \\ \vdots \\ U_{j_{n-1}}^x \\ U_n^x \end{matrix} \begin{bmatrix} \sigma_{H_{i+1}}^2 & \sigma_{H_{i+1}}^2 & \sigma_{H_{i+1}}^2 & \dots & \sigma_{H_{i+1}}^2 & \dots & \sigma_{H_{i+1}}^2 & \sigma_{H_{i+1}}^2 \\ \sigma_{H_{i+1}}^2 & \sigma_{H_{i+2}}^2 & \sigma_{H_{i+2}}^2 & \dots & \sigma_{H_{i+2}}^2 & \dots & \sigma_{H_{i+2}}^2 & \sigma_{H_{i+2}}^2 \\ \sigma_{H_{i+1}}^2 & \sigma_{H_{i+2}}^2 & \sigma_{H_{i+3}}^2 & \dots & \sigma_{H_{i+3}}^2 & \dots & \sigma_{H_{i+3}}^2 & \sigma_{H_{i+3}}^2 \\ \vdots & \vdots & \vdots & \ddots & \vdots & \vdots & \vdots & \vdots \\ \sigma_{H_{i+1}}^2 & \sigma_{H_{i+2}}^2 & \sigma_{H_{i+3}}^2 & \dots & \sigma_{H_{i+k}}^2 & \dots & \sigma_{H_{i+k}}^2 & \sigma_{H_{i+k}}^2 \\ \vdots & \vdots & \vdots & \ddots & \vdots & \vdots & \vdots & \vdots \\ \sigma_{H_{i+1}}^2 & \sigma_{H_{i+2}}^2 & \sigma_{H_{i+3}}^2 & \dots & \sigma_{H_{i+k}}^2 & \dots & \sigma_{H_{n-1}}^2 & \sigma_{H_{n-1}}^2 \\ \sigma_{H_{i+1}}^2 & \sigma_{H_{i+2}}^2 & \sigma_{H_{i+3}}^2 & \dots & \sigma_{H_{i+k}}^2 & \dots & \sigma_{H_{n-1}}^2 & \sigma_{H_n}^2 \end{bmatrix} + \begin{matrix} U_{i+1}^x \\ U_{i+2}^x \\ U_{i+3}^x \\ \vdots \\ U_{i+k}^x \\ \vdots \\ U_{j_{n-1}}^x \\ U_n^x \end{matrix} \begin{bmatrix} \sigma_{F_{i+1}}^2 & \sigma_{F_{i+2}}^2 & \sigma_{F_{i+3}}^2 & \dots & \sigma_{F_{i+k}}^2 & \dots & \sigma_{F_{n-1}}^2 & 0 \\ \sigma_{F_{i+2}}^2 & \sigma_{F_{i+2}}^2 & \sigma_{F_{i+3}}^2 & \dots & \sigma_{F_{i+k}}^2 & \dots & \sigma_{F_{n-1}}^2 & 0 \\ \sigma_{F_{i+3}}^2 & \sigma_{F_{i+3}}^2 & \sigma_{F_{i+3}}^2 & \dots & \sigma_{F_{i+k}}^2 & \dots & \sigma_{F_{n-1}}^2 & 0 \\ \vdots & \vdots & \vdots & \ddots & \vdots & \vdots & \vdots & \vdots \\ \sigma_{F_{i+k}}^2 & \sigma_{F_{i+k}}^2 & \sigma_{F_{i+k}}^2 & \dots & \sigma_{F_{i+k}}^2 & \dots & \sigma_{F_{n-1}}^2 & 0 \\ \vdots & \vdots & \vdots & \ddots & \vdots & \vdots & \vdots & \vdots \\ \sigma_{F_{n-1}}^2 & \sigma_{F_{n-1}}^2 & \sigma_{F_{n-1}}^2 & \dots & \sigma_{F_{n-1}}^2 & \dots & \sigma_{F_{n-1}}^2 & 0 \\ 0 & 0 & 0 & \dots & 0 & \dots & 0 & 0 \end{bmatrix}$$

Let

$$\Delta U^x = \begin{bmatrix} U_{i+2}^x - U_{i+1}^x \\ U_{i+3}^x - U_{i+2}^x \\ U_{i+4}^x - U_{i+3}^x \\ \vdots \\ U_{i+k}^x - U_{i+k-1}^x \\ \vdots \\ U_n^x - U_{n-1}^x \\ 0 \end{bmatrix} = \mathbf{M} U^x \quad (C-6)$$

where

$$\mathbf{M} = [M_{ik}] \quad (C-7)$$

$$M_{ik} = \begin{cases} 1, & k - i = 1 \\ 0, & i = k = j \\ -\delta_{ik}, & \text{otherwise} \end{cases}$$

$$\mathbf{M}\Sigma^e\mathbf{M}^T = \begin{bmatrix} \tilde{\sigma}_1^2 & 0 & 0 & \dots & 0 & \dots & 0 & 0 \\ 0 & \tilde{\sigma}_2^2 & 0 & \dots & 0 & \dots & 0 & 0 \\ 0 & 0 & \tilde{\sigma}_3^2 & 0 & 0 & \dots & 0 & 0 \\ \vdots & \vdots & \vdots & \ddots & & & \vdots & \vdots \\ 0 & 0 & 0 & \dots & \tilde{\sigma}_i^2 & \dots & 0 & 0 \\ \vdots & \vdots & \vdots & & & \ddots & \vdots & \vdots \\ 0 & 0 & 0 & \dots & 0 & \dots & \tilde{\sigma}_{n-1}^2 & 0 \\ 0 & 0 & 0 & \dots & 0 & \dots & 0 & 0 \end{bmatrix}$$

where (C-11)

$$\tilde{\sigma}_{i+k-1}^2 = (\sigma_{H_{i+k}}^2 - \sigma_{H_{i+k-1}}^2) - (\sigma_{F_{i+k}}^2 - \sigma_{F_{i+k-1}}^2); \sigma_{F_n}^2 \equiv 0$$

$\mathbf{M}\Sigma^x\mathbf{M}^T$ being a diagonal matrix implies that the $\Delta U_{i+k+1, i+k}^x = U_{i+k+1}^x - U_{i+k}^x$; $k = 1, \dots, n - (i + 1)$ are independent random variables. Then

$$\Pr[U_{i+k+1}^x \geq U_{i+k}^x \text{ and } U_{i+l+1}^x \geq U_{i+l}^x] = \Pr[\Delta U_{i+k+1, i+k}^x \geq 0] \cdot \Pr[\Delta U_{i+l+1, i+l}^x \geq 0] \quad (\text{C-12})$$

Let P_{i+k}^x denote the probability that HOV lane exit $i + k$ will be preferred for the trip from O to D. Then

$$P_{i+k}^x = \Pr[U_{i+k}^x \geq U_{i+l}^x; \forall l \in \mathbf{R}] \quad (\text{C-13})$$

where

$$\mathbf{R} = \{i + 1, i + 2, i + 3, \dots, i + k, \dots, n\} \quad (\text{C-14})$$

Define

$$\begin{aligned} \mathbf{R}' &= \{\forall l < i + k; l \in \mathbf{R}\} \\ \mathbf{R}'' &= \{\forall l > i + k; l \in \mathbf{R}\} \end{aligned} \quad (\text{C-15})$$

Then,

$$P_{i+k}^x = \Pr[U_{i+k}^x \geq U_l^x; \forall l \in \mathbf{R}'] \cdot \Pr[U_{i+k}^x \geq U_l^x; \forall l \in \mathbf{R}''] \quad (\text{C-16})$$

But, assuming completely myopic driver behavior: i.e., that the driver will exit the HOV lane at the first opportunity for which the decision to exit is better than the decision to exit the next available i/e point:

$$\Pr[U_{i+k}^x \geq U_l^x ; \forall l \in \mathbf{R}'] = \Pr[U_{i+k}^x \geq U_{i+k-1}^x | U_{i+k-1}^x \geq U_{i+k-2}^x] \cdot \Pr[U_{i+k-1}^x \geq U_{i+k-2}^x | U_{i+k-2}^x \geq U_{i+k-3}^x] \cdot \dots \cdot \Pr[U_{i+3}^x \geq U_{i+2}^x | U_{i+2}^x \geq U_{i+1}^x] \cdot \Pr[U_{i+2}^x \geq U_{i+1}^x] \quad (\text{C-17})$$

Or,

$$\Pr[U_{i+k}^x \geq U_l^x ; \forall l \in \mathbf{R}'] = \Pr[\Delta U_{i+k,i+k-1}^x \geq 0 | \Delta U_{i+k-1,i+k-2}^x \geq 0] \cdot \Pr[\Delta U_{i+k-1,i+k-2}^x \geq 0 | \Delta U_{i+k-2,i+k-3}^x \geq 0] \cdot \dots \cdot \Pr[\Delta U_{i+3,i+2}^x \geq 0 | \Delta U_{i+2,i+1}^x \geq 0] \cdot \Pr[\Delta U_{i+2,i+1}^x \geq 0] \quad (\text{C-18})$$

Or, since the $\Delta U_{l,l-1}^x$ are independent:

$$\Pr[U_{i+k}^x \geq U_l^x ; \forall l \in \mathbf{R}'] = \prod_{l=1}^{k-1} \Pr[\Delta U_{i+l+1,i+l}^x \geq 0] \quad (\text{C-19})$$

Then

$$P_{i+k}^x = \prod_{l=1}^{k-1} \Pr[\Delta U_{i+l+1,i+l}^x \geq 0] \cdot \Pr[U_{i+k}^x \geq U_l^x ; \forall l \in \mathbf{R}''] \quad (\text{C-20})$$

Once again invoking the assumption of myopic behavior,

$$\Pr[U_{i+k}^x \geq U_l^x ; \forall l \in \mathbf{R}''] = \Pr[U_{i+k}^x \geq U_{i+k+1}^x] = 1 - \Pr[\Delta U_{i+k+1}^x \geq 0] \quad (\text{C-21})$$

Then,

$$P_{i+k}^x = \left(1 - \Pr[\Delta U_{i+k+1,i+k}^x \geq 0]\right) \cdot \prod_{l=1}^{k-1} \Pr[\Delta U_{i+l+1,i+l}^x \geq 0] \quad (\text{C-22})$$

But,

$$\Delta U_{i+k+1,i+k}^x \text{ is } N\left[(V_{i+k+1}^x - V_{i+k}^x), \tilde{\sigma}_{i+k}^2\right]; k = 1, \dots, n-1 \quad (\text{C-23})$$

So,

$$\Pr[\Delta U_{i+k+1,i+k}^x \geq 0] = \Phi\left[\frac{(V_{i+k+1}^x - V_{i+k}^x)}{\tilde{\sigma}_{i+k}}\right] \quad (\text{C-24})$$

where $\Phi[\cdot]$ is the cumulative normal distribution function. Then

$$P_{i+k}^x = \left(1 - \Phi \left[\frac{(V_{i+k+1}^x - V_{i+k}^x)}{\check{\sigma}_{i+k}} \right] \right) \cdot \prod_{l=1}^{k-1} \Phi \left[\frac{(V_{i+l+1}^x - V_{i+l}^x)}{\check{\sigma}_{i+l}} \right] \quad (\text{C-25})$$

Appendix D: Derivation of Lane-changing Behavior

The population gap acceptance function is

$$\alpha_p(G) = \int_0^{\infty} H(G-t) \cdot \mu(t) dt = \int_0^G \mu(t) dt \quad (\text{D-1})$$

Let $\Omega(t)$ denote the probability density of delay associated with finding a gap $\geq T$. Assume that successive headways in a lane are *iid* with probability density $\phi(t)$, i.e., $\phi(t)dt$ is the probability that an arbitrary gap is between t and $t + dt$ in length.

Let $\bar{\alpha}$ denote the probability that an arbitrary gap is sufficiently large enough to activate the gap out controller function. Then

$$\bar{\alpha} = \int_0^{\infty} \alpha(\tau) \phi(\tau) d\tau \quad (\text{D-2})$$

Let the probability density function for the gap between the beginning of the observation period and the first car to pass be given by $\phi_0(t)$. If the instant at which observation is begun is uncorrelated with the arrival of any car, then no time of arrival of the next car is more likely than another. Then, the probability that the next car arrives during the interval $(t, t + dt)$ must be of the form $\hat{\lambda} dt$, where $\hat{\lambda}$ is a constant. But, this probability is conditioned on the probability that the initial gap is $\geq t$; this probability is simply:

$$\Phi(t) = \int_t^{\infty} \phi(\tau) d\tau \quad (\text{D-3})$$

So,

$$\phi_0(t) = \hat{\lambda} \Phi(t) \quad (\text{D-4})$$

where $\hat{\lambda}$ is determined by the requirement

$$\int_0^{\infty} \phi_0(\tau) d\tau = \hat{\lambda} \int_0^{\infty} \Phi(\tau) d\tau = 1 \Rightarrow \hat{\lambda} = \frac{1}{\int_0^{\infty} \Phi(\tau) d\tau} \quad (\text{D-5})$$

Then, the probability that the initial acceptable gap (and therefore, no delay), denoted by $\bar{\alpha}_0$, is given by

$$\bar{\alpha}_0 = \int_0^{\infty} \alpha(\tau) \phi_0(\tau) d\tau \quad (\text{D-6})$$

Let $w(t)dt$ denote the probability that a car in the adjacent lane passes the HOV-lane-bound car during the interval $(t, t+dt)$, conditional on the HOV-lane-bound car not having moved into the adjacent lane during the interval $(0, t)$. Then, we can express $\Omega(t)$ as

$$\Omega(t) = \bar{\alpha}_0 \delta(t) + \bar{\alpha} w(t) \quad (\text{D-7})$$

where $\delta(t)$ is the Dirac delta function; i.e.,

$$\delta(t) = \begin{cases} 1, & \text{if } t = 0 \\ 0, & \text{otherwise} \end{cases}$$

The delta function takes care of the probability that there is no delay, i.e., the initial gap is $\geq T$. The second term is the probability that the additional delay beyond the initial gap will be t , which is equal to $w(t)$, the probability density for the event ‘a gap appears in the adjacent lane at time t ’ times the probability that the current gap is acceptable; i.e., equal to $\bar{\alpha} \cdot w(t)$. Observe that $w(t)$ can be expressed as:

$$w(t) = \phi_0(t) [1 - \alpha(t)] + \int_0^t w(\tau) \phi(t - \tau) [1 - \alpha(t - \tau)] d\tau \quad (\text{D-8})$$

where the first term in the above expression is the probability that the first gap arrived during time interval $(t, t+dt)$ and was not sufficiently large (i.e., $\geq T$) to be accepted; and the second term represents the ‘‘summation’’ of all of the events that a gap appeared at time $t - \tau$, $\tau = (0, d\tau, 2d\tau, \dots, t)$, and was not sufficiently large (i.e., $\geq T$) to be accepted. Let

$$\begin{aligned} \psi(t) &= \phi(t) [1 - \alpha(t)] \\ \psi_0(t) &= \phi_0(t) [1 - \alpha(t)] \end{aligned} \quad (\text{D-9})$$

Then,

$$w(t) = \psi_0(t) + \int_0^t w(\tau) \psi(t - \tau) d\tau \quad (\text{D-10})$$

which we recognize as a convolution integral. Denote the Laplace transform of a function $F(t)$ by $\mathcal{L}[F(t)] = F^*(s)$, where

$$F^*(s) = \int_0^{\infty} e^{-st} F(t) dt$$

Then, taking the Laplace transform of the expression for $w(t)$:

$$\mathcal{L}[w(t)] = \mathcal{L}[\psi_0(t)] + \mathcal{L}\left[\int_0^t w(\tau)\psi(t-\tau)d\tau\right] \quad (\text{D-11})$$

$$w^*(s) = \psi_0^*(s) + w^*(s)\psi^*(s)$$

And, solving for $w^*(s)$, we get

$$w^*(s) = \frac{\psi_0^*(s)}{1-\psi^*(s)} \quad (\text{D-12})$$

And,

$$\begin{aligned} \mathcal{L}[\Omega(t)] &= \bar{\alpha}_0 \mathcal{L}[\delta(t)] + \bar{\alpha} \mathcal{L}[w(t)] \\ \Omega^*(s) &= \bar{\alpha}_0 + \bar{\alpha} w^*(s) \\ \Omega^*(s) &= \bar{\alpha}_0 + \frac{\bar{\alpha} \psi_0^*(s)}{1-\psi^*(s)} \end{aligned} \quad (\text{D-13})$$

The above expression can be used as a moment generating function to obtain the expected delay, \bar{t} , and its variance, \bar{t}^2 , from the relationship

$$\bar{t}^n = \int_0^{\infty} t^n \Omega(t) dt = (-1)^n \left. \frac{d^n}{ds^n} \Omega^*(s) \right|_{s=0} \quad (\text{D-14})$$

Consider $\Omega^*(s)$:

$$\begin{aligned} \Omega^*(s) &= \int_0^{\infty} e^{-st} \Omega(t) dt \\ \frac{d}{ds} \Omega^*(s) &= \frac{d}{ds} \int_0^{\infty} e^{-st} \Omega(t) dt = \int_0^{\infty} \frac{d}{ds} e^{-st} \Omega(t) dt \end{aligned}$$

But, the power series expansion for e^{-st} is given by:

$$e^{-st} = 1 - \frac{st}{1!} + \frac{s^2 t^2}{2!} - \frac{s^3 t^3}{3!} + \dots$$

Substituting,

$$\frac{d}{ds} \Omega^*(s) = \int_0^{\infty} \frac{d}{ds} \left[1 - \frac{st}{1!} + \frac{s^2 t^2}{2!} - \frac{s^3 t^3}{3!} + \dots \right] \Omega(t) dt = \int_0^{\infty} \left[-\frac{t}{1!} + \frac{2st^2}{2!} - \frac{3s^2 t^3}{3!} + \dots \right] \Omega(t) dt$$

$$\frac{d}{ds} \Omega^*(s) \Big|_{s=0} = \int_0^{\infty} \left[-\frac{t}{1!} + \frac{2 \cdot 0 t^2}{2!} - \frac{3 \cdot 0^2 t^3}{3!} + \dots \right] \Omega(t) dt = - \int_0^{\infty} t \cdot \Omega(t) dt = -E(t) = -\bar{t} \Rightarrow$$

$$\bar{t} = - \frac{d}{ds} \Omega^*(s) \Big|_{s=0}$$

Similarly,

$$\frac{d^2}{ds^2} \Omega^*(s) = \int_0^{\infty} \frac{d^2}{ds^2} \left[1 - \frac{st}{1!} + \frac{s^2 t^2}{2!} - \frac{s^3 t^3}{3!} + \dots \right] \Omega(t) dt = \int_0^{\infty} \left[\frac{2t^2}{2!} - \frac{2 \cdot 3st^3}{3!} + \dots \right] \Omega(t) dt$$

$$\frac{d}{ds} \Omega^*(s) \Big|_{s=0} = \int_0^{\infty} \left[\frac{2t^2}{2!} - \frac{2 \cdot 3 \cdot 0 t^3}{3!} + \dots \right] \Omega(t) dt = \int_0^{\infty} t^2 \cdot \Omega(t) dt = E(t^2) = \bar{t}^2 \Rightarrow$$

$$\bar{t}^2 = \frac{d^2}{ds^2} \Omega^*(s) \Big|_{s=0}$$

And, in general:

$$\bar{t}^n = E(t^n) = (-1)^n \frac{d^n}{ds^n} \Omega^*(s) \Big|_{s=0}$$

Under the usual assumption of Poisson arrivals, the headway distribution (probability density function) is given by

$$\phi(t) = \lambda \exp(-\lambda t) \tag{D-15}$$

where

$$\lambda = \int_0^{\infty} \tau \phi(\tau) d\tau \tag{D-16}$$

Then,

$$\Phi(t) = \Pr(\text{headway} > t) = \int_t^{\infty} \lambda \exp(-\lambda\tau) d\tau = \lambda \int_t^{\infty} \exp(-\lambda\tau) d\tau = e^{-\lambda t} \quad (\text{D-17})$$

From (D-4) and (D-5), i.e.,

$$\phi_0(t) = \hat{\lambda}\Phi(t) \quad (\text{D-4})$$

$$\hat{\lambda} = \frac{1}{\int_0^{\infty} \Phi(\tau) d\tau} \quad (\text{D-5})$$

$$\phi_0(t) = \hat{\lambda}\Phi(t) = \frac{\Phi(t)}{\int_0^{\infty} \Phi(\tau) d\tau} = \frac{e^{-\lambda t}}{\int_0^{\infty} e^{-\lambda\tau} d\tau} = \lambda e^{-\lambda t} = \phi(t) \quad (\text{D-18})$$

Recall that

$$\alpha(t) = H(t-T)$$

And, from (D-2) and (D-6)

$$\bar{\alpha} = \int_0^{\infty} \alpha(\tau)\phi(\tau) d\tau \quad (\text{D-2})$$

$$\bar{\alpha}_0 = \int_0^{\infty} \alpha(\tau)\phi_0(\tau) d\tau \quad (\text{D-6})$$

$$\bar{\alpha} = \bar{\alpha}_0 = \lambda \int_0^{\infty} H(\tau-T) \exp(-\lambda\tau) d\tau = \lambda \int_T^{\infty} \exp(-\lambda\tau) d\tau = \exp(-\lambda T) \quad (\text{D-19})$$

Then,

$$\begin{aligned} \psi(t) &= \phi(t)[1-\alpha(t)] = \lambda e^{-\lambda t} [1-H(t-T)] \\ \psi_0(t) &= \phi_0(t)[1-\alpha(t)] = \lambda e^{-\lambda t} [1-H(t-T)] \end{aligned} \quad (\text{D-20})$$

$$\begin{aligned} \psi^*(s) &= \psi_0^*(s) = \lambda \left\{ \mathcal{L}[e^{-\lambda t}] - \mathcal{L}[e^{-\lambda t} H(t-T)] \right\} \\ &= \lambda \cdot \frac{1}{(s+\lambda)} \cdot [1 - \exp(-(s+\lambda)T)] \end{aligned} \quad (\text{D-21})$$

And,

$$\begin{aligned}
 \Omega^*(s) &= \bar{\alpha}_0 + \frac{\bar{\alpha}\psi_0^*(s)}{1-\psi^*(s)} \\
 &= \exp(-\lambda T) \left\{ 1 + \frac{\lambda \cdot \frac{1}{(s+\lambda)} \cdot [1 - \exp(-(s+\lambda)T)]}{1 - \left\langle \lambda \cdot \frac{1}{(s+\lambda)} \cdot [1 - \exp(-(s+\lambda)T)] \right\rangle} \right\} \\
 &= \exp(-\lambda T) \left\{ \frac{1}{1 - \left\langle \lambda \cdot \frac{1}{(s+\lambda)} \cdot [1 - \exp(-(s+\lambda)T)] \right\rangle} \right\} \\
 &= \exp(-\lambda T) \left\{ \frac{(s+\lambda)}{(s+\lambda) - \left\langle \lambda \cdot [1 - \exp(-(s+\lambda)T)] \right\rangle} \right\} \\
 &= \exp(-\lambda T) \left\{ \frac{(s+\lambda)}{s + \lambda \exp[-(s+\lambda)T]} \right\}
 \end{aligned} \tag{D-22}$$

And, since

$$\bar{t}^n = \int_0^\infty t^n \Omega(t) dt = (-1)^n \left. \frac{d^n}{ds^n} \Omega^*(s) \right|_{s=0}$$

then,

$$\bar{t} = - \left. \frac{d}{ds} \Omega^*(s) \right|_{s=0} \quad ; \quad \bar{t}^2 = \left. \frac{d^2}{ds^2} \Omega^*(s) \right|_{s=0}$$

Since

$$\Omega^*(s) = \exp(-\lambda T) \left\{ \frac{(s+\lambda)}{s + \lambda \exp[-(s+\lambda)T]} \right\}$$

then,

$$\begin{aligned} \frac{d}{ds} \Omega^*(s) &= \exp(-\lambda T) \left\{ \frac{s + \lambda \exp[-(s + \lambda)T] - (s + \lambda) \{1 - \lambda T \exp[-(s + \lambda)T]\}}{\{s + \lambda \exp[-(s + \lambda)T]\}^2} \right\} \\ \bar{t} &= -\frac{d}{ds} \Omega^*(s) \Big|_{s=0} = -\exp(-\lambda T) \left\{ \frac{\lambda \exp(-\lambda T) - \lambda + \lambda^2 T \exp(-\lambda T)}{\lambda^2 \exp(-2\lambda T)} \right\} \\ &= -\frac{1}{\lambda} + \frac{1}{\lambda} \exp(\lambda T) T \\ &= \frac{1}{\lambda} [\exp(\lambda T) - 1 - \lambda T] \end{aligned} \quad (D-23)$$

Similarly, we find

$$\begin{aligned} \bar{t}^2 &= \sigma_t^2 = \frac{d^2}{ds^2} \Omega^*(s) \Big|_{s=0} \\ \frac{d^2}{ds^2} \Omega^*(s) &= \frac{d}{ds} e^{-\lambda T} \left\{ \frac{[s + \lambda e^{-(s+\lambda)T}]}{[s + \lambda e^{-(s+\lambda)T}]^2} - \frac{(s + \lambda)[1 - \lambda T e^{-(s+\lambda)T}]}{[s + \lambda e^{-(s+\lambda)T}]^2} \right\} \\ &= \frac{d}{ds} e^{-\lambda T} \left\{ [s + \lambda e^{-(s+\lambda)T}]^{-1} - (s + \lambda)[1 - \lambda T e^{-(s+\lambda)T}] [s + \lambda e^{-(s+\lambda)T}]^{-2} \right\} \\ &= e^{-\lambda T} \left\{ (-1)[s + \lambda T e^{-(s+\lambda)T}]^{-2} [1 - \lambda e^{-(s+\lambda)T}] - (1)[1 - \lambda T e^{-(s+\lambda)T}] [s + \lambda e^{-(s+\lambda)T}]^{-2} \right. \\ &\quad \left. - (s + \lambda)[\lambda T^2 e^{-(s+\lambda)T}] [s + \lambda e^{-(s+\lambda)T}]^{-2} - (-2)(s + \lambda)[1 - \lambda T e^{-(s+\lambda)T}] [s + \lambda e^{-(s+\lambda)T}]^{-3} [1 - \lambda T e^{-(s+\lambda)T}] \right\} \\ &= e^{-\lambda T} \left\{ -2[1 - \lambda T e^{-(s+\lambda)T}] [s + \lambda e^{-(s+\lambda)T}]^{-2} - [\lambda s T^2 e^{-(s+\lambda)T} + \lambda^2 T^2 e^{-(s+\lambda)T}] [s + \lambda e^{-(s+\lambda)T}]^{-2} \right. \\ &\quad \left. + 2(s + \lambda)[1 - \lambda T e^{-(s+\lambda)T}]^2 [s + \lambda e^{-(s+\lambda)T}]^{-3} \right\} \end{aligned}$$

Then,

$$\begin{aligned}
\bar{t}^2 = \sigma_t^2 &= \left. \frac{d^2}{ds^2} \Omega^*(s) \right|_{s=0} \\
&= e^{-\lambda T} \left\{ -2(1 - \lambda T e^{-\lambda T}) (\lambda e^{-\lambda T})^{-2} - (\lambda^2 T^2 e^{-\lambda T}) (\lambda e^{-\lambda T})^{-2} + 2\lambda (1 - \lambda T e^{-\lambda T})^2 (\lambda e^{-\lambda T})^{-3} \right\} \\
&= e^{-\lambda T} \left\{ - \left[2(1 - \lambda T e^{-\lambda T}) + (\lambda^2 T^2 e^{-\lambda T}) \right] (\lambda e^{-\lambda T})^{-2} + 2\lambda (1 - \lambda T e^{-\lambda T})^2 \left(\frac{1}{\lambda^3} e^{3\lambda T} \right) \right\} \\
&= e^{-\lambda T} \left\{ - \left(2 - 2\lambda T e^{-\lambda T} + \lambda^2 T^2 e^{-\lambda T} \right) \left(\frac{1}{\lambda^2} e^{2\lambda T} \right) + \frac{2}{\lambda^2} e^{3\lambda T} (1 - 2\lambda T e^{-\lambda T} + \lambda^2 T^2 e^{-2\lambda T}) \right\} \\
&= - \left(2 - 2\lambda T e^{-\lambda T} + \lambda^2 T^2 e^{-\lambda T} \right) \left(\frac{1}{\lambda^2} e^{\lambda T} \right) + \frac{2}{\lambda^2} e^{2\lambda T} (1 - 2\lambda T e^{-\lambda T} + \lambda^2 T^2 e^{-2\lambda T}) \\
&= -\frac{2}{\lambda^2} e^{\lambda T} + \frac{2}{\lambda} T - T^2 + \frac{2}{\lambda^2} e^{2\lambda T} - \frac{4}{\lambda} T e^{\lambda T} + 2T^2 \\
&= \frac{2}{\lambda^2} e^{2\lambda T} - \frac{4}{\lambda} T e^{\lambda T} - \frac{2}{\lambda^2} e^{\lambda T} + \frac{2}{\lambda} T + T^2
\end{aligned} \tag{D-24}$$

Recall that

$$w(t) = \psi_0(t) + \int_0^t w(\tau) \psi(t - \tau) d\tau$$

Let $w_n(t)dt$ denote the probability that the n th car in the adjacent lane has passed the HOV vehicle, conditional on the HOV vehicle not having found an acceptable gap. Then

$$w_{n+1}(t) = \int_0^t w_n(\tau) \psi(t - \tau) d\tau ; n = 1, 2, \dots, \infty \tag{D-25}$$

$$w_1(t) = \psi_0(t)$$

where

$$\psi(t) = \phi(t) [1 - \alpha(t)]$$

$$\psi_0(t) = \phi_0(t) [1 - \alpha(t)]$$

This is a statement of the observation that if car $n + 1$ passes the HOV vehicle at time t , then car n passed the HOV vehicle at time τ , and the gap was less than T . The probability of a gap $t - \tau$ being rejected is simply $\psi(t - \tau)$. We note then that, an equivalent expression for $w(t)$ is given by

$$w(t) = \sum_{n=1}^{\infty} w_n(t) \quad (\text{D-26})$$

Recall

$$\begin{aligned} \mathcal{L}[\Omega(t)] &= \bar{\alpha}_0 \mathcal{L}[\delta(t)] + \bar{\alpha} \mathcal{L}[w(t)] \\ \Omega^*(s) &= \bar{\alpha}_0 + \bar{\alpha} w^*(s) \end{aligned}$$

But,

$$w^*(s) = \mathcal{L}[w(t)] = \sum_{n=1}^{\infty} \mathcal{L}[w_n(t)] = \sum_{n=1}^{\infty} w_n^*(s) \quad (\text{D-27})$$

Then,

$$\Omega^*(s) = \bar{\alpha}_0 + \bar{\alpha} w^*(s) = \bar{\alpha}_0 + \bar{\alpha} \sum_{n=1}^{\infty} w_n^*(s) \quad (\text{D-28})$$

From the Convolution Theorem:

$$\begin{aligned} w_{n+1}^*(s) &= \mathcal{L}[w_{n+1}(t)] = \mathcal{L}\left[\int_0^t w_n(\tau) \psi(t - \tau) d\tau\right] = w_n^*(s) \cdot \psi^*(s); \quad n = 1, 2, \dots, \infty \\ w_1^*(s) &= \mathcal{L}[w_1(t)] = \psi_0^*(s) \end{aligned} \quad (\text{D-29})$$

Then,

$$\begin{aligned}
 w_{n+1}^*(s) &= \mathcal{L}[w_{n+1}(t)] = \mathcal{L}\left[\int_0^t w_n(\tau)\psi(t-\tau)d\tau\right] = w_n^*(s) \cdot \psi^*(s); \quad n = 1, 2, \dots, \infty \\
 w_1^*(s) &= \psi_0^*(s) \\
 w_2^*(s) &= w_1^*(s) \cdot \psi^*(s) = \psi_0^*(s) \cdot \psi^*(s) \\
 w_3^*(s) &= w_2^*(s) \cdot \psi^*(s) = \psi_0^*(s) \cdot [\psi^*(s)]^2 \\
 w_4^*(s) &= w_3^*(s) \cdot \psi^*(s) = \psi_0^*(s) \cdot [\psi^*(s)]^3 \\
 &\vdots \\
 w_n^*(s) &= w_{n-1}^*(s) \cdot \psi^*(s) = \psi_0^*(s) \cdot [\psi^*(s)]^{n-1}; \quad n = 1, 2, \dots, \infty
 \end{aligned} \tag{D-30}$$

Noting that, in the case of negative exponential headways,

$$\begin{aligned}
 \psi(t) &= \lambda e^{-\lambda t} [1 - H(t-T)] \\
 \psi_0(t) &= \lambda e^{-\lambda t} [1 - H(t-T)]
 \end{aligned}$$

Then,

$$\begin{aligned}
 w_1^*(s) &= \psi_0^*(s) \\
 w_1(t) &= \psi_0(t) = \lambda e^{-\lambda t} [1 - H(t-T)]
 \end{aligned} \tag{D-31}$$

Similarly,

$$\begin{aligned}
 w_2^*(s) &= w_1^*(s) \cdot \psi^*(s) = \psi_0^*(s) \cdot \psi^*(s) \\
 w_2(t) &= \mathcal{L}^{-1}[w_2^*(s)] = \mathcal{L}^{-1}[\psi_0^*(s) \cdot \psi^*(s)] = \lambda^2 e^{-\lambda t} \int_0^t H(T-\tau) \cdot H(T+\tau-t) d\tau \\
 &= \lambda^2 e^{-\lambda t} \{t - 2T \cdot H(t-T) - (t-2T) \cdot H(t-T) \cdot H(t-2T)\}
 \end{aligned} \tag{D-32}$$

$$w_3^*(s) = w_2^*(s) \cdot \psi^*(s)$$

$$w_3(t) = \mathcal{L}^{-1} [w_3^*(s)] = \mathcal{L}^{-1} [w_2^*(s) \cdot \psi^*(s)] = \int_0^t w_2(\tau) \psi(t-\tau) d\tau$$

$$= \lambda^3 e^{-\lambda t} \left\{ \begin{aligned} & \left[\frac{t^2}{2} - \left[\frac{(t-T)^2}{2} - \frac{(t-2T)^2}{2} + \frac{t^2}{2} \right] \cdot H(t-T) - \left[\frac{(t-3T)^2}{2} - \frac{(T-t)^2}{2} \right] \cdot H(t-T) \cdot H(t-2T) \right] \\ & \left[-\frac{(t-2T)^2}{2} \cdot H(t-2T) + \frac{(t-3T)^2}{2} \cdot H(t-2T) \cdot H(t-3T) \right] \end{aligned} \right\} \quad (\text{D-33})$$

⋮

etc.

Recalling (D-7) and (D-26), i.e.,

$$\Omega(t) = \bar{\alpha}_0 \delta(t) + \bar{\alpha} w(t) \quad (\text{D-7})$$

$$w(t) = \sum_{n=1}^{\infty} w_n(t) \quad (\text{D-26})$$

we can calculate the distribution of the delay times.

Implementation of the above procedure would involve first estimating the population distribution gap acceptance function; i.e.,

$$\alpha_p(G) = \int_0^{\infty} H(G-t) \cdot \mu(t) dt = \int_0^G \mu(t) dt \quad (\text{D-34})$$

and then computing $\hat{\alpha}(G) = H(G - \hat{T})$ based on a random draw from that distribution.